



Drivers of coastal dune dynamics on the Younghusband Peninsula, South Australia.

by

Martim Almeida Braga Moulton

Thesis
Submitted to Flinders University (Adelaide-Australia)
for the Cotutelle degree of

Doctor of Philosophy (Ph.D.)

College of Science and Engineering

March 2020

and

Submitted to Universidade Federal Fluminense (Niterói-Brazil)
for the Cotutelle degree of

Doctor of Geography (Doutor em Geografia)

Geosciences Institute (Instituto de Geociências)

Declaration

I certify that this work does not contain without acknowledgment any material previously submitted for a degree or diploma in any university. To the best of my knowledge, it also does not contain any material previously published or written by another person except where reference is made in the document.

Martim Almeida Braga Moulton.

June, 2019.

Co-authorship

Martim Almeida Braga Moulton is the primary author of all chapters in this thesis.

Co-authors listed on chapters 2 to 4 provided intellectual supervision, editorial support and field support.

Thesis acknowledgements

I would like to express my deep gratitude to Professor Patrick Hesp and Dr. Graziela Miot da Silva, my research supervisors in Australia, not only for their patient guidance and useful critiques, but also for their friendship. Their warm welcome made me feel like Adelaide and Flinders University were my second home, and definitely my learning curve in these two years with them in Australia was critical for my academic career. My grateful thanks to Flinders University for offering me the resources needed for the research and all the Flinders University staff that helped me along these years, especially Mr. Robert Keane for his help with the GIS analysis and his support on field.

I would also like to express my gratitude to Dr. Guilherme Fernandez, who has been my mentor and guide since undergraduate, and during this PhD gave me the encouragement needed to take this big step and helpful advice along the way. My gratitude for all the POSGEO-UFF staff for all the help with the cotutelle procedures and for providing me with the sandwich scholarship alongside with CAPES.

I would also like to thank Camille Bouchez and Jonas Schaper, for their immense support, encouragement, guidance, and friendship. Working late hours in the office was much more enjoyable with them.

I also wish to thank my parents, Rosário and Tim, for their support and encouragement throughout my study, they are the reason for my interest in nature and scientific research. I am very thankful for the education that you have given me.

I would like to thank so much my partner Clara Costa for her unconditional support, for listening to all my concerns and always believing in me. Also thank you for the biggest gift of all, our little Maitê, who came into this world to show us how beautiful life is. By observing the strength inside you, I became stronger and more resilient. Without you by my side, I would not have made this work possible.

I would also like to acknowledge the Ngarrindjeri people, traditional custodians of the Kurangk, who have preserved this extremely special land for so many years.

Summary

Coastal dune development and evolution has been one of the main research topics in coastal science (Martínez and Psuty, 2004). However, due to the complexity of the interactions between different driving factors that dictate coastal dune dynamics, the roles that each of the abiotic and biotic drivers play in formation and transformation of these deposits are still poorly understood (Provoost *et al.*, 2011; Barchyn and Hugenholtz, 2012).

In a historical time-scale (years to decades) dunefields can undergo significant morphological and ecological changes, shifting from an active/unvegetated state to a stabilized/vegetated state, and vice versa (Hesp, 2013). Studying how dunes evolve in a meso-scale analysis poses a significant challenge to researchers because of the difficulty in combining or obtaining spatial data with enough resolution over a significant period of time (Pickart and Hesp, 2019), and therefore studies that show medium to long-term dune changes are scarce (Hesp, 2013).

In the Younghusband Peninsula dune system (South-east coast of South Australia), the availability of high-resolution historical spatial data, combined with climatic data, oceanographic data, and specific environmental conditions, constitutes a good opportunity to study different aspects of meso-scale morphological changes and their main driving factors.

The objective of this body of work is to examine the different aspects of meso-scale driving factors of coastal dune dynamics, with the Younghusband Peninsula (YP) as a study case. This work investigates specifically: (1) What were the potential drivers of vegetation cover changes in the last ~70 years; (2) What were the geomorphological changes that occurred due to this vegetation cover

changes and how did this morphological evolution take place; and (3) What are the main drivers that dictate the foredune morphological variability identified in the southern portion of the YP.

The first part of this study (published in *Earth Surface Processes and Landforms Journal* – Moulton *et al.*, 2019) uses historical aerial images and data from potential biotic and abiotic drivers to investigate why vegetation cover has changed in the last ~70 years in the northern YP. Results show that the decline in exotic rabbit abundance, especially in the 1950s after the introduction of the Myxomatosis virus, present significant correlation to periods of greater vegetation growth. Other factors, such as wind and precipitation variability, did not present any explanatory correlation, leading to the conclusion that rabbit grazing was the most important driving factor of vegetation growth in the YP during this period.

The second part of this study investigates the geomorphological transformations induced by the vegetation changes and how the evolution of different dune types took place, with the use of historical aerial imagery and three-dimensional high-resolution topographic data. From 1949 to 2018, the dune system went through significant geomorphological changes due to vegetation stabilization, with relatively simple active transgressive dunefields changing into a complex landscape of active and vegetated blowout/parabolic dunes. Vegetation growth on the marginal interdune depressions and plains, forming narrow elongate vegetated ridges was the main process that lead to the development of a complex of blowouts and parabolic dunes, most of which are already stabilized by 2018.

The third and final part of this study investigates the role of various factors controlling foredune evolution that accounts for the alongshore geomorphological

and volumetric differences along the southeastern portion of the Youngusband Peninsula. For this study a 16 km stretch of beach on the barrier was selected, where minimal environmental changes in some factors such as wind energy and aeolian transport occur. Results show a south to north alongshore increase in foredune height and volume for the 3 years surveyed, together with an increase in wave energy, while other driving factors showed minimal to no changes. These findings indicate that wave energy has an indirect positive relationship with foredune accretion, with wave driven sediment supply to the beach increasing as wave energy rises from south to north. In this study area wave energy has more significant role than aeolian transport limitations on foredune (and relict foredune) development.

Resumo (Portuguese)

O desenvolvimento e a evolução das dunas costeiras têm sido um dos principais tópicos de pesquisa em ciências costeiras (Martínez e Psuty, 2004). No entanto, devido à complexidade das interações entre os diferentes fatores controladores que determinam a dinâmica das dunas costeiras, os papéis que cada um dos fatores abióticos e bióticos desempenham na formação e transformação desses depósitos ainda são pouco compreendidos (Provoost et al., 2011; Barchyn e Hugenholtz, 2012).

Em uma escala de tempo histórica (anos a décadas), campos de dunas podem sofrer mudanças morfológicas e ecológicas significativas, passando de um estado ativo/ não-vegetado para um estado estabilizado/vegetado e vice-versa (Hesp, 2013). Estudar como as dunas evoluem em uma análise em meso-escala representa um desafio significativo para os pesquisadores devido à

dificuldade em combinar ou obter dados espaciais com resolução suficiente durante um período de tempo significativo (Pickart e Hesp, 2019) e, portanto, estudos que mostram mudanças de médio a longo prazo em dunas costeiras são escassos (Hesp, 2013).

No campo de dunas da Península de Youngusband (costa sudeste da Austrália Meridional), a disponibilidade de dados espaciais históricos de alta resolução, combinados com dados climáticos, dados oceanográficos e condições ambientais específicas, constitui uma boa oportunidade para estudar diferentes aspectos das mudanças morfológicas em meso-escala e seus principais fatores determinantes.

O objetivo deste trabalho é examinar os diferentes aspectos dos fatores controladores da dinâmica das dunas costeiras em meso-escala, tendo a Península de Youngusband (YP) como um caso de estudo. Este trabalho investiga especificamente: (1) Quais foram os possíveis fatores controladores que implicaram nas mudanças de cobertura vegetal nos últimos ~70 anos; (2) Quais foram as mudanças geomorfológicas que ocorreram devido a essa alteração da cobertura vegetal e como se sucedeu essa evolução morfológica; e (3) Quais são os principais fatores que determinam a variabilidade morfológica das dunas frontais identificadas na porção sul da península.

A primeira parte deste estudo (publicada na revista *Earth Surface Processes and Landforms* - Moulton et al., 2019) usa imagens aéreas históricas e dados de possíveis fatores bióticos e abióticos para investigar por que a cobertura vegetal mudou nos últimos ~ 70 anos na porção norte da península de Youngusband. Os resultados mostram que o declínio da abundância de coelhos exóticos, principalmente no início da década de 1950 após a introdução do vírus

da Mixomatose, apresenta correlação significativa com períodos de maior crescimento da vegetação. Outros fatores, como a variabilidade do vento e da precipitação, não apresentaram correlação explicativa, levando à conclusão de que a redução dos coelhos foi o fator determinante mais importante do crescimento da vegetação no YP nesse período.

A segunda parte deste estudo investiga as transformações geomorfológicas induzidas pelas mudanças da vegetação e como ocorreu a evolução de diferentes tipos de dunas, com o uso de imagens aéreas históricas e dados topográficos tridimensionais de alta resolução. De 1949 a 2018, o sistema de dunas passou por mudanças geomorfológicas significativas devido à estabilização da vegetação, com campos de dunas transgressivos ativos relativamente simples mudando para uma paisagem complexa de dunas parabólicas e cortes eólicos. O crescimento da vegetação nas depressões interdunares e planícies de deflação, formando corredores alongados e estreitos de vegetação, foi o principal mecanismo que levou ao desenvolvimento de uma série de cortes eólicos e dunas parabólicas, a maioria dos quais já se encontravam estabilizados em 2018.

A terceira e última parte deste estudo investiga o papel de vários fatores que controlam a evolução das dunas frontais, responsáveis pelas diferenças geomorfológicas e volumétricas encontradas ao longo da linha de costa da porção sudeste da Península de Younghusband. Para este estudo, foi selecionado um trecho de 16 km de praia, onde mudanças ambientais mínimas ocorrem em relação a certos fatores, como energia eólica e transporte eólico. Os resultados mostram um aumento de sul para norte na altura e no volume das dunas frontais nos três anos pesquisados, juntamente com um aumento na

energia das ondas, enquanto outros fatores determinantes mostraram mudanças mínimas ou inexistentes. Essas descobertas indicam que a energia das ondas tem uma relação indireta positiva com a acumulação eólica das dunas frontais, sugerindo que as ondas têm um papel importante no suprimento de sedimentos em direção à praia, aumentando à medida que a energia das ondas sobe de sul para o norte. Nesta área de estudo, a energia das ondas tem um papel mais significativo do que as limitações de transporte eólico no desenvolvimento de dunas frontais (e dunas frontais relíquias).

Table of contents

Declaration	ii
Co-authorship	iii
Thesis acknowledgements.....	iv
Summary.....	v
Table of contents	xi
List of figures.....	xiv
List of tables	xvii
Chapter 1- Thesis introduction.....	1
1.1. Research problem	1
1.2. Research questions and aims.....	3
1.3. Literature review	4
1.3.1. Coastal transgressive dunefields.....	4
1.3.2. Vegetation cover changes in large-scale transgressive coastal dune systems	5
1.3.3. Historical geomorphological changes in large-scale coastal transgressive dunefields due to vegetation changes	6
1.3.4. Surfzone-beach-dune models and the controls of foredune evolution ..	8
Chapter 2 - Changes in vegetation cover on the Youngusband Peninsula transgressive dunefields (Australia) 1949 – 2017	10
2.1. Abstract	10
2.2. Introduction.....	11
2.3. Study site.....	15
2.4. Methods	17
2.4.1. Quantification of the changes in vegetation cover	17
2.4.1.1. Grayscale pixel-based classification	19
2.4.1.2. Point-based grid sampling classification.....	20
2.4.2. Analysis of climate data	20
2.4.3. Analysis of rabbit density data	21
2.5. Historical vegetation changes.....	22
2.5.1. Long-term changes (1949-2017)	22
2.5.2. Short-term Recent Annual Changes (2010 to 2017).....	26
2.6. Potential driving factors of vegetation change.....	28
2.6.1. Long-term changes (1949-2017)	28
2.6.1.1. Rainfall.....	30
2.6.1.2. Wind	31

2.6.2.3. Rabbits.....	32
2.6.2. Short-term Recent Annual Changes (2010 to 2017).....	33
2.6.3. Other potential driving factors.....	35
2.7. Conclusion.....	37
2.8. Acknowledgements.....	38
2.9. References.....	39
2.10. Supplementary materials.....	45
Chapter 3 - Historical evolution of transgressive dunefields to parabolic-blowout dunefields, Younghusband Peninsula, South Australia.....	48
3.1. Abstract.....	48
3.2. Introduction.....	49
3.3. Study site.....	52
3.4. Methods.....	54
3.5. Results.....	56
3.5.1. Geomorphological changes between 1949 and 2018.....	56
3.5.2. Decadal geomorphological changes.....	60
3.5.2.1. Foredune-blowout complex evolution.....	60
3.5.2.2. Parabolic dune evolution.....	62
3.5.2.3. Active transgressive dunefield evolution.....	64
3.5.2.3.1. Evolution into a parabolic dune complex.....	64
3.5.2.3.2. Evolution into a single large-scale parabolic dune.....	66
3.6. Discussion.....	68
3.7. Conclusion.....	73
3.8. Acknowledgments.....	74
3.9. References.....	74
Chapter 4 - Surfzone-beach-dune interactions along a variable low wave energy dissipative beach.....	78
4.1. Abstract.....	78
4.2. Introduction.....	79
4.2.1. The development of Surfzone-beach-dune interaction models.....	82
4.2.2. Connection to the backshore and dunes.....	83
4.2.3. Controlling factors of foredune development.....	84
4.2.3.1. Beach morphology and wind flow.....	84
4.2.3.2. Beach Width.....	85
4.2.3.3. Beach Mobility.....	86
4.2.3.4. Wave Energy.....	87

4.3. Study area	88
4.4. Methods	91
4.4.1. Topography and bathymetry	92
4.4.2. Beach width	94
4.4.3. Grain size analysis	94
4.4.4. Wave energy	95
4.4.5. Shoreline orientation and aeolian drift potential	96
4.5. Results	98
4.5.1. Beach and Foredune Topographic Variability	98
4.5.2. Beach Width	103
4.5.3. Grain size analysis	104
4.5.4. Shoreline orientation and aeolian drift potentials	105
4.5.5. Wave energy alongshore variability	107
4.6. Discussion	113
4.7. Conclusion	115
4.8. Acknowledgments	116
4.9. References	116
Chapter 5 - Thesis final conclusions	125
5.1. Summary of findings	125
5.2. Future work	129
Thesis references	131

List of figures

Figure 2.1 Map of the study site, showing the location of the Youngusband Peninsula (YP) in the south-east Coast of South Australia. The detailed image (c.) shows the northern section of the YP where most of the active transgressive dune system is situated and the sand rose indicates the resultant aeolian drift potential (Data from Robe weather station), (d.) shows in detail the survey area where most of the vegetation cover analysis was performed (image from 2017).....	14
Figure 2.2 - Comparison of the vegetation cover between 1949 and 2017, the first and the latest aerial photographs for the northern section of the YP transgressive dunefield (black outlined area). The 2017 orthomosaic shows a significant decrease in sand area and increase in vegetation cover.....	15
Figure 2.3 - Long-term (68 years) changes in vegetation cover within the study area expressed in percentages. The blue columns represent the percentages obtained by the GPC method and the orange columns show the PGSC percentages. The calculated averages between the two classifications are represented by the numbers inside the bars and the dotted line, here used as an estimate for the vegetation cover for each year. The error bars show the difference between the two classification methods for each of the images.....	23
Figure 2.4 - Sequence of images utilising the results of Grayscale Pixel-based Classification (GPC) for the different years of aerial images available in the survey area. A trend of increasing vegetation cover occurs since the first aerial imagery was taken in 1949. The vegetation cover growth has led to the connection of the initially discrete patches of vegetation, and stabilization of a significant portion of the dune system, resulting in the development of parabolic dunes.	25
Figure 2.5 - Short-term (8 years) annual vegetation changes for 2010 to 2017. An increasing trend in vegetation cover is observed. The error bars show the difference between the two classification methods (PGSC in orange and GPC in blue) for each of the images.....	27
Figure 2.6 - (a) Vegetation cover estimates compared to (b) the variations in rainfall anomalies (Meningie weather station rainfall data; average annual rainfall is 469 mm), (c) Aeolian drift potential (calculated from Robe weather station wind data), and (d) rabbit density: data from Witchitie (Flinders Ranges - SA) in blue (Saunders et al. 2010) and data from Salt Creek (Coorong Region - SA), in orange (Mutze et al. 2014a), interpolated data are represented in the dotted lines. The vertical dashed lines separate the data in the periods determined by the year of each aerial photograph.	29
Figure 2.7 - Annual vegetation cover for the last 8 years (2010-2017) using satellite imagery compared to annual rainfall (Meningie Meteorological Station), aeolian drift potential (DP) (Robe Meteorological Station) and rabbit density (sources: Mutze et al., 2014; Cox, unpublished).....	35
Figure SM-8 - Historical annual rainfall record for Meningie (1864-2017), showing rainfall before and during the studied period. The 5-year moving average shows two periods of below average rainfall (1925-1944 and 1993-2008) followed by two periods of above average rainfall (1945-1956 and 2009-2013).....	45
Figure 3.1 – Location of the northern Youngusband Peninsula. The dashed line (c) represents the study area. Images d, e, f, and g show the location of the representative areas chosen to show the detailed evolutionary paths of the main geomorphological changes that occurred in the past 7 decades.....	51
Figure 3.2 – Oblique aerial photos showing: a) the complex nested relict and active parabolic-blowout dune morphology within the YP; b) an active parabolic dune	

migrating towards the Coorong Lagoon; c) elongate parabolic dunes in the last stage of vegetation colonization within a densely vegetated, formerly active transgressive dunefield area (Images courtesy of Michael Hilton).....	53
Figure 3.3 – Geomorphological maps showing the changes between 1949 (a) and 2018 (b) within the northern YP. Datum: GDA 2020.....	58
Figure 3.4 – Elevation data of the northern YP dunes obtained from the 2018 LiDAR (Base image: 2018 orthomosaic). Horizontal datum: GDA2020. Vertical datum: AHD (Australian Height Datum).....	60
Figure 3.5 - Example of the geomorphological changes that occurred within foredunes from 1949 to 2018 (Location in figure 3.1).....	61
Figure 3.6 – Example of the geomorphological changes that occurred within parabolic dunes from 1949 to 2018. (Location in figure 3.1).	63
Figure 3.7 – Example of the geomorphological changes that occurred within a portion of the active transgressive dunefield from 1949 to 2018, with vegetation colonization transforming it into a series of parabolic dunes (Location in figure 3.1).	65
Figure 3.8 - Example of the geomorphological changes that occurred within an active transgressive dunefield from 1949 to 2018, with vegetation colonization transforming it into a single parabolic dune (Location in figure 3.1).	67
Figure 3.9 – Annual rainfall record for Meningie (SA).....	69
Figure 4.1 – Location of the study area in South Australia (a), at the southern end of the YP system (b), and the location of the 9 profile sites (P1 to P9) where topographic surveys were performed. (c) Bathymetric information adapted from the Australian Hydrographic Service (2001).	81
Figure 4.2 – (a) Wind rose and (b) Sand rose (based on $m\ sec^{-1}$ data) for the study area, arrow indicates the resultant sediment transport vector. (Wind data from Cape Jaffa Meteorological Station - 1991 to 2017 - Bureau of Meteorology [2017]).	91
Figure 4.3 – Wave modelling domain showing the large and nested grids. Wave propagation for average and storm conditions were simulated across the large domain (a) which provided boundary conditions to the nested domain. (b) Model validation was performed using measured significant wave height (Hs) from the Cape du Couedic wave buoy (black triangle next to Kangaroo Island).	96
Figure 4.4 – Illustration showing the definitions used for determining onshore, alongshore and offshore winds.	98
Figure 4.5 –Two-dimensional topographic profile measurements for the 9 sites between 2016 and 2018. Dune height increases from P1 to P9.	99
Figure 4.6 – South to North alongshore variation in (a) foredune height and (b) foredune volume at each site for each of the 3 years surveyed. In all surveys, a northwards increase in both foredune height and volume occurs from P1 to P9). Trendlines are indicated for the different years.	100
Figure 4.7 – RPA derived Digital Surface Models for P1, P5, and P9, showing the significant northwards increase in height and volume of the foredune from South (P1) to North (P9).	101
Figure 4.8 – LiDAR DEM of the study area showing elevational changes alongshore and the 5 selected profiles (P1, P3, P5, P7 and P9). A substantial difference in height and volume of the modern (blue line) and relict foredunes (red line) from south to north. LiDAR - Horizontal datum: GDA2020. Vertical datum: AHD (Australian Height Datum).	103
Figure 4.9 – Average beach width and dry beach width for each of the profile sites. The linear trendline shows a decrease in wet and dry beach width from North to South, but little variation in terms of dry-beach width.	104

Figure 4.10 – Mean grain size diameter of beach and dune samples for each of the 9 sites. Black dashed lines represent the limits of each sediment size class.	105
Figure 4.11 – Sand roses (a, b and c) for the 3 different sections of shoreline orientation observed in the study area. The dotted blue line in each sand rose indicates the mean orientation for that section of coast. The red solid lines are the drift potential (DP) of offshore winds and the orange solid line the DP of alongshore winds. The dashed black arrow is the RDP/RDD excluding offshore DP's. The dashed and dotted arrow is the RDP/RDD excluding offshore and alongshore DP's.	107
Figure 4.12 – Breaker wave height estimated by the model (square plots) and measured in-the field (round plots) at each site. Both methods show an increase in breaker wave height from South to North.	108
Figure 4.13 – Foredune volumes plotted against; (a) Breaker wave height estimated by the numerical model Delft3d; b) Breaker wave height visually measured; (c) Number of breaking waves; (d) Surfzone width and (e) Distance to seagrass. All wave energy proxy indicators show a good to significant correlation with foredune volumes for the 3 different years.	109
Figure 4.14 – Aerial photograph (2013) of the study area showing the seagrass meadow in the nearshore. An increase in the distance between the shoreline and the landward edge of the seagrass (white dashed line) can be observed from South to North, correlating with an increase in wave energy.	110
Figure 4.15 – Significant wave height (Hs) simulation for the study area using (a) storm conditions (wave direction 225° - wave period 7.7 s) and (b) average conditions (wave direction 225° - wave period 10.6 s). An increase in significant wave height (Hs) can be observed from South to North in both simulations. (c) Wave dissipation simulation results for average conditions. There is a clear increase from South to North indicating higher energy and more extensive surf zone towards the north.	111
Figure 4.16 – (a) Detailed nearshore bathymetry for the study area (Adapted from the Australian Hydrographic Service, 2001) and location of the nearshore topographic profiles for each of the sites. (b) Subaqueous nearshore topographic profiles from each site revealing the slight increase in slope gradient from P1 to P9.	112

List of tables

Table 2.1 - Information regarding the aerial photographs selected for the long-term vegetation cover analysis.....	18
Table 2.2 - Vegetation change between periods analysed (periods are based on the years of the available aerial photographs).....	24
Table SM-03 Percent of vegetation cover for the long-term analysis obtained from the Grayscale pixel-based classification method (GPC) and the Point-based grid sampling manual classification method (PGSC) using the available aerial photography for the study area.....	45
Table SM-02 – Percent of vegetation cover for the long-term analysis obtained from the GPC method and the PGSC method using annual satellite imagery for the study area.	46
Table SM-03 – Values for vegetation cover and averages for the different variables per period used to perform the Pearson correlation coefficient (PCC) statistical analysis for the long-term data (1949-2017).....	46
Table SM-04 – Values for vegetation cover and averages for the different variables per year used to perform the Pearson correlation coefficient (PCC) statistical analysis for the annual short-term data (2010-2017).....	47
Table SM-05 – Results from the Pearson correlation coefficient statistical analysis for the long-term data (1949-2017).....	47
Table SM-06 – Results from the Pearson correlation coefficient statistical analysis for the short-term data (2010-2017).	47
Table 3.1 – Area of the different geounits mapped in 1949 (a) and 2018 (b).....	59
Table 4.1 – Shoreline angle and estimates of aeolian drift potential and their relative rate of sand drift for sites P1 to P9 assuming equal beach sediment supply.	106
Table 4.2 - Indicators of wave energy measured for each site. Numbers correspond to an average calculated from both field measurements and imagery for 8 different years.	108

Chapter 1- Thesis introduction

1.1. Research problem

Coastal sand dunes are dynamic geomorphological landforms that represent the interface between the land and the sea. Dunefields can be seen as a hazard to properties and infrastructure since they can migrate inland, creating negative impacts for governments and landowners, and have been historically subjected to artificial stabilization or even complete removal for economic reasons (Nordstrom, 2008). However, they can also provide a wide range of ecosystem services to society and promote socio-economic benefits that are greatly overlooked or undervalued (Everard *et al.*, 2010).

In many sites around the world, coastal dunes contribute to coastal defence, acting as a physical barrier that mitigates the impacts of coastal flooding induced by storm waves, extreme weather events (e.g. tropical cyclones) and sea-level rise (Everard *et al.*, 2010), as well as being an important source of sediment for natural beach recovery (Psuty, 2004). Given that approximately 10% of the world's population lives in coastal areas less than 10 meters above sea level (McGranahan *et al.*, 2007), and a Global Mean Sea Level rise of 0.2 to 2.5 m (Sweet *et al.*, 2017) together with a 2% to 11% increase in extreme weather event intensity is expected by the end of the 21st century (Knutson, 2010), it is imperative that we increase our understanding of resilient natural features such as coastal sand dunes.

Although coastal dune systems have been one of the main objects of study for coastal scientists for at least 180 years (Martínez and Psuty, 2004), still little is known in terms of the association with biotic and abiotic driving factors that influence the formation and morphological changes of these systems at a meso-scale (annual to decadal time-scale) (Hesp, 2013).

Coastal dunes are depositional landforms derived from processes that have different time scales (Walker *et al.* 2017). At a historical time-scale (years to decades) dunefields can undergo significant morphological and ecological changes, shifting from an active/unvegetated state to a stabilized/vegetated state, and vice versa (Hesp, 2013).

How and why coastal dunefields change have been an important research topic in coastal geomorphology, dating back to pioneer studies on the West Coast of the U.S. made by Cooper (1958; 1967) and Lake Michigan beaches by Oslen (1958). However, studying the evolution of dunes in a meso-scale analysis poses a significant challenge to researchers due to the difficulty to combine or obtain spatial data with enough resolution over a significant period of time (Pickart and Hesp, 2019), and therefore studies that show medium-term dune changes are scarce (Hesp, 2013).

The Youngusband Peninsula (South East coast of the State of South Australia) is one of the longest Holocene coastal dune systems in the world (190 km long), with great geodiversity that includes a wide variety of dune types. Located in an isolated and protected area (within the Coorong National Park), this long barrier is an excellent laboratory to study different processes related to coastal dune dynamics.

Because of its geographical location, as part of the Coorong estuary and the mouth of Australia's largest river, the Murray River, a considerable amount of high-resolution historical spatial data, climatic data, and oceanographic data, are available. Combined with specific environmental conditions, the Youngusband Peninsula constitutes a good location to investigate different aspects of meso-scale morphological changes and their main driving factors.

1.2. Research questions and aims

Within the central questions that still pose challenges to coastal geomorphology, three guide this study: (1) What drives vegetation changes in large scale coastal dune systems? (2) What are the evolutionary paths of different dune types in a dunefield stabilization phase? (3) What are the main controlling factors of foredune evolution?

With the Younghusband Peninsula dunefield as a case study, the objective of this thesis is to examine why dune vegetation cover has changed in the past decades, what were the morphological implications of this vegetation cover change, how did these transformations occurred, and what factors drive alongshore foredune morphological variations. Therefore, the specific aims of this thesis are to investigate:

- i. The potential drivers of vegetation cover changes in the last ~70 years within the northern Holocene dune system of the Younghusband Peninsula.
- ii. The geomorphological changes that occurred due to the vegetation cover changes and how did this morphological evolution take place in the last ~70 years within the northern Holocene dune system of the Younghusband Peninsula.
- iii. The main drivers that dictate the foredune morphological variability identified in the southern portion of the Younghusband Peninsula.

1.3. Literature review

1.3.1. Coastal transgressive dunefields

Coastal transgressive dunefields are aeolian sand deposits that were formed by the downwind movement of sand in vegetated to semi-vegetated areas (Hesp and Thom, 1990). These dunefields often comprise an extensive area and typically occur in regions with strong winds, high wave energy, and high sediment supply coasts (Davies, 1980; Short and Hesp, 1982; Pye and Tsoar 1990; Hesp and Thom, 1990; Hesp, 2011; Hesp *et al.*, 2011; Hesp and Walker, 2013).

The definition of “transgressive dunefield” used in this work is similar to the one presented in Hesp and Thom (1990), where the term is employed to describe active and stabilized dunes that are currently migrating, or had a past of landwards migration, over a pre-existing terrain (forest, wetland, etc.). These dunefields often exhibit a range of simple to complex landforms and one to multiple phases of development (Cooper, 1958; 1967; Orme and Tchakerian, 1986; Hesp and Thom, 1990; Clemmensen *et al.*, 1996; 2001; 2006; Hesp, 2011; 2013).

Transgressive dunefields can range from highly mobile systems to fully stabilized systems (relict transgressive dunefields) (Hesp, 2013). The stabilization of these systems is dependent on the competition between aeolian sand transport/supply and vegetation growth (Durán and Herrmann, 2006; Arens *et al.*, 2013; Hesp, 2013; Hesp and Hilton, 2013; Pickart and Hesp, 2019). They can switch from an active and largely unvegetated state to a stabilized and predominantly vegetated state, and vice versa (Hugenholtz and Wolfe, 2005; Yizhaq *et al.*, 2007, 2009; Hesp, 2013), resulting in substantial morphological changes (Hesp *et al.*, 2011; Hesp, 2013).

1.3.2. Vegetation cover changes in large-scale transgressive coastal dune systems

Vegetation is the main, and commonly the only stabilizing agent of coastal transgressive dune systems (Hesp and Thom, 1990; Durán and Herrmann, 2006). Changes in dune vegetation cover can result in a complete transition of the state of the dunefield (stable or active) (Hesp, 2013). Provoost *et al.* (2011) emphasize that dune vegetation changes are usually caused by a number of different factors that usually cannot be easily separated, and local or regional specific interactions between the different processes and feedback mechanisms suggest a complex scenario.

Climate is often regarded as the main factor for vegetation change in coastal (and desert) dune systems, mainly due to: rainfall variability (Marcomini and Maidana, 2006; Wolfe and Hugenholtz, 2009), changes in the wind patterns (Tsoar, 2005; Tsoar *et al.*, 2009; Levin, 2011) or a combination of both (Jones *et al.*, 2010; Martinho *et al.*, 2010; Miot da Silva *et al.*, 2013; Miot da Silva and Hesp, 2013; Jackson *et al.*, 2019b).

However, a number of other factors have been considered as drivers of coastal vegetation changes. Among them are: climatic factors linked to storm events, such as the degree of cyclonic activity (Levin, 2011) and intensity of storm wave activity (Hesp and Thom, 1990; Clemmensen and Murray, 2006; Clarke and Rendell, 2009); geological factors, such as sediment supply from the beach (Tastet and Pontee, 1998); ecological factors, such as deliberate and natural dispersion of exotic and invasive plants (Clemmensen and Murray, 2006; Hilton *et al.*, 2006; Hesp and Hilton, 2013), and grazing of native and exotic fauna (Ranwell, 1960; White, 1961; Harris and Davy, 1986); human-induced changes, such as alterations in land use (Gilbertson *et al.*, 1999; Tsoar and Blumberg,

2002; Kutiel *et al.*, 2004; Provoost *et al.*, 2011, Jackson and Nordstrom, 2019), or nitrogen deposition due to industrial and agricultural development and urbanization (Provoost *et al.*, 2011).

By analysis of historical aerial imagery, recent studies have revealed that in the past decades a number of coastal transgressive dunes, in different parts of the world, have undergone vegetation growth and stabilization due to various reasons (Tsoar and Blumberg, 2002; Kutiel *et al.*, 2004; Marcomini and Maidana, 2006; Jones *et al.*, 2010; Martinho *et al.*, 2010; Levin, 2011; Provoost *et al.*, 2011; Miot da Silva *et al.*, 2013; Jackson *et al.*, 2019b). Although these studies have contributed to a better comprehension of the reasons behind this increase in coastal vegetation, the links between the driving factors and dunefield changes in coastal or desert dunefields are still far from being completely understood (Provoost *et al.*, 2011; Barchyn and Hugenholtz, 2012).

1.3.3. Historical geomorphological changes in large-scale coastal transgressive dunefields due to vegetation changes

The geomorphological implications of vegetation changes in coastal dunefields have been verified by several studies (Tsoar and Blumberg, 2002; Kutiel *et al.*, 2004; Dúran and Herrmann, 2006; Marcomini and Maidana, 2006; Jones *et al.*, 2010; Martinho *et al.*, 2010; Levin, 2011; Miot da Silva *et al.*, 2013; Yizhaq, 2013; Hesp and Martinez, 2007; Fernandez *et al.*, 2017; Hesp and Smyth, 2019). However, few of these studies investigate the medium-term (meso-scale) changes of transgressive dunefields (Pickart and Hesp, 2019), and therefore little is known about the evolutionary paths that these dune systems take (Hesp, 2013).

Within the evolutionary stages of transgressive dunefields, phases of greater stabilization due to vegetation growth are very common (Hesp, 2013; Hernández-Cordero *et al.*, 2018; Jackson *et al.*, 2019a). In a stabilization phase, vegetation will tend to grow and fixate the different dune forms, until they reach an equilibrium with the sand deposition rate. That is unless something triggers another destabilization phase (which can happen at any evolutionary stage of the stabilization process) (Hesp, 2013). Phases of dune transgression and stabilization are usually well defined in the landscape by the evolutionary stage of vegetation and morphological aspects of the dunefield (Cooper, 1958; 1967; Orme and Tchakerian, 1986; Clemmensen *et al.*, 1996; 2001; 2006).

During the stabilization process, significant geomorphological alterations within the dune system can occur, with active mobile dunes (i.e., active transgressive dunes, transverse dunes, etc.) evolving into dune types that have their genesis linked to vegetation fixation (i.e., 'anchored' dunes), such as parabolic dunes, blowouts, trailing ridges, for example (Tsoar and Blumberg, 2002; Kutiel *et al.*, 2004; Marcomini and Maidana, 2006; Jones *et al.*, 2010; Martinho *et al.*, 2010; Levin, 2011; Miot da Silva *et al.*, 2013; Yizhaq, 2013; Hesp and Martinez, 2007; Fernandez *et al.*, 2017; Hesp and Smyth, 2019; Pickart and Hesp, 2019). However, very little is known in terms of how these transformations proceed, and the relationship between vegetation cover and morphological changes at a decadal time scale (Pickart and Hesp, 2019).

Hesp (2013) presented one of the few conceptual models for coastal transgressive dunefield meso-scale evolution. This model consists of three main scenarios of development and evolutionary paths of transgressive dunefields: (1) direct development from the backshore; (2) development because of foredune

and/or dunefield erosion; and (3) development from parabolic dunes. For each of these scenarios, Hesp presents different evolutionary pathways, with special emphasis on the role of vegetation in the evolutionary process. However, in deriving these conceptual models, Hesp (2013) noted the critical need for further empirical investigations.

1.3.4. Surfzone-beach-dune models and the controls of foredune evolution

Empirical and conceptual models have tried to explain interactions between the surfzone, beach, and dunes in order to understand wave and aeolian driven sediment transport dynamics and foredune and dunefield formation and evolution. Examples include Hesp (1982), Short and Hesp, (1982), Psuty (1988, 1992), Sherman and Bauer (1993), Hesp and Smyth (2016). Several studies have subsequently attempted to either summarise these models to various degrees or analyse individual driving factors of foredune evolution related to these models (Hesp, 1988; Sherman and Lyons, 1994; Aagaard, *et al.*, 2004; Psuty, 2008; Bauer *et al.*, 2009; Houser, 2009; Davidson-Arnott, 2010; Hesp, 2012; Aagaard *et al.*, 2013; Hesp and Smyth, 2016).

According to these studies, the most relevant controlling factors of the long-term evolution of foredunes are: (1) Differences in wind flow due to variations in intertidal/subaerial beach morphologies (Hesp, 1982; Short and Hesp, 1982; Sherman and Lyons, 1994; Namikas and Sherman, 1997; Hesp and Smyth, 2016); (2) Beach width affecting sand moisture and wind fetch (Short and Hesp, 1982; Davidson-Arnott and Law, 1996; Bauer and Davidson-Arnott, 2003; Davidson-Arnott *et al.*, 2005; Bauer *et al.*, 2009; Houser and Hamilton, 2009; Houser and Mathew, 2011; Silva *et al.*, 2019); (3) The degree of topographic

variation of a beach over time, termed beach mobility (Short and Hesp, 1982; Short, 1988; Battiau-Queney *et al.*, 2003; Hesp and Smyth, 2016); and (4) Sediment supply and erosion by wave energy (Short and Hesp, 1982; Short, 1988; Psuty, 1988; Aagaard *et al.*, 2004; Miot da Silva *et al.*, 2012; Dillenburg *et al.*, 2016; Cohn *et al.*, 2018; 2019a). All these factors are directly and indirectly linked to the surfzone-beach modal state (Dissipative, Reflective or Intermediate states), as shown in the surfzone-beach-dune model of Short and Hesp (1982).

Despite many efforts, the role and degree of importance of each factor driving the dune-building process is still debatable and this is primarily due to the fact that in nature these factors cannot be easily separated (Bauer *et al.*, 2009).

In the following chapters, these meso-scale problems of coastal dune evolution and functioning are examined.

Chapter 2 - Changes in vegetation cover on the Youngusband Peninsula transgressive dunefields (Australia) 1949 – 2017

Martim A.B. Moulton ^{1,4},
Patrick A. Hesp¹,
Graziela Miot da Silva¹,
Camille Bouchez²,
Muriel Lavy³,
Guilherme B. Fernandez⁴.

¹ Beach and Dune Systems (BEADS) Laboratory, College of Science and Engineering, Flinders University, Adelaide, Australia.

³ National Centre for Groundwater Research and Training, College of Science and Engineering, Flinders University, Adelaide, Australia.

³ Polytechnic University of Turin, DIATI - Department of Environmental, Transport and Infrastructure Engineering, Turin, Italy.

⁴ Department of Geography, Universidade Federal Fluminense, Niterói, Brazil.

Published in *Earth Surface Processes and Landforms* Journal: Moulton, M., Hesp, P.A., Miot da Silva, G., Bouchez, C., Lavy, M., Fernandez, G. B. 2018. Changes in vegetation cover on the Youngusband Peninsula transgressive dunefields (Australia) 1949–2017. *Earth Surface Processes and Landforms*, 44: 459– 470. <https://doi.org/10.1002/esp.4508>. License Number: 4791590161275.

2.1. Abstract

Studies have shown that the impact of climate change, human and animal actions on coastal vegetation can turn stabilized dunes into active mobile dunes and vice versa. Yet, the driving factors that trigger vegetation changes in coastal dunes are still not fully understood. In the transgressive dunefields of the Youngusband Peninsula (south-east coast of South Australia) historical aerial photographs show an increase in vegetation cover over the last ~70years. This study attempts to identify the causes of the changes in vegetation cover (1949 to 2017) observed in a typical section of the coastal dune systems of the Peninsula. Vegetation cover was first estimated for various years using the available historical aerial photography (long-term changes – 1949 to 2017) and recent

satellite imagery (short-term annual changes – 2010 to 2017) for the area, and then results were discussed against the observed changes in climatic variables and rabbit density, factors that could have played a role in this transformation. Results of long-term changes show that the vegetation cover has increased significantly from 1949 to 2017, from less than 7% vegetation cover to almost 40%, increasing dune stabilization and forming parabolic dune systems. Periods with the largest growth in vegetation cover (1952-1956 and 2009-2013) coincide with a significant decline in rabbit numbers. Rabbit density was found to be the primary factor linked to the rapid vegetation growth and stabilization of the dunefield, for both decadal long-term (last 68years) and annual short-term changes (last 8years). Other factors such as changes in rainfall, aeolian sediment transport, land use practices, and the introduction of invasive plants have apparently played a limited to negligible role in this stabilization process.

Key words: coastal dunes, vegetation change, coastal vegetation, rabbits, climate variability.

2.2. Introduction

Transgressive dunefields are extensive coastal aeolian sand deposits that have or had a history of migration (transverse, oblique or alongshore, depending of the prevailing winds) over time, often exhibiting a range of simple to complex landforms and one to multiple phases of development (Hesp and Thom, 1990; Hesp *et al.*, 2011; Hesp and Walker, 2013). The stabilization of transgressive dunefields is dependent on the competition between aeolian sand transport and vegetation growth (Durán and Herrmann, 2006; Arens *et al.*, 2013; Hesp, 2013; Hesp and Hilton, 2013). These dunefields can switch from an active and largely unvegetated state to a stabilized and predominantly vegetated state, and vice versa (Hugenholtz and Wolfe, 2005; Yizhaq *et al.*, 2007, 2009; Hesp, 2013).

The colonization and growth rate of dune vegetation not only affects the rate of landward migration of individual dunes and transgressive dunefields but

also their morphology (Hesp *et al.*, 2011; Hesp, 2013). Since vegetation is the main, and commonly the only stabilizing agent of coastal dune systems (Hesp and Thom, 1990; Durán and Herrmann, 2006), investigating the mechanisms that trigger changes in vegetation cover is essential to provide a better understanding of how dune systems transition from an active to a stable state, and potentially produce useful information for future coastal management.

Climate is often regarded as the main factor for vegetation change in coastal (and desert) dune systems, mainly due to; rainfall variability (Marcomini and Maidana, 2006; Wolfe and Hugenholtz, 2009), changes in the wind patterns (Tsoar, 2005; Tsoar *et al.*, 2009; Levin, 2011) or a combination of both (Jones *et al.*, 2010; Martinho *et al.*, 2010; Miot da Silva *et al.*, 2013; Miot da Silva and Hesp, 2013). However, a number of other factors have been considered as drivers coastal vegetation changes. Among them; climatic factors linked to storm events, such as the degree of cyclonic activity (Levin, 2011) and intensity of storm waves (Hesp and Thom, 1990; Clemmensen and Murray, 2006; Clarke and Rendell, 2009); geological factors, such as sediment supply from the beach (Tastet and Pontee, 1998); ecological factors, such as deliberate and natural dispersion of exotic and invasive plants (Clemmensen and Murray, 2006; Hilton *et al.*, 2006; Hesp and Hilton, 2013), and grazing of native and exotic fauna (Ranwell, 1960; White, 1961; Harris and Davy, 1986); human-induced changes, such as alterations in land use (Gilbertson *et al.*, 1999; Tsoar and Blumberg, 2002; Kutiel *et al.*, 2004; Provoost *et al.*, 2011), or nitrogen deposition due to agricultural development and urbanization (Provoost *et al.*, 2011).

However, Provoost *et al.* (2011) emphasizes that vegetation changes in dunes are usually caused by a number of different factors that usually cannot be

easily separated, and local or regional specific interactions between the different processes and feedback mechanisms suggest a complex scenario.

Using historical aerial imagery, recent studies have revealed that in the past decades a number of coastal transgressive dunes, in different parts of the world, have undergone vegetation growth and stabilization due to various reasons (Tsoar and Blumberg, 2002; Kutiel *et al.*, 2004; Marcomini and Maidana, 2006; Jones *et al.*, 2010; Martinho *et al.*, 2010; Levin, 2011; Provoost *et al.*, 2011; Miot da Silva *et al.*, 2013). Although these studies have contributed to a better comprehension of the reasons behind this increase in coastal vegetation, the links between the driving factors and dunefield changes in coastal or desert dunefields are still far from being completely understood (Provoost *et al.*, 2011; Barchyn and Hugenholtz, 2012).

Aerial photography and satellite imagery of transgressive dune systems along the South Australian (SA) coast reveal significant changes in vegetation cover, with an apparent increase in vegetation cover along the entire SA coast. In the transgressive dune systems of the Youngusband Peninsula (YP, Figure 2.1) this increase in vegetation cover in the last ~70years is very well marked, as shown in the difference between images from 1949 (the earliest aerial photographic record) and 2017 (Figure 2.2), especially in the central and northern section of the coastal barrier. Because of the long record of aerial photographs and the low human interference due to the isolation from the continent imposed by the Coorong Lagoons, the northern YP represents an ideal area for a case study (Figure 2.1).

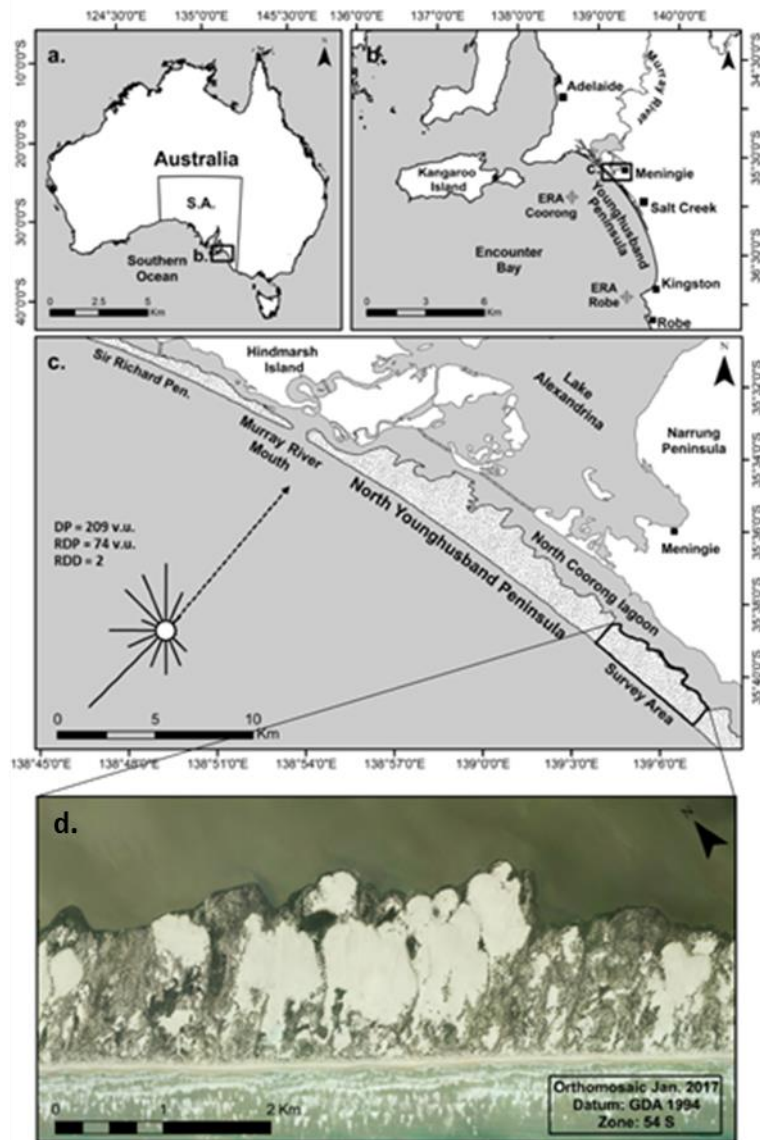


Figure 2.1 Map of the study site, showing the location of the Younghusband Peninsula (YP) in the south-east Coast of South Australia. The detailed image (c.) shows the northern section of the YP where most of the active transgressive dune system is situated and the sand rose indicates the resultant aeolian drift potential (Data from Robe weather station), (d.) shows in detail the survey area where most of the vegetation cover analysis was performed (image from 2017).

Hence, the objective of this study is to analyse the vegetation cover changes and the stabilization of the dunes that has taken place in the last ~70years in the northern Younghusband Peninsula transgressive dunefield system (south-east coast of South Australia, Figure 2.1) in order to better

understand the causes that drive these changes in this location, and potentially elsewhere along the South Australian Coast.

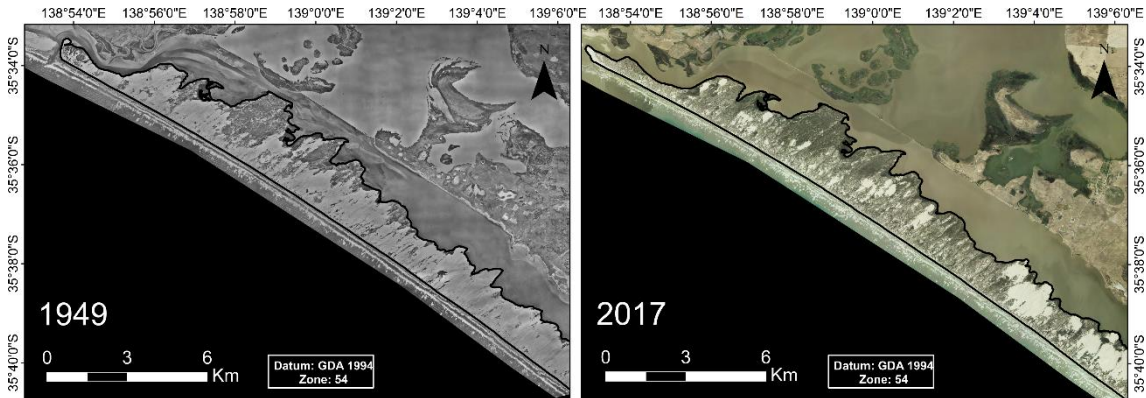


Figure 2.2 - Comparison of the vegetation cover between 1949 and 2017, the first and the latest aerial photographs for the northern section of the YP transgressive dunefield (black outlined area). The 2017 orthomosaic shows a significant decrease in sand area and increase in vegetation cover.

2.3. Study site

One of the longest continuous transgressive dune systems in Australia is situated on the Youngusband Peninsula (YP) (Figure 2.1). Located within the Coorong National Park, the dunes cover approximately 150 km² in extent, range from 1 to 2 km wide, and can reach up to 40m high in some areas (Short and Hesp, 1984). At the present time, active transgressive dunes are found only in the northern and central-northern parts of the Peninsula.

From the Murray mouth down to about 110 km south-east, the beach and dunes are separated from the continent by an extensive lagoon, the Coorong Lagoon. South of that, the lagoon starts to become intermittent and the YP is eventually connected to a Last Interglacial barrier (Harvey, 2006).

The climate of the region can be classified as warm-summer Mediterranean (Csb - Köppen classification), with high temperatures and low

rainfall averages during the summer, and more humid and lower temperatures during autumn and winter. A rainfall gradient is observed along the Peninsula, ranging from 468mm/yr at the north-western end (average for Meningie) and 586mm/yr in the south-eastern end (average for Kingston). The Peninsula is subjected to strong predominantly southwesterly winds, with gusts that can reach up to 18m/s (data from the Robe weather station – Australian Bureau of Meteorology), producing a net sand transport resultant from south-west to north-east (see sand rose in Figure 2.1c) and the migration of the dune system towards the lagoon and continent.

Data from different studies (Luebbers, 1981; Short and Hesp, 1984; Short, 1988; Bourman *et al.*, 2000; Harvey, 2006; Bourman *et al.*, 2006), suggest that the modern YP coastal barrier began to form ~ 6500 to 7000years ago, when sea-level stabilized at similar levels to present, after an extended period of post-glacial sea-level rise (Belperio *et al.*, 2002).

The YP dune field is a very dynamic system, and in its ~ 6500–7000years of existence, various phases of natural stabilization and destabilization or new transgressive dune field phases have occurred. The presence of palaeosols within the dunes suggests that the YP dune system has undergone several phases of stabilization although it remains unclear how many phases or episodes or when these occurred (Gilbertson, 1981; Short and Hesp, 1984; Harvey, 2006). Despite being protected and relatively isolated since they are separated from the mainland by an extensive lagoon, the dunefields have undergone moderate human pressure in the past (Paton, 2010). Pastoral activities and especially the introduction of invasive species of fauna and flora such as European rabbits

(*Oryctolagus cuniculus*), have changed the landscape of the YP and its dunefilled to various degrees (Hilton *et al.*, 2007; Mutze *et al.*, 2010; Paton, 2010).

A specific area of the northern part of the YP was chosen to investigate the vegetation changes of the Peninsula in the last ~70years (Figure 2.1d). This area was selected for two reasons; one, it is the section of the peninsula with the largest number of available historical aerial photographs, enabling the quantification of long-term changes in vegetation every ~7years on average, and, two, this section is representative of the entire transgressive dune system. The presence of largely active dunes in the first aerial photographs (1949), also means that historical pastoral activities were minimal (Hilton *et al.*, 2007; Paton, 2010), thus having less impact on the vegetation and landscape than in other areas of the dune system.

2.4. Methods

The methodology of this work consists of three parts: (1) quantification of the changes in vegetation cover; (2) analysis of climatic data; (3) analysis of rabbit density data.

2.4.1. Quantification of the changes in vegetation cover

To quantify the changes in coastal dune vegetation cover in the last ~70years, historical aerial photographs from the study area were obtained from the Department of Environment, Water and Natural Resources of South Australia (DEWNR). The photographs used in this study were selected taking into account their spatial resolution, the percent cloud cover, and the date in which they were taken (Table 2.1). Pixel resolution resampling was performed using the largest pixel size within the images (1967 – 1m pixel resolution), matching all images to

the same pixel resolution in order to reduce spatial errors in the classifications. Geometric corrections were made in each image to correct inherent distortions and to geo-reference them in a standard projection system. This process was performed using ArcGis 10.6 software, selecting the 2017 orthorectified image as the reference base map. In order to perform standard vegetation classification methods, all images were normalized to match the same number of bands, meaning that all 3band (RGB) images were transformed into 1 band (BandW) using the Grayscale function in ArcGis 10.6. The vegetation cover of the selected area was extracted for each dataset using two different methods of classification: Grayscale pixel-based classification (GPC), and a point-based grid sampling classification (PGSC).

Table 2.1 - Information regarding the aerial photographs selected for the long-term vegetation cover analysis.

Date	Original scale	Pixel resolution (m)
1949 (Apr.)	1:15,000	0.25
1956 (Sept.)	1:40,000	0.6
1967 (Sept.)	1:53,000	1.0
1975 (Apr.)	1:10,000	0.15
1984 (Mar.)	1:20,000	0.8
1995 (Apr.)	1:10,000	0.25
2000 (Jul.)	1:10,000	0.35
2008 (Mar.)	1:10,000	0.3
2013 (Jan.)	1:10,000	0.5
2017 (Jan.)	1:10,000	0.4

To quantify the annual vegetation changes in the same study area in the last 8years (2010–2017), Rapid-Eye (5m pixel resolution) satellite imagery were obtained from Planet Team (2017). Satellite images were chosen consistently from late December of each of the 8years so that the survey interval was

approximately 12 months apart from each other, in order to minimize possible effects of seasonal variations in plant growth. Both the GPC and the PGSC methods were performed after all images were transformed into 1 band. Rapid-Eye images were treated to the same standard geometric and radiometric corrections by the provider (Planet Team, 2017).

2.4.1.1. Grayscale pixel-based classification

The Grayscale pixel-based classification (GPC) was performed using the Image Classification tool in ArcGis 10.6 software, via an iso-cluster unsupervised classification method. This type of classification combines the iso-cluster method with the maximum likelihood classification algorithm, enabling a classification based on the distribution of the pixel values (Atkinson and Lewis, 2000).

The pixels from grayscale images vary from black (0 = black) to white, (255 = white). By knowing the distribution of the pixel values that cover a certain type of feature, the classes are then determined automatically by the classification technique according to the number of classes defined by the user. In this study, two classes were defined, bare sand and vegetated surface. The high contrast between sand (bright pixels) and vegetation (dark pixels) in the grayscale images collected over coastal dunes facilitates the classification process which returns a satisfying delineation of the vegetated area.

Manual corrections, such as exclusion of shaded areas misclassified as vegetation were performed in order to better represent the real extent of vegetation cover and reduce potential uncertainties related to shadows on the original aerial images (Fensham and Fairfax, 2002).

2.4.1.2. Point-based grid sampling classification

The point-based grid sampling manual classification method (PGSC) consists of classifying the land cover using a defined grid of sample points for the area (Fensham and Fairfax, 2002). For this study, a grid of labelled points was utilized, and created in ArcGis 10.6 to remotely assign the class to each point by visualizing the correspondent features within the digitized aerial photography. A grid of 965 sample points regularly distributed every 100m was created for the study area. The classification was done visualizing individually each mosaic in a proper scale (1:1000), enabling classification of features with precision. The class of bare sand or vegetation was associated to each point in order to evaluate the vegetation cover percentages over the total sample grid. This simple manual classification is proven to be one of the most precise methods of remotely assessing vegetation change, since it overcomes the problems inherent to pixel automated classifications, such as inconsistent boundary delimitation and shaded areas mistakenly classified as vegetation (Fensham and Fairfax, 2002).

2.4.2. Analysis of climate data

Climate data series were obtained from the Australian Bureau of Meteorology. Measurements of monthly rainfall from as early as 1864 were obtained from the Meningie Meteorological Station (20 km south-east from the study area – location of Meningie in Figure 2.1b), providing a monthly long-term record of rainfall for the study area.

Hourly measurements of wind speed and wind direction from 1957 to 2017 were obtained from Robe Meteorological Station, located 180 km south of the study area (Figure 2.1c).

Reanalysis wind data (ERA-Interim), available between 1979 and 2017, of the closest grid-point to the study area (location of the centre of the grid in Figure 1b), and of the closest grid-point to the Robe station (location of the centre of the grid in Figure 2.1b), were obtained in order to evaluate the bias linked to the use of climatic data 180 km away from our study area. Wind speed monthly reanalysis data at Robe and in the YP are strongly correlated (Pearson correlation coefficient (PCC): $r = 0.856$; $n = 20454$) showing that the wind regime at Robe and at the study site are very similar. This validates the use of data from the Robe Weather Station for this study.

Annual estimates of aeolian drift potential (DP) were calculated using the “Fryberger Method” (Fryberger and Dean, 1979), based on Robe Weather Station wind data and mean grain size determined from sediment samples collected in the study area (following the methods described in Miot da Silva *et al.*, 2013).

2.4.3. Analysis of rabbit density data

This study uses long-term rabbit density estimates from Saunders *et al.* (2010), Mutze *et al.* (2014a) and Cox (unpublished) to investigate the impact of this invasive herbivore on vegetation cover within the study area.

Data from Saunders *et al.* (2010) provide the only available long-term rabbit density estimates for South Australia (1927– 2010), covering the entire period analysed in this study. Rabbit numbers have been measured at Witchitie, in the Flinders Ranges, which is 390 km north-west from our study site. This dataset provides important information regarding long-term variation of rabbit numbers and the effects of bio-control measures. Absolute numbers of rabbits are expected to be different between the Witchietie site and the YP because of

distinct climatic and environmental conditions. However, the observed rabbit density variations in Witchietie are likely to be representative of variations in our study as bio-control measures were implemented all over South Australia at approximately the same time. This dataset is therefore used later to discuss vegetation cover changes over the last ~70year (long-term changes).

Mutze *et al.* (2014a) and Cox (unpublished) provide the closest rabbit measurements to our study site (60 km south-east from our study site). The two datasets were collected in locations very proximate to each other in Salt Creek, however at different time periods, 1992–2014 for Mutze *et al.* (2014a) and 2011–2017 for Cox (unpublished). Missing years of the dataset provided by Mutze *et al.* (2014a) (from 2015 to 2017), were filled in using the dataset provided by Cox (unpublished) using the linear regression between the two datasets calculated from the overlapping period ($r^2 = 0.97$). This dataset is used later to discuss vegetation cover changes over the last 8years (recent annual short-term changes).

All rabbit datasets were standardized to rabbits per ha² (rabbit density) using the conversion formulas suggested by Mutze *et al.* (2014b).

2.5. Historical vegetation changes

2.5.1. Long-term changes (1949-2017)

The estimated vegetation cover from the GPC and PGSC classification methods were shown to be consistent, as both show an overall increase in vegetation cover through the years, with differences between the two methods being below 4% (Figure 2.3).

In general, the GPC method indicated smaller values of percentage vegetation cover than the PGSC method (see Supplementary Material (SM) Table SM-01). It is possible that the GPC method underestimated the percentage of vegetation cover due to the low threshold value given to the vegetation class in order to avoid shaded areas from being classified as vegetation. On the other hand, an overestimation of the vegetation cover determined by the PGSC method due to the random predisposition of analysed points within the sampling grid could have possibly occurred. For this reason, the averaged vegetation cover percentage of results from the two classifications was used as the best estimate of vegetation cover (Figure 2.3). Results show a net increase in the vegetation cover from ~7% to ~39% in the period 1949 to 2017 (Figure 2.3), corresponding to an average growth of 0.5% per year over 70years.

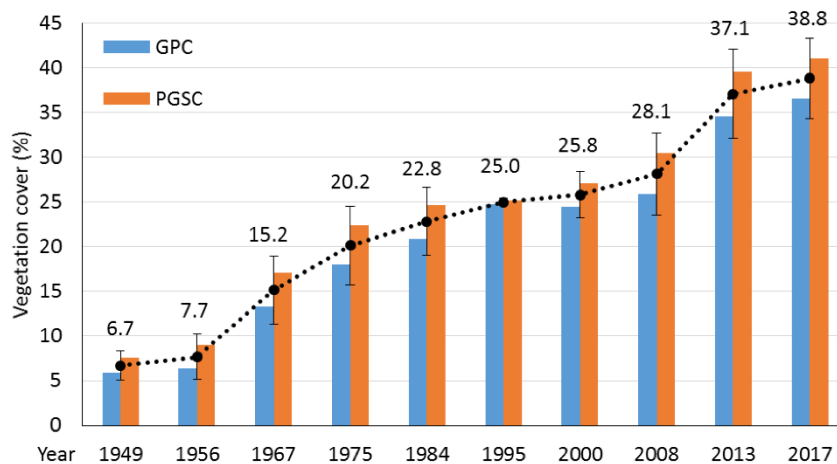


Figure 2.3 - Long-term (68 years) changes in vegetation cover within the study area expressed in percentages. The blue columns represent the percentages obtained by the GPC method and the orange columns show the PGSC percentages. The calculated averages between the two classifications are represented by the numbers inside the bars and the dotted line, here used as an estimate for the vegetation cover for each year. The error bars show the difference between the two classification methods for each of the images.

Table 2.2 - Vegetation change between periods analysed (periods are based on the years of the available aerial photographs).

Time period	Absolute change (%)	Relative change (%)	Annual average vegetation change (%)
1949-1956	0.97	14.38	0.14
1956-1967	7.49	97.31	0.68
1967-1975	4.99	32.85	0.62
1975-1984	2.64	13.11	0.29
1984-1995	2.22	9.74	0.20
1995-2000	0.79	3.15	0.16
2000-2008	2.33	9.02	0.29
2008-2013	8.95	31.79	1.79
2013-2017	1.98	5.72	0.49

Annual average vegetation cover changes (Table 2.2), were calculated by using the difference between the vegetation cover (%) of a given aerial image and the one prior to it, divided by the number of years separating them. This value was used as the indicator of vegetation growth rate of each period.

Results of annual average vegetation cover change show two periods of low, gradual increase in vegetation cover (1949–1956 and 1995–2000) and two periods of higher increase in vegetation cover (1956–1967–1975 and 2008–2013) (Table 2.2 and Figure 2.3). The low increase in vegetation cover between 1949 and 1956 (+0.14% per year, Table 2.2) and subsequent abrupt increase between 1956 and 1967 and between 1967 and 1975 (+0.68 and +0.62 per year, Table 2.2), suggest that conditions changed significantly at some time between 1956 and 1967. The highest increase in vegetation cover, about 10%, occurred between 2008 and 2013 (+1.79% per year, Table 2.2, Figure 2.3).

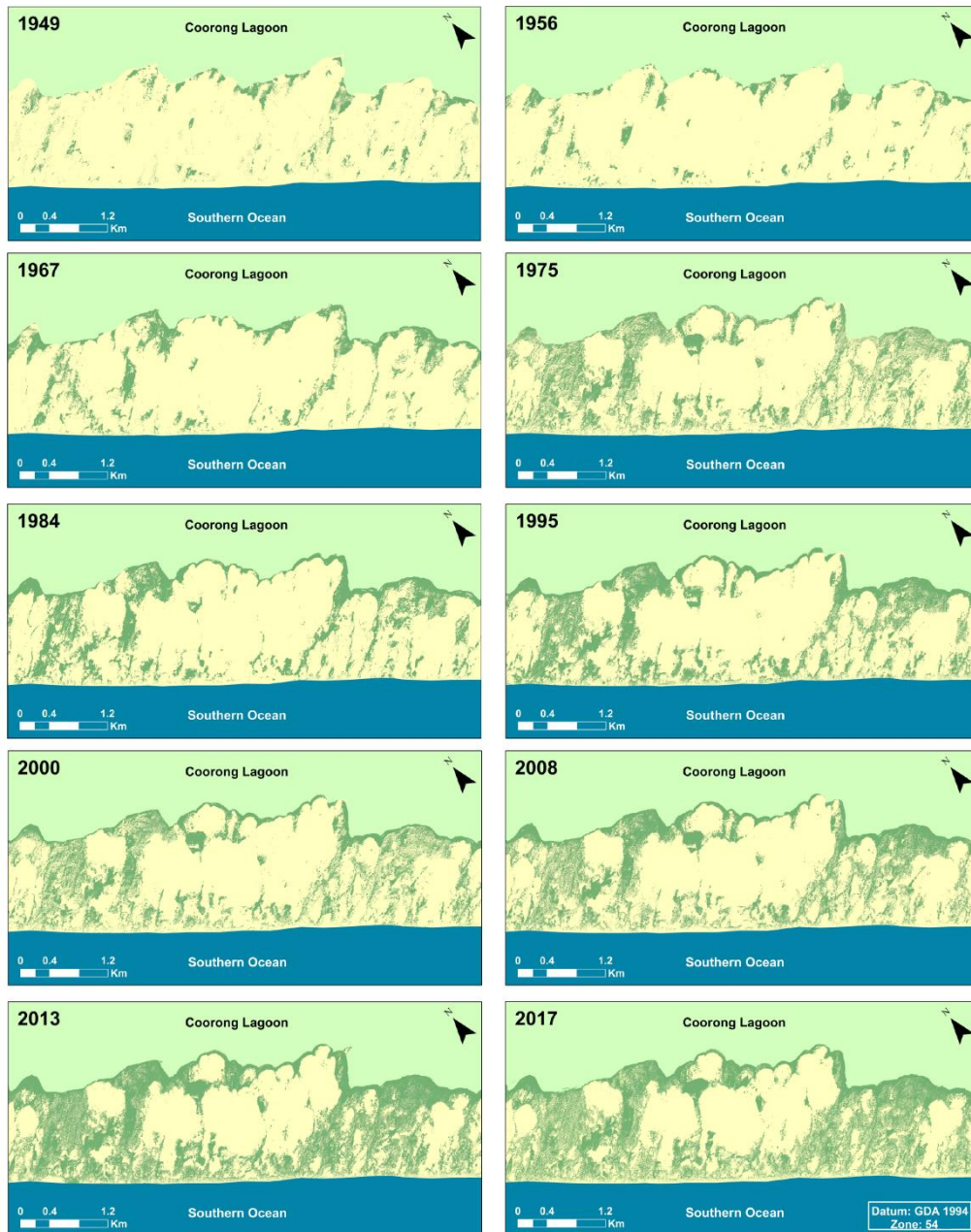


Figure 2.4 - Sequence of images utilising the results of Grayscale Pixel-based Classification (GPC) for the different years of aerial images available in the survey area. A trend of increasing vegetation cover occurs since the first aerial imagery was taken in 1949. The vegetation cover growth has led to the connection of the initially discrete patches of vegetation, and stabilization of a significant portion of the dune system, resulting in the development of parabolic dunes.

The long-term spatial dynamics of vegetation change between 1949 and 2017 are more easily observed when the GPC results are displayed in map form (Figure 2.4). In 1949, a very small percentage of the area was covered with

vegetation, and only small patches of vegetation were present on the landward margin of the dunefield between the lagoon and the transgressive dunes, and in isolated portions of the deflation plain. In contrast, the 2017 classification shows vegetation cover extending from the lagoonal margin across the dunefield to the seaward foredune (Figure 2.4).

A substantial change in the geographical distribution of the vegetation can be observed from 1967 onwards. The aerial photographic record shows vegetation beginning to form corridors along the lateral margins of the dunes and into the deflation plains (Figure 2.4), initiating a connection between the backshore/foredune and the lagoonal margin of the transgressive dunes.

The 1967 classification also shows an expansion of the vegetation on the lagoon margins, forming another corridor of vegetation in a NW-SE direction (Figure 2.4). In subsequent years, the vegetation continues to increase, and this occurs mainly with the expansion of these vegetation corridors, stabilizing most of the margins of the transgressive dunes. The deflation plains increase at the same rate as the vegetation expansion and only the higher and more active transgressive dunes are still unvegetated (Figure 2.4). These active dunes still constitute a large area of the north and central-north sections of the YP.

2.5.2. Short-term Recent Annual Changes (2010 to 2017)

To understand the nature of annual variations in vegetation cover, both the GPC and PGSC methods were using recent satellite imagery (2010–2017). The results of this short-term annual vegetation cover analysis also show an increasing trend in vegetation cover in recent years (Figure 2.5 and Table SM-02). Results obtained from the satellite imagery of December 2012 (5m resolution) were compared with results from the aerial photograph in January

2013 (1m resolution) to evaluate the bias linked to different image sources. Both GPC and PGSC methods showed higher vegetation cover for the 2012 satellite imagery (respectively 49% and 56% - Table SM-02), than the 2013 aerial photograph (respectively 35% and 40% - Table SM-01). However, when down sampling the pixel resolution of the 2013 aerial photograph to match the 5m resolution of the satellite image the vegetation cover increased to 44% for the GPC, and to 55% for the PGSC, almost matching the results obtained with the Rapid-Eye satellite image. Therefore, the disparities between the vegetation cover estimates can at first order be attributed to the difference in pixel resolution.

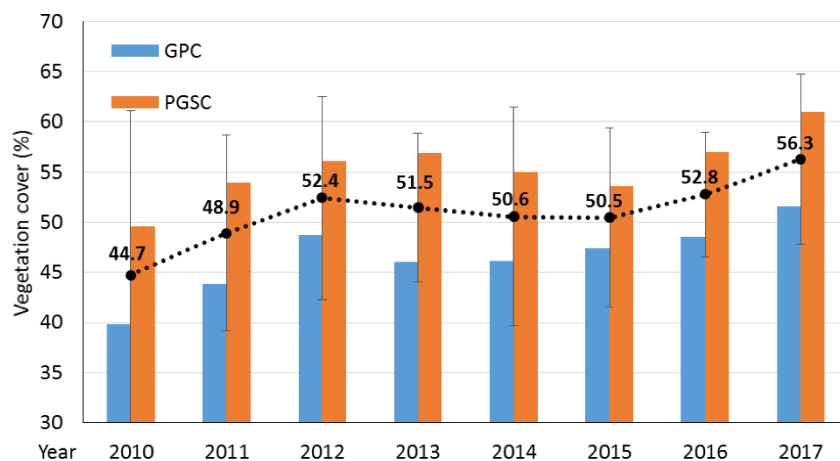


Figure 2.5 - Short-term (8 years) annual vegetation changes for 2010 to 2017.

An increasing trend in vegetation cover is observed. The error bars show the difference between the two classification methods (PGSC in orange and GPC in blue) for each of the images.

However, instead of downscaling all aerial photographs to 5m pixel resolution to match satellite images and therefore lose information, results of the two image sources were analysed independently from each other. Rapid-Eye images were used mainly to estimate annual dynamics of vegetation cover for the past 8 years, knowing that absolute vegetation cover estimates from this

dataset produces an overestimation and cannot be directly compared with the long-term dataset.

The short-term annual vegetation cover classification also shows an increasing trend, with a higher rate of vegetation growth between 2010 and 2012 (Figure 2.5). However, in this short-term analysis an annual variability in vegetation cover that is masked in the long-term classification by the larger interval between the images (~7years on average), can be observed. For instance, some years reveal a slight decrease in vegetation cover (e.g. 2013–2014) (Figure 2.5) that cannot be detected in the long-term analysis.

2.6. Potential driving factors of vegetation change

2.6.1. Long-term changes (1949-2017)

The variability of the driving factors that we consider as being the most probable predictors of changes in dune vegetation are here compared with the calculated vegetation cover changes determined for the study area in the past 68years. Available data regarding (1) rainfall, (2) wind (expressed as aeolian drift potential), and (3) presence of rabbits (expressed as rabbit density), are presented and compared with the vegetation growth observed within the nine periods defined by the dates of the available aerial photography (Figure 2.6).

For each variable, a Pearson correlation coefficient (PCC) was calculated between the vegetation cover (%) at the end of each period and the average of the variable of interest over the whole period. Therefore, PCC analyses were undertaken with nine observations, corresponding to the nine periods.

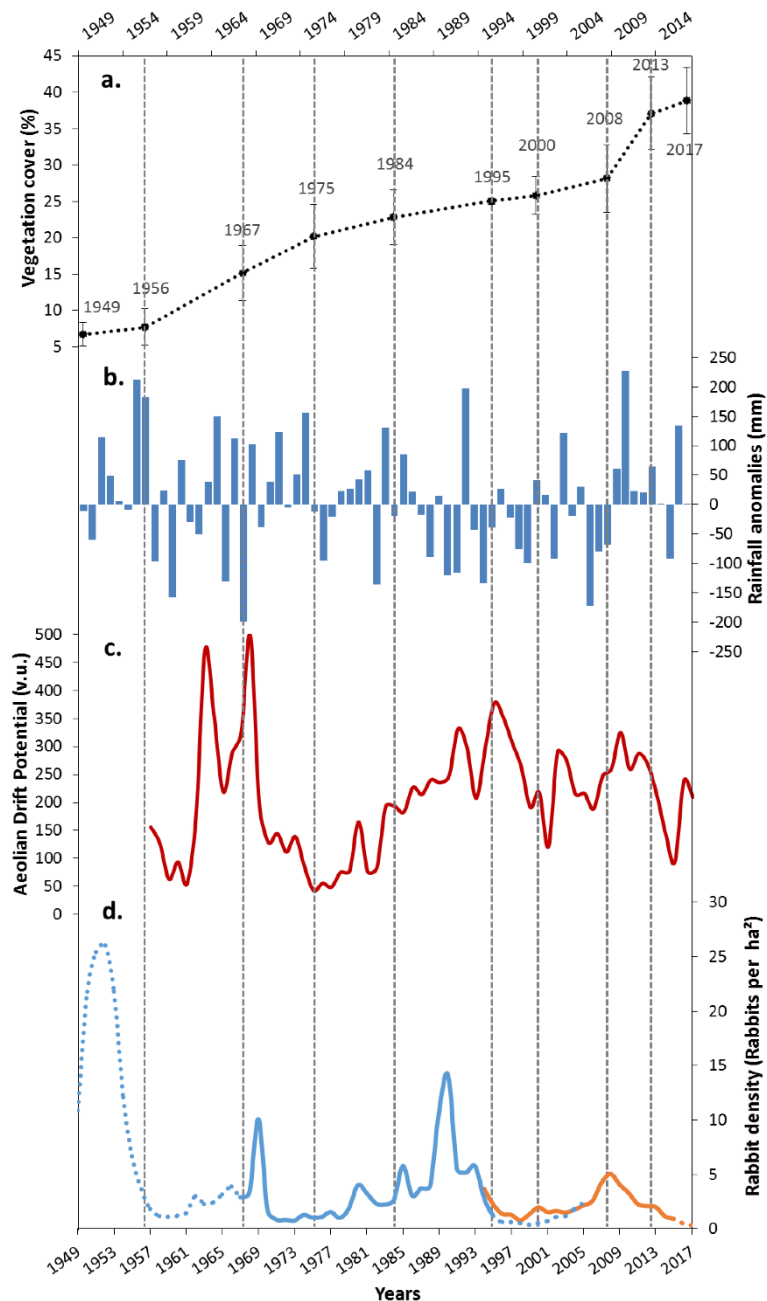


Figure 2.6 - (a) Vegetation cover estimates compared to (b) the variations in rainfall anomalies (Meningie weather station rainfall data; average annual rainfall is 469 mm), (c) Aeolian drift potential (calculated from Robe weather station wind data), and (d) rabbit density: data from Witchitie (Flinders Ranges - SA) in blue (Saunders et al. 2010) and data from Salt Creek (Coorong Region - SA), in orange (Mutze et al. 2014a), interpolated data are represented in the dotted lines. The vertical dashed lines separate the data in the periods determined by the year of each aerial photograph.

2.6.1.1. Rainfall

Results from the long-term vegetation cover classifications suggests that, if rainfall was a strong predictor of vegetation change, the overall trend of rainfall for the study area would increase over time. However, annual rainfall data from Meningie (153 years of record) shows a relatively stable long-term trend (Figure SM-1). In fact, a slight decline in annual rainfall can be seen in the last 5 decades (Figure 2.6b; Figure SM-1), consistent with the observed decline in autumn–winter rainfall in the past 5 decades in Southern Australia associated with the positive phase of the Southern Annular Mode (SAM) (Nicholls, 2010).

Despite the relatively stable rainfall pattern and slight decline in the past 5 decades, year to year variability in rainfall can be observed when the data are shown in terms of rainfall anomalies (above or below annual average rainfall) (Figure 2.6b). Over the last century (Figure SM-1) two periods of prolonged drought (1925-1944 and 1993–2008, correspond respectively to the ‘World War II drought’ and the ‘Millennium drought’) were followed by two periods of consecutive years of above-average rainfall (Figure 2.6b), 1945–1956 and 2009–2013. This pattern of above- average rainfall years following periods of prolonged droughts is common for South Australia, as noted by Verdon-Kidd and Kiem (2009).

The two periods of higher vegetation growth rate in the study area (see ‘average annual average vegetation change’ in Table 2.2) coincide with the two wet periods mentioned above (Figure 2.6b). In particular, during the last above average rainfall period (2009–2013), related to La Niña/ENSO events during two successive summers (2010–2011) that produced the wettest 24-month period in Australia since instrumented records began (Australian Bureau of Meteorology,

2017) and the wettest year in Meningie (2010 – 696.2mm), substantial vegetation growth was observed in the YP (Figure 2.6a).

Contrarily, the occurrence of the 'Big Dry' (~1997–2008) did not seem to have a large impact on the vegetation cover since a net increase in vegetation is observed within this period, rising from ~25% in 1995 to ~28% in 2008 (Table 2.2). However, the rate of change was particularly low, 0.16%/year between 1995 and 2000 and 0.29 %/year between 2000 and 2008 (Table 2.2).

The Pearson correlation coefficient (PCC) analysis carried out between the vegetation cover and average rainfall does not show a significant correlation ($r = -0.086$; $n = 9$; $P = 0.013$) (Tables SM-03 and SM-05), suggesting that averaged rainfall over several years is not a good predictor of the long-term vegetation changes observed.

However, vegetation dynamics seem to have some degree of relationship to rainfall, as wet events correlate with high vegetation growth periods. Moreover, effects of dry periods seem to be less significant, showing the resilience of coastal vegetation towards drought periods and a nonlinear response of vegetation to rainfall that cannot be seen by the use of PCC statistical analysis.

2.6.1.2. Wind

The wind regime determines the direction and rate of sediment transport on sand dunes (Pye and Tsoar, 1990), and therefore affects dune migration rates, amount of vegetation burial, and consequently vegetation cover in transgressive dunefields. Therefore, one might expect that an increase in vegetation cover in the study area could be associated with a decrease in the aeolian sediment transport (here indicated by drift potential, DP) over time (and vice versa).

DP calculations using the observed wind data at Robe show, however, a slight increase in potential aeolian transport between 1956 and 2017. Moreover, the DP variability shown in the data seems to contradict the common assumption that high DP (high sediment transport) limits the growth of vegetation by sand burial and/or surface deflation, and low DP values (low sediment transport) favours expansion of vegetation colonization processes (Tsoar, 2005). High DP values observed in the 1960s (Figure 2.6c) for instance, coincide with a period of significant increase in vegetation cover (Figure 2.6a), and, in the 1970s to early 1980s, low DP values (Figure 2.6c) occur during a period of low annual vegetation growth rate (Table 2.2).

The PCC between vegetation cover and the annual averaged DP did not yield significant results ($r = -0.274$; $n = 8$; $P = 0.511$) (see Tables SM-03 and SM-05), indicating that wind does not seem to be a first-order driver of vegetation change in the study area.

2.6.2.3. Rabbits

Exotic herbivores such as the European Rabbits (*Oryctolagus cuniculus* L.) are known to suppress native coastal vegetation, especially by suppressing the regeneration of native trees and shrubs (Bird *et al.*, 2012; Cooke, 2014; Mutze *et al.*, 2016). Rabbits suppress native vegetation at a much higher rate than native herbivores (e.g. kangaroos, wombats and emus), and can also enable the regeneration of certain species that are not impacted by grazing of native animals (Bird *et al.*, 2012). Introduced in Australia in 1788, rabbit numbers built to plague proportions by the early 1900s in much of Australia, including South Australia (Saunders *et al.*, 2010). Rabbit density calculations from Witchitie (390 km north

of the YP) indicates up to ~27 rabbits per hectare in the early 1950s in Witchitie (Saunders *et al.*, 2010) (Figure 2.6d).

In order to reduce the rabbit population a number of different measures were implemented by the Australian Government at various times including the introduction of viruses as biocontrol agents. Thus, Myxomatosis was introduced in South Australia and in the YP-Coroong region in 1952, the rabbit flea in 1968, and the Rabbit Haemorrhagic Disease Virus (RHD) in 1995.

The drastic drop in rabbit density observed in the long-term estimates for Witchitie (Figure 2.6d) in the beginning of the 1950s due to Myxomatosis coincides with the increase in vegetation cover between 1949 and 1967 (Figure 6a). Likewise, the increase in vegetation cover observed between 2008 and 2013 (Figure 2.6a) was followed by a decrease in rabbit density as shown in the data from Salt Creek.

The PCC analysis shows a statistically significant negative correlation between vegetation cover and the average rabbit density, for the periods between the aerial photographs using the long-term rabbit data from Witchitie ($r = -0.778$; $n = 7$; $P = 0.039$) (Tables SM-03 and SM-05). These results suggest that rabbit grazing plays a major role in the long-term dynamics of the dune vegetation.

2.6.2. Short-term Recent Annual Changes (2010 to 2017)

The annual vegetation cover changes observed on satellite images between 2010 and 2018 were also compared with data for the three main possible driving factors; rainfall; aeolian DP and rabbit density (Figure 2.7). In this short-term annual analysis, the observed increase in vegetation also coincides

with a decrease in the rabbit density at Salt Creek, while annual rainfall shows a steady trend (Figure 2.7).

Annual rainfall for the past 8 years shows a steady trend while annual vegetation cover increases, with some years even showing a negative relationship (e.g. 2010–2011), indicating that vegetation changes do not appear to be directly correlated to annual rainfall. However, it is important to note that annual rainfall within the entire 8 years analysed shows above average values for Meningie (only 2015 shows below average annual rainfall). The years of 2010 and 2016 for instance were well above average and could be also influencing the vegetation growth observed between 2010 and 2012 and 2015–2017.

Regarding wind sediment transport potential, the DP calculations show no indication of a direct negative relationship with vegetation cover, as the period of slight decrease in DP (2012–2015) corresponds to a slight decrease of vegetation, and the increase in DP in 2015–2016 coincides with an increase in vegetation cover for the same period (Figure 2.7).

The PCC analysis provides a strong negative correlation between vegetation cover and rabbit density ($r = -0.818$; $n = 8$; $P = 0.013$) and statistically insignificant correlations between vegetation cover and DP ($r = -0.167$; $n = 8$; $P = 0.693$), and rainfall ($r = -0.496$; $n = 8$; $P = 0.211$) (see Tables SM-04 and SM-06).

These results are in agreement with the findings of Cooke (1988) and Bird *et al.* (2012) who obtained significant correlations between the reduction of the rabbit population and the regeneration of spring germinating shrubs in the Coorong National Park.

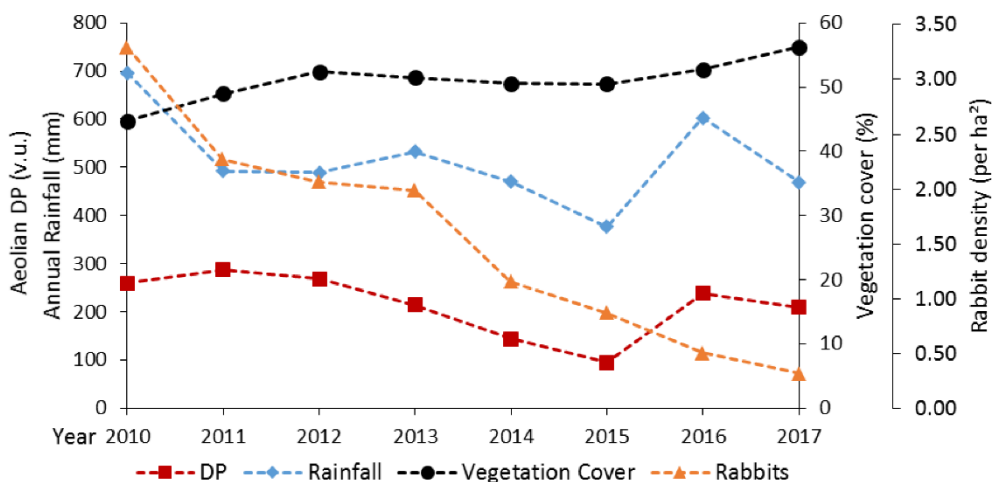


Figure 2.7 - Annual vegetation cover for the last 8 years (2010-2017) using satellite imagery compared to annual rainfall (Meningie Meteorological Station), aeolian drift potential (DP) (Robe Meteorological Station) and rabbit density (sources: Mutze et al., 2014; Cox, unpublished).

2.6.3. Other potential driving factors

Vegetation cover changes in the YP dunefields have been previously reported and attributed to different factors, such as grazing by domesticated animals; degradation by off-road vehicles; and invasion of exotic plants.

Sutton (1925) stated that the reduction of vegetation cover and dune mobility observed by land owners in the 1920s was the result of overgrazing by cattle in some locations of the YP dunefields. Even though the cessation of pastoral activities in the dunefields in the 1930s could have aided the vegetation regeneration, it is unlikely that this was the main cause of the observed changes in the past ~70years, especially in the study region which was dominated by active transgressive dunes. Moreover, McCourt and Mincham (1987) refuted Sutton's (1925) statement arguing that stock numbers were very limited on the peninsula and the more probable cause was the increase of the rabbit population (McCourt and Mincham, 1987).

In the 1970's, an increase in the numbers of off-road vehicles (ORV's) in the YP created serious concerns regarding their impact on the erosion and destabilization of the dunes (Welsh, 1975). Gilbertson (1977, 1981) concluded from aerial photography analysis that the rate of landward sand drift was significant and that the areas of greater dune migration coincided with the areas with the highest numbers of ORV tracks in the southern end of the peninsula. Since 1975, the use of ORVs within the dunes has been significantly reduced, mainly as a result of more strict regulations within the National Park (Gilbertson, 1981), and this could also have contributed to the observed increase in vegetation in the past 7 decades. However, the impact of ORVs was located mainly in the south of the YP. In addition, and as the results of this study proves, vegetation cover in the north of the Peninsula increased significantly between 1967 and 1975 when ORV use was also increasing in the Coorong National Park according to Gilbertson (1981).

Another factor that could have contributed to vegetation changes in the YP was the presence of exotic pioneer plants (Hilton *et al.*, 2007; James, 2012). Due to natural and deliberate introduction, exotic plants are present along the YP dune system. Sea-wheat grass (*Thinopyrum junceiforme*) in particular, has been proven to have impacted the stabilization of the dunes to some extent. Sea-wheat grass established almost along the entire YP coastline post-1978, causing significant displacement of *Spinifex* and possibly other native species, and changing the dunefield morphology by (i) forming significant incipient foredunes and ii) therefore restricting sediment movement inland on some sections of the coast leading to the stabilization of blowouts in foredunes (Hilton *et al.*, 2007; James, 2012; Levin *et al.*, 2017). Although Sea-wheat grass has likely contributed

to the observed changes in vegetation cover, the incipient foredune is a very minor part of the much larger dunefield examined in this study. In addition, Hilton *et al.* (2007) states that this grass was only found in the YP after the 1980s and therefore it could not have been the cause of the vegetation cover increase observed between 1949 and 1975, and it certainly has no presence in the larger transgressive dunefield, being restricted to the backshore-incipient foredune region.

The net increase in vegetation over the last ~70years could also be partially linked to more general factors, such as the natural growth of vegetation due to the hysteretic nature of vegetation growth once a trend towards increasing cover is established (Tsoar, 2005), an increase in photosynthetic productivity (Long, 1991) linked to rising CO₂ concentrations (Cape Grim Greenhouse Gas Data – CSIRO, 2018), and/or a slight increase in mean temperature in South Australia (~1°C increase in the last 5 decades) (Steffen and Hughes, 2011). At this time, we have no way to ascertain the degree of importance of these factors in the YP.

2.7. Conclusion

The Youngusband Peninsula transgressive dunefields have undergone major changes in vegetation cover and geomorphology over the last ~70years. Vegetation has increased significantly and with it, active transgressive dunes have been and are being stabilized and transformed into stabilized dunes and parabolic dunes in many areas.

Both decadal long-term and recent annual short-term data indicate that the principal factor driving this vegetation cover change is the decline in exotic rabbit

populations in the region. Periods of large decrease in rabbit numbers coincide with periods of higher vegetation increase, showing a significant negative correlation. In particular the drop in rabbit numbers in the 1950s, after the introduction of Myxomatosis, seems to have been a significant turning point for the growth and/or regeneration of dune vegetation.

However, variations in rabbit density alone does not explain the whole variance in vegetation cover observed. Wind power/sand transport appear to have had little effect on the vegetation changes observed, but large rainfall events might have contributed to the overall increase in vegetation cover. Moreover, data suggest that dune vegetation is not directly affected by extended dry periods, most likely due to the resilient nature of the coastal vegetation to arid conditions. The impact of the reduction of rabbit grazing on dunes vegetation is very clear in the northern YP, and therefore other dunefields across South Australia have possibly undergone similar changes, since all dunefields except those on Kangaroo Island were subjected to rabbit infestations.

Higher spatial and temporal resolution open source satellite data in the near future should aid higher precision analyses of the changes and the dynamics of vegetation cover within dune systems that will enable a better understanding of the causes behind this phenomenon.

2.8. Acknowledgements

MM and GBF thank the Department of Geography, Universidade Federal Fluminense, and Flinders University for scholarships and cotutelle support for MM's research. PH and GMdS thank the College of Science and Engineering, Flinders University for support. Grateful thanks to Robert Keane (Flinders

University) for GIS support, and also Brian Cooke (University of Canberra), Tarnya Cox (NSW Department of Primary Industries) and Greg Mutze (Department of Primary Industries and Regions SA) for their support in providing important data on rabbit densities.

2.9. References

Arens, S.M., Slings Q.L., Geelen, L.H., Van der Hagen, H.G. 2013. Restoration of dune mobility in the Netherlands. In: Restoration of Coastal Dunes. Martínez, L.M., Gallego-Fernández, J.B., Hesp, P.A. (eds.) Springer: Berlin; 107–124.

Atkinson, P.M., Lewis P. 2000. Geostatistical classification for remote sensing: an introduction. *Computers and Geosciences*, 26(4): 361–371. [https://doi.org/10.1016/S0098-3004\(99\)00117-X](https://doi.org/10.1016/S0098-3004(99)00117-X)

Australian Bureau of Meteorology. 2017. La Niña – Detailed Australian Analysis. Retrieved 23 January, 2017 from <http://www.bom.gov.au/climate/enso/Inlist/>

Barchyn, T.E., Hugenholtz, C.H. 2012. Aeolian dune field geomorphology modulates the stabilization rate imposed by climate. *Journal of Geophysical Research*, 117: (F02035). <https://doi.org/10.1029/2011JF002274>.

Belperio, A.P., Harvey, N., Bourman RP. 2002. Spatial and temporal variability in the Holocene sea-level record of the South Australian coastline. *Sedimentary Geology*, 150(1): 153–169. [https://doi.org/10.1016/S0037-0738\(01\)00273-1](https://doi.org/10.1016/S0037-0738(01)00273-1).

Bird, P., Mutze, G., Peacock D., Jennings S. 2012. Damage caused by low density exotic herbivore populations: the impact of introduced European rabbits on marsupial herbivores and *Allocasuarina* and *Bursaria* seedling survival in Australian coastal shrubland. *Biological Invasions*, 14(3): 743–755. <https://doi.org/10.1007/s10530-011-0114-8>.

Bourman, R.P., Murray-Wallace, C.V., Belperio, A.P., Harvey, N. 2000. Rapid coastal geomorphic change in the River Murray Estuary of Australia. *Marine Geology*, 170(1): 141–168 [https://doi.org/10.1016/S00253227\(00\)00071-2](https://doi.org/10.1016/S00253227(00)00071-2).

Bourman, R., Harvey, N., James, K.F. 2006. Evolution of the Youngusband Peninsula, South Australia: new evidence from the northern tip. *South Australian Geographical Journal*, 105: 37–50.

Cape Grim Greenhouse Gas Data – CSIRO. 2018. CSIRO Marine and Atmospheric Research and the Australian Bureau of Meteorology (Cape Grim Baseline Air Pollution Station). Retrieved from <http://capegrim.csiro.au/>

Clarke, M.L., Rendell, H.M. 2009. The impact of North Atlantic storminess on western European coasts: a review. *Quaternary International*, 195(1): 31–41. <https://doi.org/10.1016/j.quaint.2008.02.007>.

-
- Clemmensen, L.B., Murray, A. 2006. The termination of the last major phase of aeolian sand movement, coastal dunefields, Denmark. *Earth Surface Processes and Landforms*, 31(7): 795–808. <https://doi.org/10.1002/esp.1283>.
- Cooke, B.D. 1988. The effects of rabbit grazing on regeneration of sheoaks, *Allocasuarina verticillata* and saltwater ti-trees, *Melaleuca halmaturorum*, in the Coorong National Park, South Australia. *Australian Journal of Ecology*, 13(1): 11–20. <https://doi.org/10.1111/j.1442-9993.1988.tb01414.x>.
- Cooke, B.D. 2014. *Australia's War Against Rabbits: the Story of Rabbit Haemorrhagic Disease*. CSIRO Publishing: Collingwood, Victoria.
- Durán, O., Herrmann, H.J. 2006. Vegetation against dune mobility. *Physical Review Letters* 97(18): 188001. <https://doi.org/10.1103/PhysRevLett.97.188001>.
- Fensham, R.J., Fairfax, R.J. 2002. Aerial photography for assessing vegetation change: a review of applications and the relevance of findings for Australian vegetation history. *Australian Journal of Botany*, 50(4): 415–429. <https://doi.org/10.1071/BT01032>.
- Fryberger, S.G., Dean, G. 1979. Dune forms and wind regime. In: *A Study of Global Sand Seas*, McKee, E.D. (ed.), Vol. 1052; 137–169. U.S. Geological Survey Professional Paper.
- Gilbertson, D.D. 1977. The off-road use of vehicles and aspects of the bio-physical systems of the lower Coorong region. In: *The Southern Coorong and Lower Youngusband Peninsula of South Australia*, Gilbertson, D.D., Foale, M.R. (eds.). The Nature Conservation Society of South Australia: Adelaide, South Australia; 71–91.
- Gilbertson, D.D. 1981. The impact of past and present land use on a major coastal barrier system. *Applied Geography*, 1(2): 97–119. [https://doi.org/10.1016/0143-6228\(81\)90028-X](https://doi.org/10.1016/0143-6228(81)90028-X).
- Gilbertson, D.D., Schwenninger JL, Kemp RA, Rhodes EJ. 1999. Sand drift and soil formation along an exposed North Atlantic coastline: 14,000 years of diverse geomorphological, climatic and human impacts. *Journal of Archaeological Science* 26(4): 439–469. <https://doi.org/10.1006/jasc.1998.0360>.
- Harris, D., Davy, A. 1986. Strandline Colonization by *Elymus Farctus* in Relation to Sand Mobility and Rabbit Grazing. *The Journal of Ecology*, 74(4): 1045–1056. <https://doi.org/10.2307/2260232>.
- Harvey, N. 2006. Holocene coastal evolution: barriers, beach ridges, and tidal flats of South Australia. *Journal of Coastal Research*, 22(1): 90–99. <https://doi.org/10.2112/05A-0008.1>.
- Hesp, P.A. 2013. Conceptual models of the evolution of transgressive dunefield systems. *Geomorphology*, 199: 138–149. <https://doi.org/10.1016/j.geomorph.2013.05.014>.

-
- Hesp, P.A., Hilton, M.J. 2013. Restoration of foredunes and transgressive dunefields: case studies from New Zealand. In: Restoration of Coastal Dunes, Martínez, M.L., Gallego-Farnadez, J.B., Hesp, P.A. (eds.), Springer: Berlin/Heidelberg; 67–92 https://doi.org/10.1007/978-3-642-33445-0_5.
- Hesp, P.A., Martinez, M., Miot da Silva, G., Rodríguez-Revelo, N., Gutierrez, E., Humanes, A., Lainez D., Montano, I., Palacios, V., Quesada, A., Storero, L., Trilla, G.G., Trochine, C. 2011. Transgressive dunefield landforms and vegetation associations, Doña Juana, Veracruz, Mexico. *Earth Surface Processes and Landforms*, 36(3): 285–295. <https://doi.org/10.1002/esp.2035>.
- Hesp, P.A., Thom, B.G. 1990. Geomorphology and evolution of transgressive dunefields. In: Coastal Dunes: Processes and Morphology, Nordstrom, K., Psuty, N., Carter, R.W.G. (eds.). John Wiley & Sons: Chichester; 235–288.
- Hesp, P.A., Walker, I.J. 2013. Aeolian environments: coastal dunes. In: Treatise on Geomorphology, vol. 11, Aeolian Geomorphology, Shroder, J. (Editor in Chief), Lancaster, N., Sherman, D.J., Baas, A.C.W. (eds.), Academic Press: San Diego, CA; 109–133.
- Hilton, M., Harvey, N., Hart, A., James, K., Arbuckle, C. 2006. The impact of exotic dune grass species on foredune development in Australia and New Zealand: a case study of *Ammophila arenaria* and *Thinopyrum junceiforme*. *Australian Geographer*, 37(3): 313-334. <https://doi.org/10.1080/00049180600954765>.
- Hilton, M., Harvey, N., James, K.F. 2007. The impact and management of exotic dune grasses near the mouth of the Murray River, South Australia. *Australasian Journal of Environmental Management*, 14(4): 220–228. <https://doi.org/10.1080/14486563.2007.9725171>.
- Hugenholtz, C.H., Wolfe, S.A. 2005. Biogeomorphic model of dunefield activation and stabilization on the northern Great Plains. *Geomorphology*, 70(1-2): 53–70. <https://doi.org/10.1016/j.geomorph.2005.03.011>.
- James, K.F. 2012. Gaining new ground: *Thinopyrum junceiforme*, a model of success along the South Eastern Australian coastline. The University of Adelaide. Doctoral Thesis. 221 p.
- Jones, M.L.M., Sowerby A, Rhind PM. 2010. Factors affecting vegetation establishment and development in a sand dune chronosequence at Newborough Warren, North Wales. *Journal of Coastal Conservation*, 14(2): 127–137. <https://doi.org/10.1007/s11852-009-0071-x>.
- Kutielm P., Cohen, O., Shoshany, M., Shub, M. 2004. Vegetation establishment on the southern Israeli coastal sand dunes between the years 1965 and 1999. *Landscape and Urban Planning*, 67(1): 141–156. [https://doi.org/10.1016/S0169-2046\(03\)00035-5](https://doi.org/10.1016/S0169-2046(03)00035-5).

-
- Levin, N. 2011. Climate-driven changes in tropical cyclone intensity shape dune activity on Earth's largest sand island. *Geomorphology*, 125(1): 239–252. <https://doi.org/10.1016/j.geomorph.2010.09.021>.
- Levin, N., Jablon, P.E., Phinn, S., Collins, K. 2017. Coastal dune activity and foredune formation on Moreton Island, Australia, 1944–2015. *Aeolian Research*, 25: 107–121. <https://doi.org/10.1016/j.aeolia.2017.03.005>.
- Long, S.P. 1991. Modification of the response of photosynthetic productivity to rising temperature by atmospheric CO₂ concentrations: has its importance been underestimated? *Plant, Cell and Environment*, 14(8): 729–739. <https://doi.org/10.1111/j.1365-3040.1991.tb01439.x>.
- Luebbers, R.A. 1981. The Coorong Report: An Archaeological Survey of the Southern Youngusband Peninsula. Report for the South Australian Department of Environment and Planning.
- Marcomini, S.C., Maidana, N. 2006. Response of eolian ecosystems to minor climatic changes. *Journal of Coastal Research*, sp39: 204–208.
- Martinho, C.T., Hesp, P.A., Dillenburg, S.R. 2010. Morphological and temporal variations of transgressive dunefields of the northern and midlittoral Rio Grande do Sul coast, Southern Brazil. *Geomorphology*, 117(1): 14–32. <https://doi.org/10.1016/j.geomorph.2009.11.002>.
- Miot da Silva, G., Hesp, P.A. 2013. Increasing rainfall, decreasing winds, and historical changes in Santa Catarina dunefields, southern Brazil. *Earth Surface Processes and Landforms*, 38(9): 1036–1045. <https://doi.org/10.1002/esp.3390>.
- McCourt, T, Mincham H. 1987. The Coorong and lakes of the lower Murray (p. 205). Adelaide: Gillingham Printers.
- Miot da Silva G., Martinho, C.T., Hesp, P.A., Keim, B.D., Ferligoj, Y. 2013. Changes in dunefield geomorphology and vegetation cover as a response to local and regional climate variations. *Journal of Coastal Research*, 65(sp2): 1307–1312. <https://doi.org/10.2112/SI65-221.1>.
- Mutze, G., Bird, P., Jennings, S., Peacock, D., de Preu N., Kovaliski, J., Cooke B, Capucci, L. 2014a. Recovery of South Australian rabbit populations from the impact of rabbit haemorrhagic disease. *Wildlife Research*, 41(7): 552–559. <https://doi.org/10.1071/WR14107>.
- Mutze, G., Cooke, B., Jennings, S. 2016. Estimating density-dependent impacts of European rabbits on Australian tree and shrub populations. *Australian Journal of Botany*, 64(2): 142–152. <https://doi.org/10.1071/BT15208>.
- Mutze, G., Cooke, B., Lethbridge, M., Jennings, S. 2014b. A rapid survey method for estimating population density of European rabbits living in native vegetation. *The Rangeland Journal*, 36(3): 239–247. <https://doi.org/10.1071/RJ13117>.
- Mutze, G., Kovaliski, J., Butler, K., Capucci, L., McPhee, S. 2010. The effect of rabbit population control programmes on the impact of rabbit haemorrhagic

disease in south-eastern Australia. *Journal of Applied Ecology*, 47(5): 1137–1146. <https://doi.org/10.1111/j.13652664.2010.01844.x>.

Nicholls, N. 2010. Local and remote causes of the southern Australian autumn-winter rainfall decline, 1958–2007. *Climate Dynamics*, 34(6): 835–845. <https://doi.org/10.1007/s00382-009-0527-6>.

Paton, D.C. 2010. *At the end of the River: the Coorong and Lower Lakes*. David. ATF Press: Adelaide <https://doi.org/10.1071/PC110290>.

Provoost, S., Jones, M.L.M., Edmondson, S.E. 2011. Changes in landscape and vegetation of coastal dunes in northwest Europe: a review. *Journal of Coastal Conservation*, 15(1): 207–226. <https://doi.org/10.1007/s11852-009-0068-5>.

Pye, K., Tsoar, H. 1990. *Aeolian Sands and Sand Dunes*. Unwin Hyman: London.

Ranwell, D.S. 1960. Newborough Warren, Anglesey: III. Changes in the vegetation on parts of the dune system after the loss of rabbits by myxomatosis. *The Journal of Ecology*, 48(2): 385–395. <https://doi.org/10.2307/2257524>.

Saunders, G., Cooke, B., McColl, K., Shine, R., Peacock, T. 2010. Modern approaches for the biological control of vertebrate pests: an Australian perspective. *Biological Control*, 52(3): 288–295. <https://doi.org/10.1016/j.biocontrol.2009.06.014>.

Short, A.D. 1988. Holocene coastal dune formation in southern Australia: a case study. *Sedimentary Geology*, 55(1-2): 121–142. [https://doi.org/10.1016/0037-0738\(88\)90093-0](https://doi.org/10.1016/0037-0738(88)90093-0).

Short, A.D., Hesp, P. 1984. Beach and dune morphodynamics of the South East Coast of South Australia. Coastal Studies Unit Technical Report 84/1, Department of Geography, The University of Sydney.

Steffen, W., Hughes, L. 2011. *The critical decade: South Australian impacts* (Report). ACT Climate Commission Secretariat: Canberra Retrieved from <https://climatecommission.angrygoats.net/report/the-critical-decade-south-australian-impacts/>.

Sutton, J. 1925. A trip to the Coorong. *South Australian Ornithologist*, 8(3): 75–95.

Tastet, J.P., Pontee, N.I. 1998. Morpho-chronology of coastal dunes in Médoc. A new interpretation of Holocene dunes in Southwestern France. *Geomorphology*, 25(1–2): 93–109. [https://doi.org/10.1016/S0169-555X\(98\)00035-X](https://doi.org/10.1016/S0169-555X(98)00035-X).

Team, P. 2017. Planet Application Program Interface. In: *Space for Life on Earth*: San Francisco, California <https://api.planet.com>.

Tsoar, H. 2005. Sand dunes mobility and stability in relation to climate. *Physica A: Statistical Mechanics and its Applications*, 357(1): 50–56. <https://doi.org/10.1016/j.physa.2005.05.067>.

-
- Tsoar, H., Blumberg, D.A.N. 2002. Formation of parabolic dunes from barchan and transverse dunes along Israel's Mediterranean coast. *Earth Surface Processes and Landforms*, 27(11): 1147–1161. <https://doi.org/10.1002/esp.417>.
- Tsoar, H., Levin, N., Porat, N., Maia, L.P., Herrmann, H.J., Tatumi, S.H., Claudino Sales, V. 2009. The effect of climate change on the mobility and stability of coastal sand dunes in Ceará State (NE Brazil). *Quaternary Research*, 71(2): 217–226. <https://doi.org/10.1016/j.yqres.2008.12.001>.
- Verdon-Kidd, D.C., Kiem, A.S. 2009. Nature and causes of protracted droughts in southeast Australia: comparison between the Federation, WWII, and Big Dry droughts. *Geophysical Research Letters*, 36(22): L22707. <https://doi.org/10.1029/2009GL041067>.
- Welsh, A. 1975. Report of Off-Road-Recreational-Vehicles. South Australian Department of Environment and Conservation, Environment Division, SADEC 3, Adelaide.
- White, D.J.B. 1961. Some observations on the vegetation of Blakeney Point, Norfolk, following the disappearance of the rabbits in 1954. *Journal of Ecology*, 49(1): 113–118. <https://doi.org/10.2307/2257428>.
- Wolfe, S.A., Hugenholtz, C.H. 2009. Barchan dunes stabilized under recent climate warming on the northern Great Plains. *Geology*, 37(11): 1039–1042. <https://doi.org/10.1130/G30334A.1>.
- Yizhaq, H., Ashkenazy, Y., Tsoar, H. 2007. Why do active and stabilized dunes coexist under the same climatic conditions? *Physical Review Letters*, 98(18): 188001. <https://doi.org/10.1103/PhysRevLett.98.188001>.
- Yizhaq, H., Ashkenazy, Y., Tsoar, H. 2009. Sand dune dynamics and climate change: a modeling approach. *Journal of Geophysical Research*, 114 (F01023). <https://doi.org/10.1029/2008JF001138>.

2.10. Supplementary materials

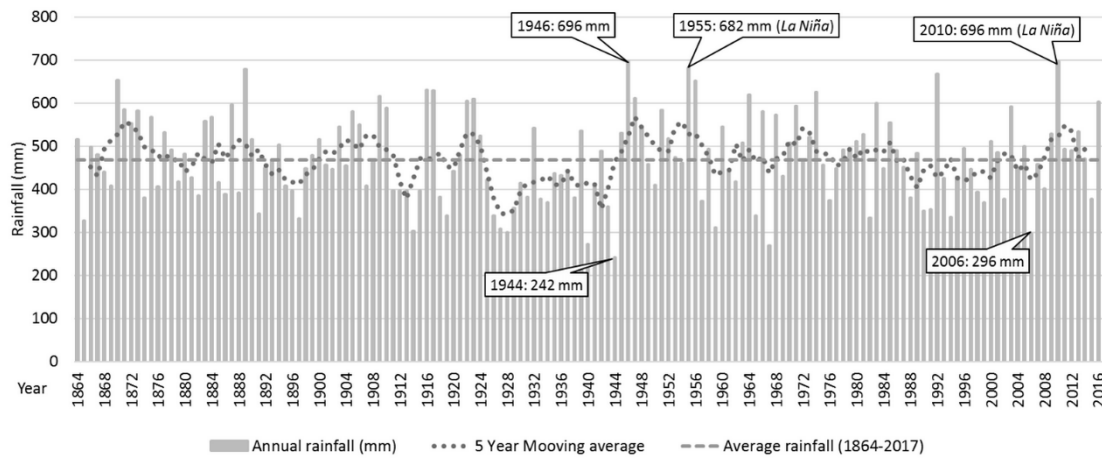


Figure SM-8 - Historical annual rainfall record for Meningie (1864-2017), showing rainfall before and during the studied period. The 5-year moving average shows two periods of below average rainfall (1925-1944 and 1993-2008) followed by two periods of above average rainfall (1945-1956 and 2009-2013).

Table SM-03 Percent of vegetation cover for the long-term analysis obtained from the Grayscale pixel-based classification method (GPC) and the Point-based grid sampling manual classification method (PGSC) using the available aerial photography for the study area.

	GSC	PGSC	Difference	Average
1949	5.90	7.56	1.66	6.73
1956	6.43	8.96	2.53	7.69
1967	13.27	17.09	3.82	15.18
1975	17.97	22.36	4.38	20.16
1984	20.91	24.70	3.79	22.81
1995	24.82	25.24	0.42	25.03
2000	24.51	27.13	2.62	25.82
2008	25.84	30.45	4.61	28.15
2013	34.59	39.60	5.00	37.09
2017	36.57	41.10	4.53	38.84

Table SM-02 – Percent of vegetation cover for the long-term analysis obtained from the GPC method and the PGSC method using annual satellite imagery for the study area.

	GPC	PGSC	Difference	Average
2010	39.86	49.60	9.74	44.73
2011	43.87	54.00	10.13	48.93
2012	48.72	56.10	7.38	52.41
2013	46.03	56.90	10.87	51.47
2014	46.10	55.00	8.90	50.55
2015	47.37	53.60	6.23	50.48
2016	48.54	57.00	8.46	52.77
2017	51.57	61.00	9.43	56.29

Table SM-03 – Values for vegetation cover and averages for the different variables per period used to perform the Pearson correlation coefficient (PCC) statistical analysis for the long-term data (1949-2017).

Period	Vegetation cover (%)*	Rabbit density average for Witchitie (Rabbits per ha²)**	Rabbit density average for Salt Creek (Rabbits per ha²)***	Rainfall average for Meningie (mm)	DP average for Robe (v.u.)
1949-1956	7.70	17.80	NA	511.71	NA
1956-1967	15.20	2.29	NA	479.28	200.18
1967-1975	20.20	2.71	NA	497.36	203.48
1975-1984	22.80	2.05	NA	470.38	90.93
1984-1995	25.00	6.60	NA	448.69	242.77
1995-2000	25.80	0.65	1.40	426.30	298.06
2000-2008	28.10	1.82	2.18	457.61	221.33
2008-2013	37.10	NA	3.13	523.32	106.90
2013-2017	38.80	NA	0.74	479.76	171.18

*Vegetation cover of each period is represented as the value obtained at the end of that period (e.g. 1949-1956 = Vegetation cover of 1956). Vegetation cover percentages were calculated using the average of GPC and PGSC techniques for the available historical aerial photographs, as described in the methods.

** Rabbit density averages for Witchitie (Flinders Ranges – SA) was calculated based on the data from Sauders et al. (2010).

*** Rabbit density average for Salt Creek (Coorong Region – SA) was calculated based on the data from Mutze et al., 2014a and Cox, unpublished).

Table SM-04 – Values for vegetation cover and averages for the different variables per year used to perform the Pearson correlation coefficient (PCC) statistical analysis for the annual short-term data (2010-2017).

Year	Vegetation cover (%)	Annual Rabbit density for Salt Creek (Rabbits per ha ²)*	Annual rainfall for Meningie (mm)	Annual DP for Robe (v.u.)
2010	44.70	3.30	696.20	259.83
2011	48.90	2.29	492.20	287.06
2012	52.40	2.08	489.10	267.90
2013	51.50	2.00	533.10	214.10
2014	50.60	1.17	470.20	142.96
2015	50.50	0.89	377.00	93.94
2016	52.80	0.53	602.80	238.05
2017	56.30	0.35	469.05	209.76

* Annual rabbit density for Salt Creek (Coorong Region – SA), based on the data from Mutze et al., 2014a and Cox, unpublished).

Table SM-05 – Results from the Pearson correlation coefficient statistical analysis for the long-term data (1949-2017).

Pearson Correlations – long-term data (68 years)				
	Vegetation cover	Rabbit density	Rainfall	DP
r ²	1	-0.778	-0.086	-0.274
Sig. (2-tailed)*		0.039	0.013	0.511
N	9	7	9	8

*Significance level used was p<0.05.

Table SM-06 – Results from the Pearson correlation coefficient statistical analysis for the short-term data (2010-2017).

Pearson Correlations – short-term data (8 years)				
	Vegetation cover	Rabbit density	Rainfall	DP
r ²	1	-0.818	-0.167	-0.496
Sig. (2-tailed)*		0.013	0.693	0.211
N	8	8	8	8

*Significance level used was p<0.05.

Chapter 3 - Historical evolution of transgressive dunefields to parabolic-blowout dunefields, Youngusband Peninsula, South Australia

*Martim A.B. Moulton^{1,2},
Patrick A. Hesp¹,
Graziela Miot da Silva¹,
Guilherme B. Fernandez²,
Robert Keane¹.

¹ Beach and Dune Systems (BEADS) Laboratory, College of Science and Engineering, Flinders University, Adelaide, Australia.

² Laboratório de Geografia Física (LAGEF), Geography Department, Universidade Federal Fluminense (UFF), Niterói, Brazil.

3.1. Abstract

Coastal sand dunes present different morphological patterns as a result of aeolian processes and vegetation density. At times dune systems switch from a vegetated/stabilized state to an unvegetated/transgressive stage, and vice-versa, changing their geomorphological characteristics. Although many studies regarding geomorphological changes of coastal dunes have been made all around the world, few have investigated the medium-term evolutionary paths of transgressive dunefields. This study examines the geomorphological changes that occurred on the Youngusband Peninsula (YP) dune system in South Australia due to vegetation cover changes in the past ~70 years. Recent studies have shown that vegetation cover density has significantly increased by the anthropogenic control of exotic fauna (principally rabbits). Using a sequence of historical aerial photographs between 1949 and 2018, along with high-resolution LiDAR data (2018), the geomorphological changes and the evolutionary patterns were analyzed. In 1949 the dune system displayed well-developed active transgressive dunefields and active parabolic dunes connected to the beach. By 2018, major geomorphological changes occurred. Active transgressive dunefields, that occupied 60% of the northern YP area, evolved into vegetated and active blowouts and parabolic dunes, and in 2018 only represented 10% of the total study area. Results show that vegetation growth has triggered a new stabilization phase of the YP dunes and caused major geomorphological changes in 88% of the dunefield. If no significant environmental change takes place, the northern YP will have all its dunes stabilized in the next few decades.

Key Words: Transgressive dunefields; parabolic-blowout complex; coastal dunefield evolution, geomorphological changes.

3.2. Introduction

Transgressive dunefields, when active, are large-scale mobile dune systems that typically occur on high energy dissipative, high sediment supply coasts and migrate as the result of onshore, obliquely onshore, or alongshore aeolian sediment transport (Hesp, 2013). These dunefields usually display various types of dunes depending on the sediment supply, wind regime, vegetation density, and evolutionary stage (Hesp *et al.*, 2011). At the final evolutionary stage, they may be fully vegetated (Hesp and Thom, 1990).

Natural geomorphological changes in these typically large-scale coastal dunefields can be largely attributed to changes in vegetation cover (Hernández-Cordero *et al.*, 2018). As seen in continental dunefields, coastal transgressive dune systems can switch from a vegetated/stabilized state to an unvegetated/transgressive state, and vice-versa, changing the geomorphological characteristics and dynamics (Miot da Silva *et al.*, 2013; Hugenholtz and Wolfe, 2005).

While many studies regarding geomorphological changes of coastal dunes have been made around the world (Tsoar and Blumberg, 2002; Kutiel *et al.*, 2004; Duran and Hermann, 2006; Marcomini and Maidana, 2006; Jones *et al.*, 2010; Martinho *et al.*, 2010; Levin, 2011; Miot da Silva *et al.*, 2013; Yizhaq *et al.*, 2013; Hesp and Martinez, 2007; Fernandez *et al.*, 2017; Hesp and Smyth, 2019), very few investigate the medium-term changes of transgressive dunefields (Pickart and Hesp, 2019), and therefore little is known about the evolutionary paths that these dune systems take (Hesp, 2013).

Within the evolutionary stages of transgressive dunefields, phases of greater stabilization due to vegetation growth are very common (Hesp, 2013; Hernández-Cordero *et al.*, 2018; Jackson *et al.*, 2019a). In a stabilization phase, vegetation will tend to grow and fixate the different dune forms until it reaches an equilibrium with the sand deposition rate, unless something triggers another destabilization phase (which can happen at any evolutionary point within the stabilization process) (Hesp, 2013). During the stabilization process, significant geomorphological alterations within the dune system can occur, with active mobile dunes evolving into dune types that have their genesis linked to vegetation fixation (i.e., 'Anchored' dunes), such as parabolic dunes, blowouts, trailing ridges, etc. (Tsoar and Blumberg, 2002; Hesp and Martinez, 2007; Guan *et al.* 2017; Yan and Bass, 2017; Hesp and Smyth, 2019).

By examining transgressive dunefields around the world, Hesp (2013) presented one of the few conceptual models for coastal transgressive dunefield evolution. This model consists of three main scenarios of development or initiation, and evolutionary paths of transgressive dunefields: (1) direct development from the backshore; (2) development because of foredune and/or dune field erosion; and (3) development from parabolic dunes. For each of these scenarios the author presents different evolutionary pathways. In deriving these conceptual models, Hesp (2013) noted the need for empirical investigations.

In a recent study, Moulton *et al.* (2019) quantified the vegetation cover changes that occurred on the Youngusband Peninsula (YP) dunefield (South Australia) in the last 7 decades revealing that the reduction of the invasive rabbit population (*Oryctolagus cuniculus*) in the region led to a rapid increase in vegetation cover and significant stabilization process that is still in progress.

Although this study elucidates the magnitude of the vegetation changes and the principal reasons for it, the impact of the 40% increase in vegetation cover over the past 70 years on the geomorphology of the dunes was not explored.

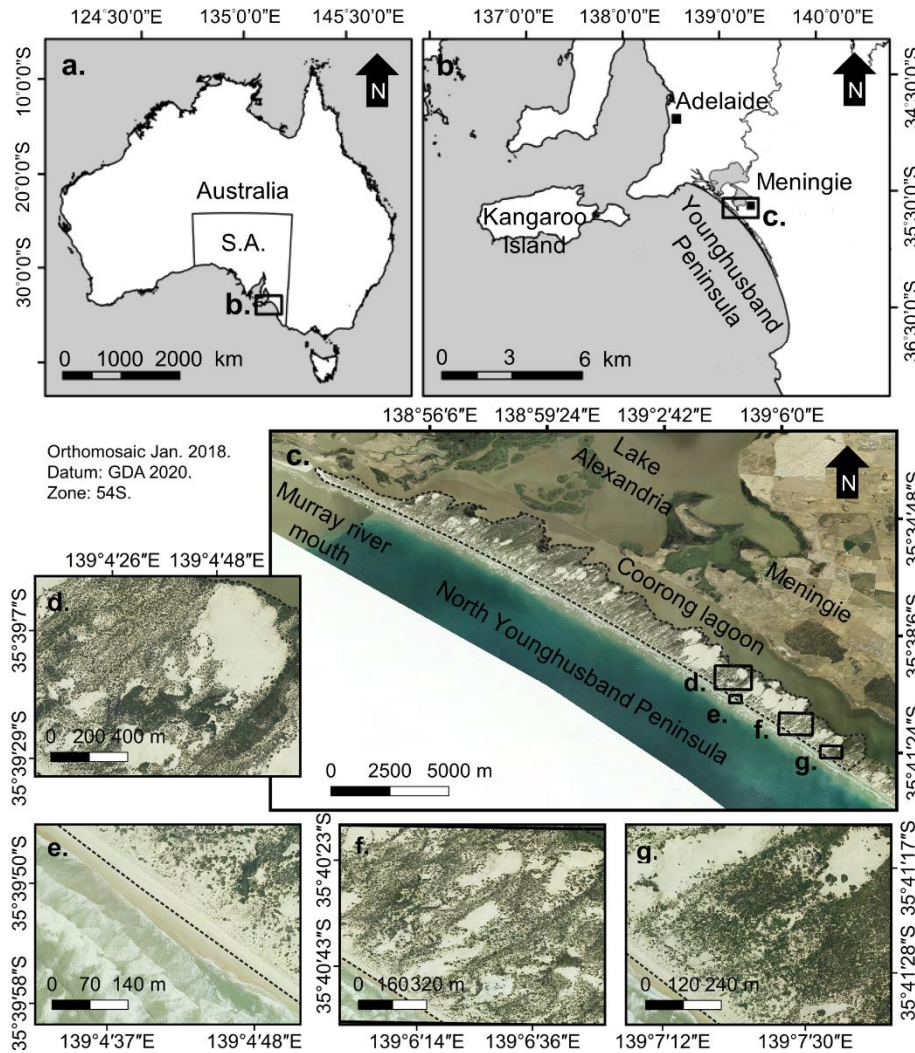


Figure 3.1 – Location of the northern Younghusband Peninsula. The dashed line (c) represents the study area. Images d, e, f, and g show the location of the representative areas chosen to show the detailed evolutionary paths of the main geomorphological changes that occurred in the past 7 decades.

This study examines the geomorphological changes that occurred on the northern YP dune system (Figure 3.1) due to vegetation cover changes in the past ~70 years, focusing on the evolutionary paths of different dune types.

3.3. Study site

The Youngusband Peninsula is a narrow (1-2 km wide) and long (190 km) Holocene coastal sand barrier partially separated from older Pleistocene barrier systems by an inter-barrier lagoon (Coorong Lagoon) (Figure 3.1). This extensive barrier comprises one of the largest coastal dune systems of Australia, with more than 40 m high transgressive and parabolic dunes in the northern section (Figure 3.2), decreasing in size in the mid-section of the barrier, until the barrier is connected to the continent further south and the landscape is composed of series of relict foredunes (Short and Hesp, 1984; Paton, 2010; Bourman *et al.*, 2016; Murray-Wallace, 2018; Moulton *et al.*, 2019).

The YP has a warm-summer Mediterranean climate (Csb - Köppen classification), with high temperatures and lowest mean monthly rainfall average during the summer (20 mm), and more humid (60 mm) and lower temperatures during winter (Meningie Weather Station - Source: Australian Bureau of Meteorology, 2018). The resultant wind direction is North-east, with predominant winds ranging from the South to West quadrants (Moulton *et al.*, 2019).

While the evolution of this Holocene barrier is not yet fully understood, radiocarbon dating from archeological sites (Luebbers, 1981, 1982) and sedimentary facies (Short and Hesp, 1984; Harvey *et al.*, 2006) have established that it began to be formed approximately 6500-7000 years ago when large quantities of sediment from the continental shelf were driven landwards by the Postglacial Marine Transgression (PMT). Short and Hesp (1984) obtained an age of $6,180 \pm 90$ years BP on shell hash (SUA-1430) on the seaward side of the barrier at Coorong 104 km (i.e. 104 km from the River Murray mouth), indicating the barrier was at least in place by ~6000 years BP. Harvey *et al.* (2006) reported

a suite of ages on dune and beach sediments ranging from 5,020 to 885 years BP in an area ESE of Barker Knoll (approx. 3km SE of the Murray Mouth). The presence of various palaeosols throughout the dunefield indicates that the system evolved via the development of several relatively discrete dunefield phases (Gilbertson, 1981; Short and Hesp, 1984; Harvey, 2006).

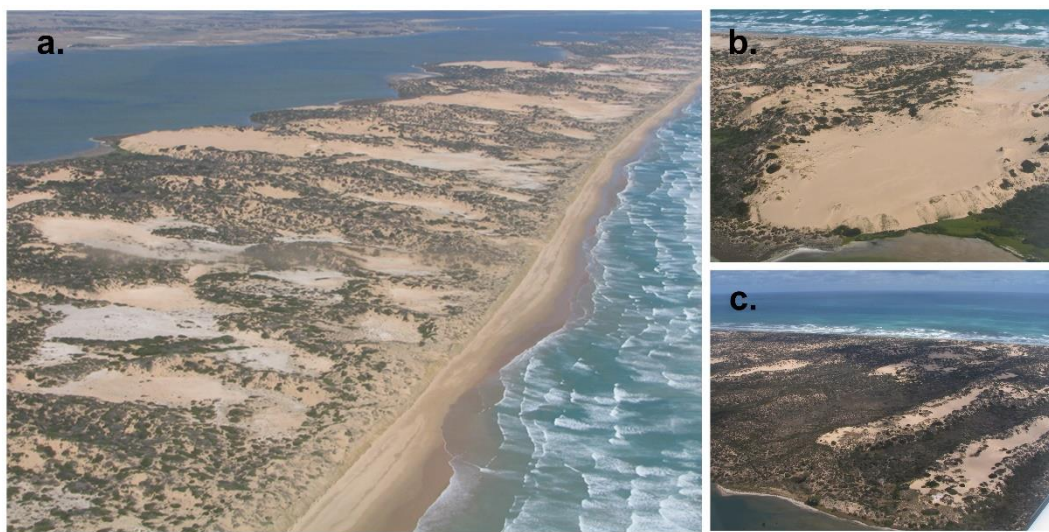


Figure 3.2 – Oblique aerial photos showing: a) the complex nested relict and active parabolic-blowout dune morphology within the YP; b) an active parabolic dune migrating towards the Coorong Lagoon; c) elongate parabolic dunes in the last stage of vegetation colonization within a densely vegetated, formerly active transgressive dunefield area (Images courtesy of Michael Hilton).

In 1802, while navigating past the Youngusband Peninsula, Matthew Flinders noted in his journal that the coastline landscape was predominantly of widespread active dunes with very little vegetation (Flinders, 1814). Recently, a stabilization phase, which intensified between 1956 and 1975 (Moulton *et al.*, 2019), has transformed the morphology of the transgressive dune systems to form the present-day landscape. In addition to the remaining active dune forms from the transgressive phase and the anchored dune forms associated to the

recent stabilization phase, older stabilized dunes representing one or more earlier phases are present in some areas (Short and Hesp, 1984; Paton, 2010).

3.4. Methods

To investigate the geomorphological changes of the Younghusband Peninsula dunefields, historical aerial photographs and high-resolution *Light Detection and Ranging* (LiDAR) data were used. All data were obtained from the South Australian *Department for Environment and Water* (DEW), totaling 10 different years of digital images (1949, 1956, 1967, 1975, 1984, 1995, 2000, 2005, 2008, 2013 and 2018) with a 7-year interval between them (on average), covering the past 7 decades, and one year of LiDAR data (2018). The LiDAR data obtained was part of the Climate adaptation project led by DEW, the SA Coast Protection Board, SA Water, and local governments, to collect high precision elevation of the entire coast of the state of South Australia.

The first aerial photographic record, 1949, and the last, 2018, were chosen for the large-scale mapping of geomorphic units (geounits). These two images are orthorectified vertical photographs with enough resolution and clarity for the purposes of this study. Ortho rectification and mosaic were produced by the supplier, with +/- 2 GSD RMSE horizontal spatial accuracy for each and pixel size of 25 cm and 40 cm GSD, respectively. The area of the YP chosen for this mapping is limited by the extension of the 1949 survey, which extends from the eastern margin of the Murray River mouth (35°33'25"S / 138°52'56"E) to a location called Nine Mile Point (35°40'55"S / 139° 8'19"E), covering 27 km of the northern section of the barrier and 21 km² in area (Figure 3.1).

The two maps were produced via manual classification in ArcGis 10.6 software at a 1: 20,000 scale and presented at a 1: 100,000 scale, using vegetation and three-dimensional elevation data to distinguish the different geounits. Three-dimensional information was obtained from traditional stereo imaging techniques, using aerial photographs where image overlap existed (mostly for the 1949 images), and from the 2018 high resolution LiDAR data (\pm 50 cm horizontal and \pm 15 cm vertical spatial accuracy). LiDAR data provided the possibility of creating a Digital Elevation Model (DEM) of the entire study area (GDS – 1m), enabling a more accurate mapping of the morphological features present.

In the 1949 and 2018 images, the following geomorphic units were identified and mapped: (1) Foredunes and remnant knobs wherein the most seaward dune morphologies bounded by the seaward edge of the pioneer vegetation line or scarp, and the landward edge adjacent to the lee swale; (2) active blowouts and parabolic dunes as defined by their outer erosional or trailing ridge edges, upwind margins of deflation basins or plains and downwind margins of depositional lobes; (3) vegetated blowouts and parabolic dunes; (4) active transgressive dunes characterized by large-scale dune morphologies with transverse, oblique and linear dunes present on the surface; (5) Pre-1949 stabilized dunefield; (6) Dune flats and marsh vegetation adjacent to the Coorong Lagoon; and (7) Beach characterized by bare sand located between the swash zone limit and the edge the pioneer vegetation line. Transverse and linear dune ridges on transgressive dunefields, and the limits of individual active blowouts and parabolic dunes were mapped as line features.

Due to the significant length of the barrier, a more detailed analysis of the geomorphological changes was performed in representative areas, where the evolutionary paths of the main geomorphic units and dune types of the YP can be observed (Figure 3.1). For this, aerial photographs from all the available years were used to show examples of the approximately decadal geomorphological changes. These images were georectified in ArcGIS 10.6 software using the 2018 orthorectified mosaic as the base map.

Two field campaigns were made to collect ground-control points (GCPs) to assess the accuracy of the georectification and verify the mapped geounits. Given the isolation of the Youngusband Peninsula dunefield, very few fixed man-made structures were found within the study site. Therefore, old bushes and lake margins detectable in both 1949 and 2018 composed the majority of the GCPs.

3.5. Results

3.5.1. Geomorphological changes between 1949 and 2018

Results from the geomorphological mapping of the Northern YP in 1949 and 2018 revealed that considerable geomorphological changes took place (Figure 3.3). More than 88% of the study area changed due to the increase in vegetation cover. The observed changes represent a major stabilization process. In 1949, 73% of the barrier consisted of active dunes (active transgressive dunefields + active blowouts and parabolic dunes), reducing to only 32% in 2018 (Table 3.1).

Active transgressive dunefields were predominant in the 1949 landscape (Figure 3.3a), with 60% of the study area being composed of these dunes (Table

3.1). In 2018, these areas were significantly reduced, and only 10.3% of the active transgressive dunefields remained. Most of the active transgressive dunefield areas present in 1949 have either changed into vegetated blowouts and parabolic dunes, (47.3% of the 2018 landscape - See table 3.1), or into active blowouts and parabolic dunes (21.7% in 2018 - See table 3.1), these being the most significant geomorphological changes observed in the last 70 years in the northern YP (Figure 3.3).

The majority of the active parabolic dunes mapped in 1949 have either undergone a complete stabilization process or migrated inland in the past decades. These dunes were predominantly found connected to the beach system in 1949, while in 2018 these dunes are predominantly found in the middle of the barrier. An increase in the total area of active blowouts and parabolic dunes in the past few decades (See table 3.1) can be attributed to the fact that they have mostly evolved from the fixation of active transgressive dunefields.

Another important stabilization process in this period occurred adjacent to the beach, where a major foredune formation and stabilization process was observed. Continuous foredunes were only seen close to the Murray mouth in 1949, with isolated remnant knobs presumably from a prior foredune erosional process being the most predominant seaward dunes. In 2018, a continuous and well developed foredune ridge was observed along the entire shoreline of the study area.

The only areas of the dunefield where little to no change occurred were isolated patches of previously (older) stabilized dunefields close to the Lagoon margins (the dark green areas of figure 3.3), and the remaining areas of active transgressive dunes (the orange areas of figure 3.3b).

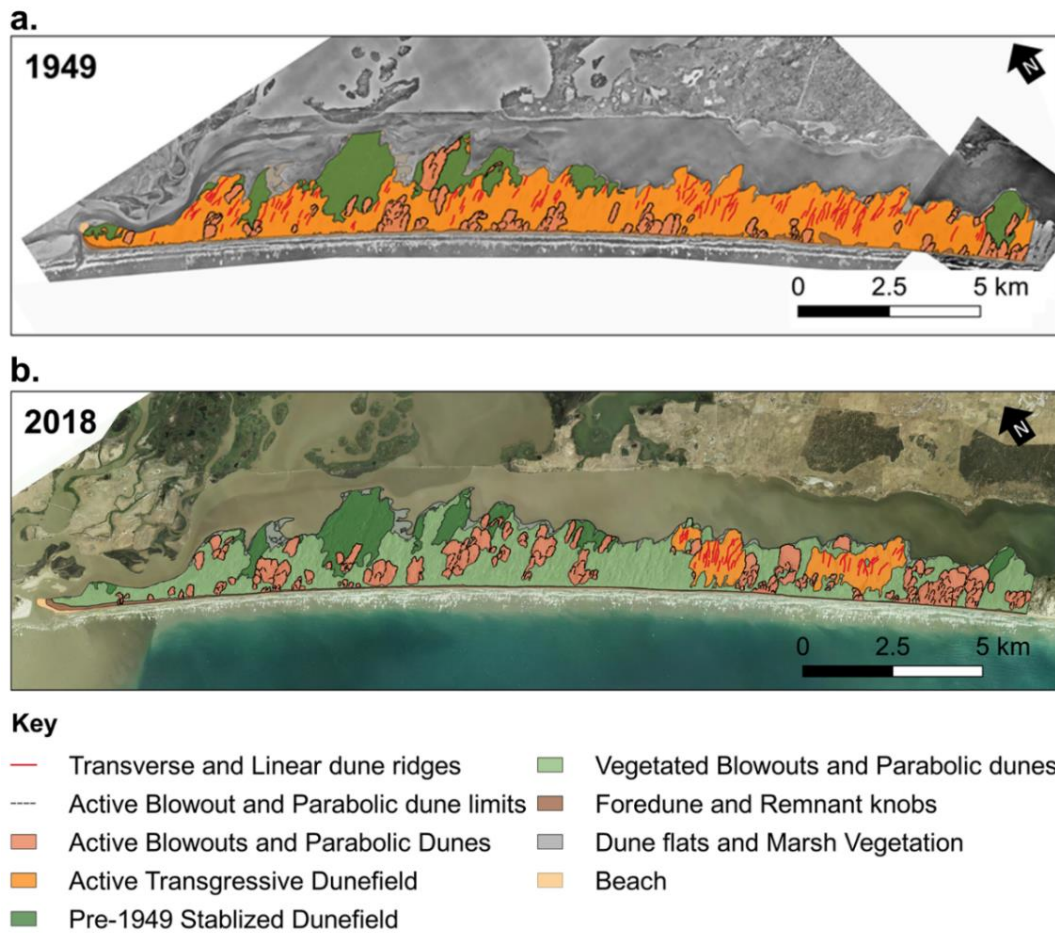


Figure 3.3 – Geomorphological maps showing the changes between 1949 (a) and 2018 (b) within the northern YP. Datum: GDA 2020.

The previously stabilized areas denominated “Pre-1949 stabilized dunefield” unit, consists of old trailing ridges of parabolic and transgressive dunes, as well as deflation plains and basins, that were completely stabilized during a previous stabilization phase of the dunefield. Although in some sites active parabolic dunes have migrated into these areas, much of the older system remained intact since 1949 (Figure 3.3), “surviving” the last dune transgression phase.

In 1949, blowouts and parabolic dunes presented little vegetation, being considered as active (figure 3.3a). Over the last 7 decades, most of them were stabilized by vegetation, therefore being classified as vegetated blowouts and

parabolic dunes in 2018 (figure 3.3b and table 3.1). New active blowouts and parabolic dunes can also be seen in 2018, increasing by 8% in comparison to 1949. This is likely the result of vegetation separating transgressive dunes into parabolics, and, in some cases, the development of blowouts.

Table 3.1 – Area of the different geounits mapped in 1949 (a) and 2018 (b).

a.	1949 Geounits	Area (m²)	Area (%)
	Active Blowouts and Parabolic Dunes	5793802	13.4
	Active Transgressive Dunefield	26001780	60.0
	Pre-1949 Stabilized Dunefield	7715147	17.8
	Vegetated Blowouts and Parabolic Dunes	0	0
	Foredune and Remnant Knobs	915752	2.1
	Dune flats and Marsh Vegetation	1685390	3.9
	Beach	1170146	2.7
	Total	43282017	100
b.	2018 Geounits	Area (m²)	Area (%)
	Active Blowouts and Parabolic Dunes	9535899	21.7
	Active Transgressive Dunefield	4514359	10.3
	Pre-1949 Stabilized Dunefield	5582482	12.7
	Vegetated Blowouts and Parabolic Dunes	20719964	47.3
	Foredune and Remnant Knobs	820549	1.9
	Dune flats and Marsh Vegetation	1792112	4.1
	Beach	859417	2.0
	Total	43824782	100

The remaining active transgressive dunefields present in 2018, despite having their area significantly reduced in size (Figure 3.3), still constitute relatively large-scale sand deposits that migrate inland and have changed very little in terms of their original morphology. These dunefields are still the highest points of

the barrier (more than 40 m above mean sea level – Figure 3.4) and present transverse or linear dunes (Figure 3.3), that distinguish them from previous transgressive dunefield areas that have been transformed into large-scale parabolic dunes (Figure 3.3).

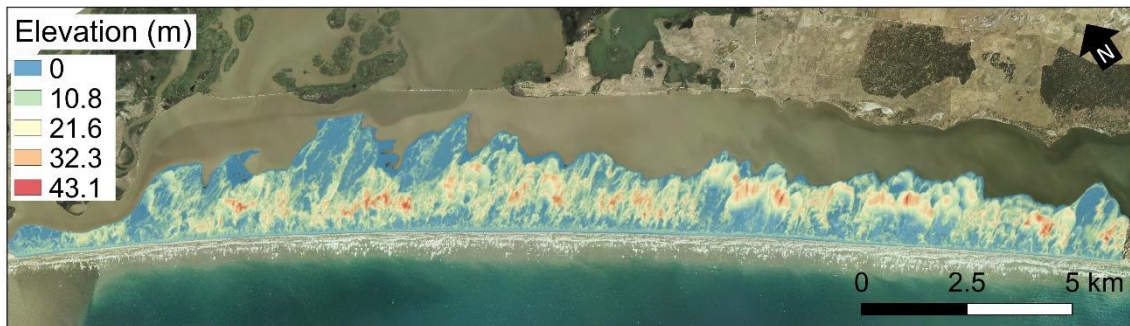


Figure 3.4 – Elevation data of the northern YP dunes obtained from the 2018 LiDAR (Base image: 2018 orthomosaic). Horizontal datum: GDA2020. Vertical datum: AHD (Australian Height Datum).

3.5.2. Decadal geomorphological changes

The evolutionary paths of the dunefields that took place in the northern YP dunes in the past 7 decades are presented in the section below, with 4 examples of the changes that occurred in the foredune-blowout complex, parabolic dunes, and transgressive dunefields (Figure 3.1).

3.5.2.1. Foredune-blowout complex evolution

Historical imagery shows a considerable increase in vegetation cover adjacent to the shoreline along with the connectivity and stabilization of the foredunes (Figure 3.5). In 1949, vegetation was scarce and foredunes were limited to disconnected remnant knobs (Figure 3.5). Until the 1975 image disconnected foredunes still dominated, despite the evident increase in

vegetation cover. Areas of overwash fan deposits can be observed in these early images (Figure 3.5).

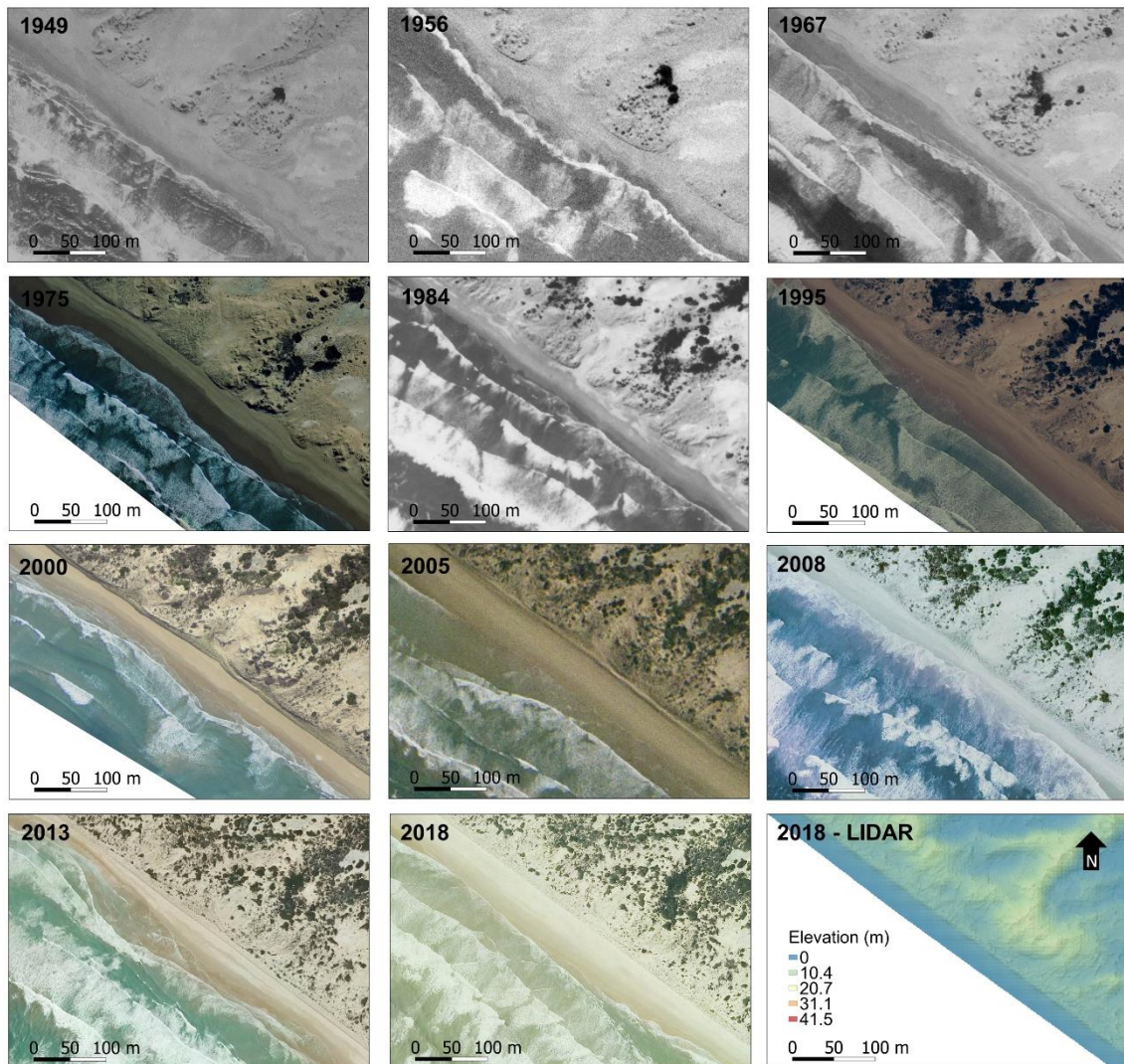


Figure 3.5 - Example of the geomorphological changes that occurred within foredunes from 1949 to 2018 (Location in figure 3.1).

By 1975, the alongshore connectivity of the foredunes starts to become more evident. Although the presence of blowouts still separates the foredunes in some areas, the isolated remnant knobs no longer dominate this landform unit (Figure 3.5).

20 years later, the 1995 images show that blowout erosion within the foredunes is significantly reduced. Prior blowouts become filled by sand deposition and stabilized by vegetation. Foredune stabilization and alongshore connectivity improved following vegetation colonization and increase in cover. From 2000 onwards, a clear ridge connecting the foredunes can be seen and pioneer vegetation advances towards the sea. In 2013, incipient dune formation alongshore is evident and is present through to 2018. By 2018 vegetation has considerably stabilized the foredune-blowout complex.

3.5.2.2. Parabolic dune evolution

Parabolic dunes identified in the 1949 image, also evolved through significant morphological changes in the past 7 decades. In different parts of the YP, parabolic dunes can be observed attached to the beach in 1949 (Figure 3.6). The deflation basin of parabolic dunes, in most cases, show little or no vegetation at this stage, and the dunes are typically long-walled parabolic dunes as seen in figure 3.6.

From 1949 to 1975, vegetation increases considerably at the back of the parabolic depositional lobe, trailing arms, and within the deflation basin (Figure 6). In the 1975 image, significant stabilization of the deflation basin can be observed (Figure 3.6). By 1995, the vegetation expansion within the deflation basin has led to complete separation of the parabolic dune from the beach and the parabolic dune is in part stabilized (Figure 3.6).

The parabolic dune depositional lobe is initially just one lobe in 1949, but by 1967, a line of nebkha developing since 1956, act to split the lobe into two lobes. This initial nebkha line develops further into the 1970's and two separate deflation basins are formed with clearly separate depositional lobes. The more

NW dune becomes significantly stabilized by 2005, while the larger, more SE dune is still active in 2018. A somewhat similar, but significantly smaller version of this occurred in Israel where nebkhas initiated the transformation of a barchan dune into a parabolic dune (Ardon *et al.*, 2009).

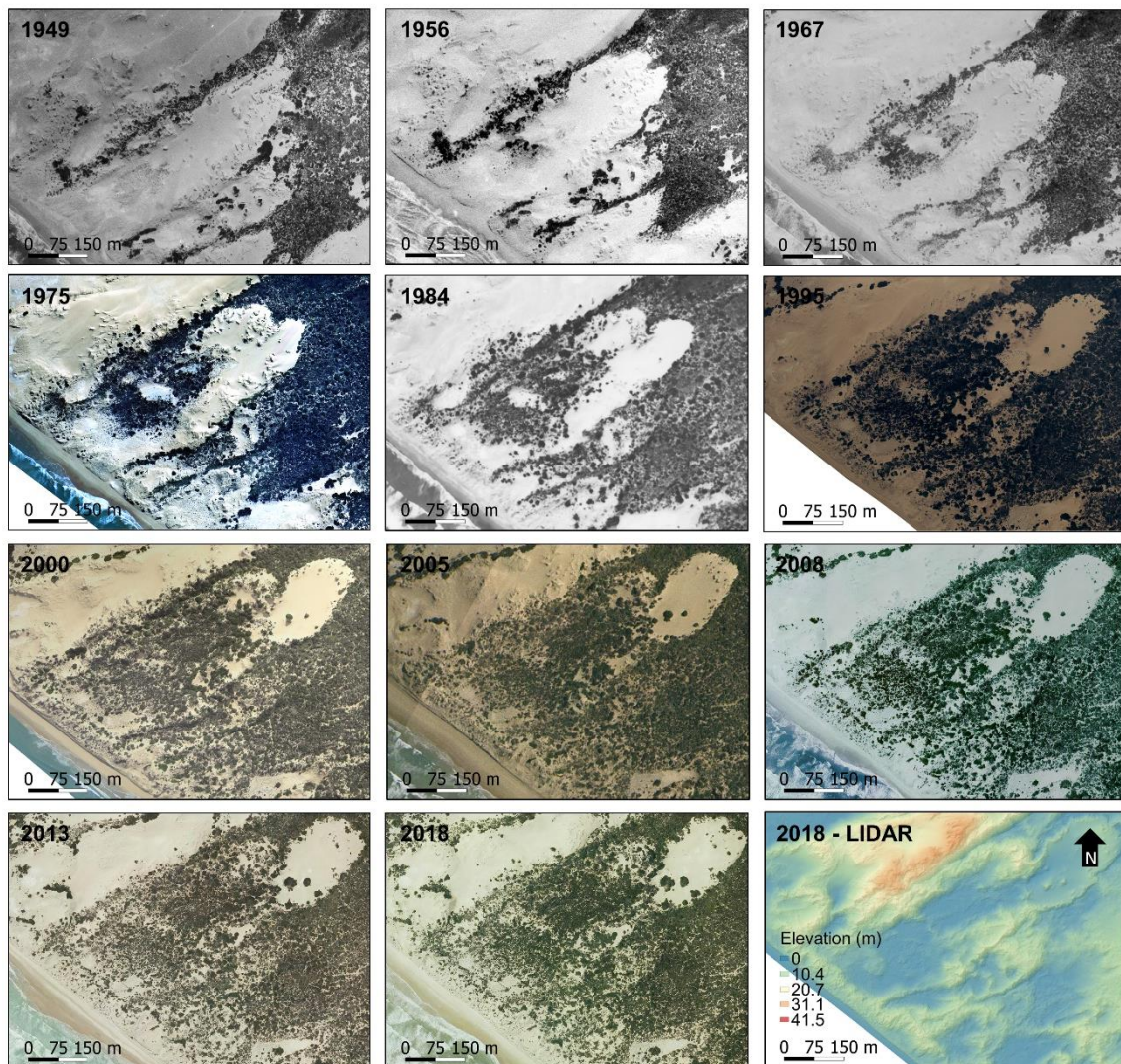


Figure 3.6 – Example of the geomorphological changes that occurred within parabolic dunes from 1949 to 2018. (Location in figure 3.1).

Vegetation continues to increase between 1995 and 2018, bare sand areas are reduced, and the SE dune continues the stabilization process. Despite this general stabilization, some parabolic dunes continue to migrate inland (Figure 3.6).

3.5.2.3. Active transgressive dunefield evolution

Active transgressive dunefields composed the majority of the YP landscape in 1949, extending the entire width of the barrier at most sites as shown above in the larger-scale geomorphological mapping (Figure 3.3a). Transgressive dunefields were highly mobile, presenting a single depositional unit with transverse/linear dune ridges with the vegetation cover being mostly limited to the back of the precipitation ridge, interdune depression and deflation plains (Figures 3.7, and 3.8). These dunefields have transformed either into (a) a complex of parabolic dunes or (b) a single large-scale parabolic dune.

3.5.2.3.1. Evolution into a parabolic dune complex

In this case of transgressive dune evolution, vegetation started to form corridors within the across-barrier interdune depression around 1967, separating one transgressive dunefield segment from the other (Figure 3.7). The increase of vegetation cover within the active transgressive dunefield area also leads to the establishment of nebkha and patches of vegetation on the upper portions of the dunes.

In the 1975 image, these vegetation patches and nebkha fields that occur mainly in the higher areas within the dunes start to become larger. Interdune depressions and deflation basins and plains also start to become more vegetated and instead of a single transgressive dunefield, vegetation corridors start to form stabilized ridges that separate the dunefield into large-scale elongated parabolic dunes. By 1975 separate depositional lobes begin to form (Figure 3.7).

By 1984, nebkha fields are beginning to coalesce, and start to break up the larger parabolic dunes into smaller units. Several of these become vegetated

ridges by 1995, and the elongated parabolic dunes are divided into many smaller parabolic dunes (Figure 3.7).

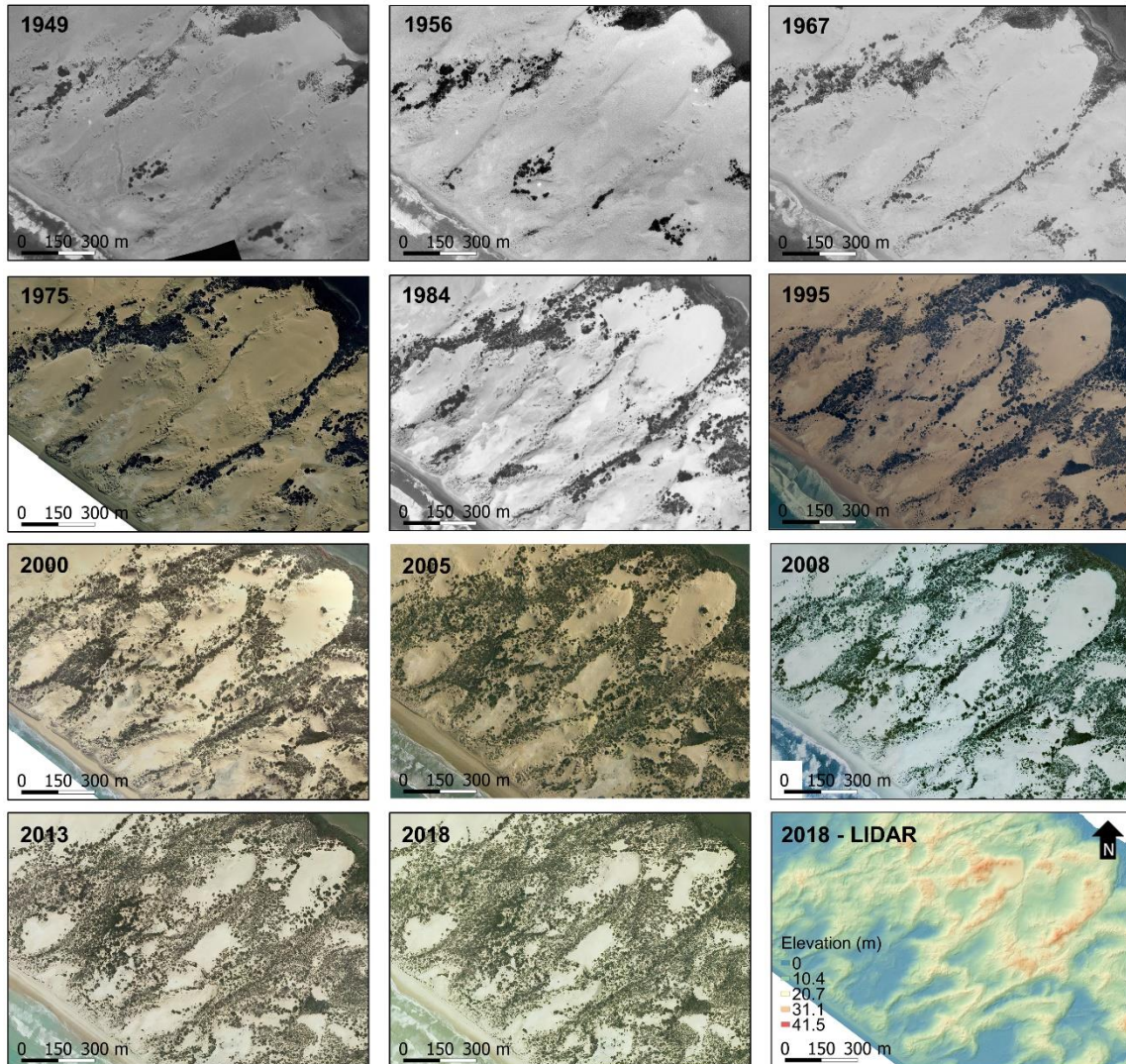


Figure 3.7 – Example of the geomorphological changes that occurred within a portion of the active transgressive dunefield from 1949 to 2018, with vegetation colonization transforming it into a series of parabolic dunes (Location in figure 3.1).

These dune forms become more evident with the vegetation growth around the downwind toe of the depositional lobes. Lower deflation basin areas become stabilized as the vegetation cover also increases. At this stage (1995), most of the transgressive dunefields have become either blowouts or active

parabolic dunes, and the dunefield has converted from a relatively simple form to a complex, chaotic, multi-dune form.

With the vegetation increase in the subsequent years, the bare sand areas of these blowouts and parabolic dunes reduces in size. Although these dunes become significantly stabilized by 2018, when compared to the 2013 images, migration of the depositional lobes of many of the parabolics/blowouts still occurs (Figure 3.7). In 1995 there were roughly 17 individual active parabolic dunes and by 2018 there were approximately 8.

3.5.2.3.2. Evolution into a single large-scale parabolic dune

This transgressive dunefield evolutionary path is similar to the previous one. However, in this case, the vegetation growth is limited to the interdune depressions and plains on each side of a larger dune. The vegetation patches present in the upper left and lower right portions of the 1949 photograph provides the site from which significant plant colonization proceeds and then spreads. The interdune depressions and plains are quickly vegetated, and by 1975 the active transgressive dunefield in the middle of the photograph is completely separated from the rest of this now very well vegetated dunefield portion (Figure 3.8).

As the transgressive dunefield migrates inland an extensive deflation plain is formed. Vegetation rapidly colonizes this lower area between 1967 and 1975, and by 1995 the dune is no longer connected to the beach and vegetation completely separates the dunefield and a single large-scale parabolic dune is formed (Figure 8).

The transgressive dunefield displays transverse N facing dunes ridges and a lateral SE precipitation ridges in 1975, and these can be seen up until 1984

(Figure 3.8). By 1995 vegetation has colonized up the SE and N facing precipitation ridges, and the former transverse dune dominated surface has begun to develop a deflation basin. By 2018 a fully developed and active large-scale parabolic dune was formed (Figure 3.8).

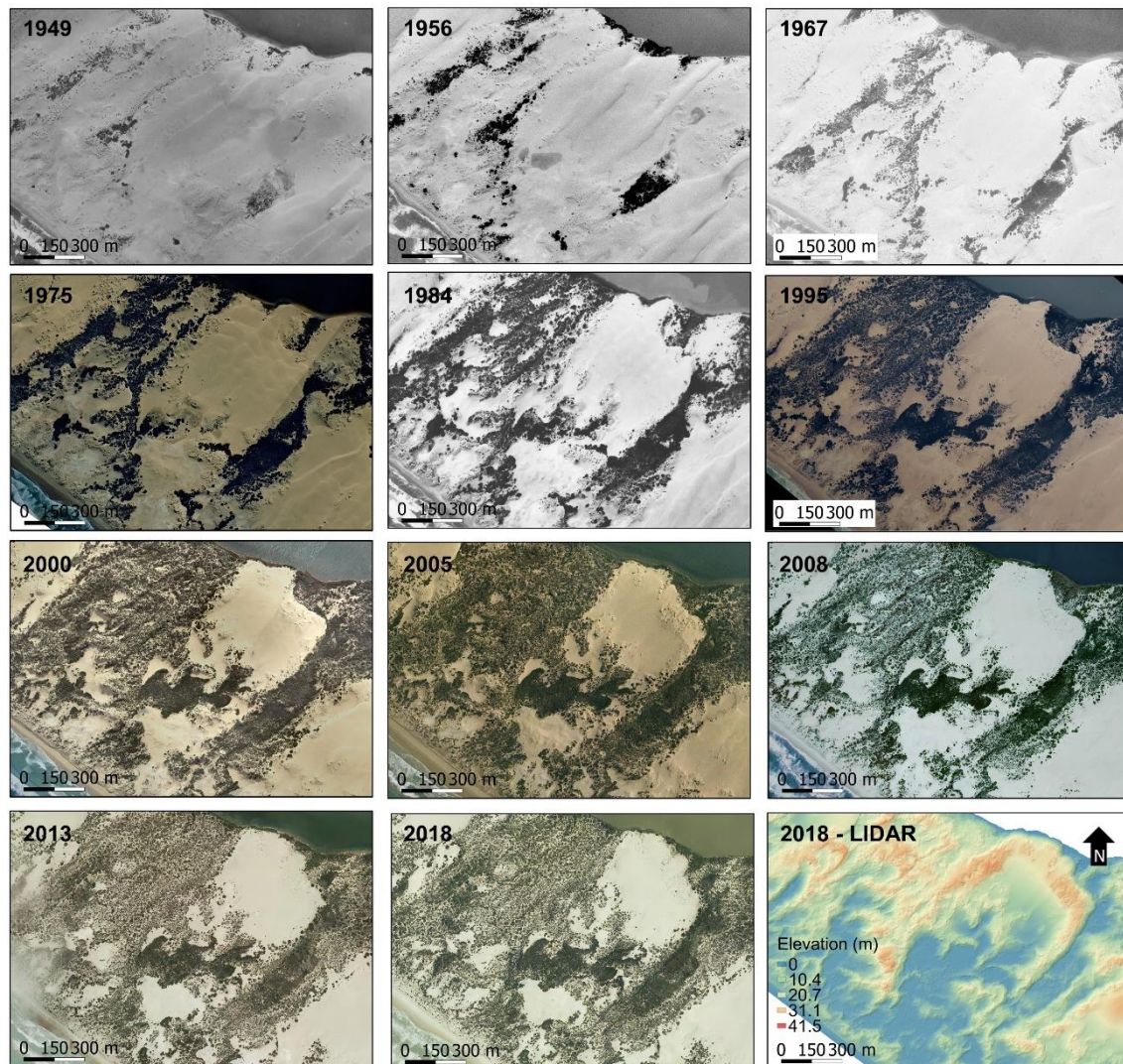


Figure 3.8 - Example of the geomorphological changes that occurred within an active transgressive dunefield from 1949 to 2018, with vegetation colonization transforming it into a single parabolic dune (Location in figure 3.1).

It is also possible to observe the process of blowout formation close to the deflation plain. Patches of vegetation in the lower part of the dunefield, just above

the deflation plain, start to form in 1967. By 1975 these patches become larger and fixate the sand creating nebkhas that have their windward slope eroded by wind creating semicircular blowouts (Figure 3.8). As vegetation increases, most of these blowouts become circular blowouts (Figure 3.8). A similar process is described by Hesp (2002).

3.6. Discussion

The geomorphological changes observed in the aerial photographs between 1949 and 2018 are clearly the result of a major dune stabilization phase following a pre-1949 transgressive phase of the YP dune system. Vegetation largely outcompeted sand deposition in the last ~70 years, with the majority of the existing active dunes (active transgressive dunefields and active blowouts/parabolics) turning into semi-fixed to fixed dunes (vegetated and active blowouts/parabolics and parabolic dunes) (Figure 3.3).

Tsoar and Blumberg (2002) noted a similar scenario of geomorphological changes in Israel's Mediterranean coast as transgressive dunes became vegetated, as did Guan *et al.* (2017) in the Hobq Desert (China), and Yan and Bass (2017) in their modelling of barchan to parabolic transformations.

The major factors that enabled this generalized vegetation growth within the dunefield was discussed in Moulton *et al.* (2019), where the authors found that the decline of the rabbit population on the Peninsula had the largest contribution, with climatic controls, having a secondary role. It is unclear, however, what triggered the destabilization stage that formed the extensive transgressive dune sheets present in 1949, since that are no aerial imagery and very little environmental data for the YP prior to this date.

The annual rainfall record from Meningie (20 km south-east from the study area), however, dates to 1864. This data shows a relatively stable long-term trend when the entire period is analysed, with a slight decline in the linear trend and the 5-year moving average demonstrating some periods of above and below average rainfall (Figure 3.9).

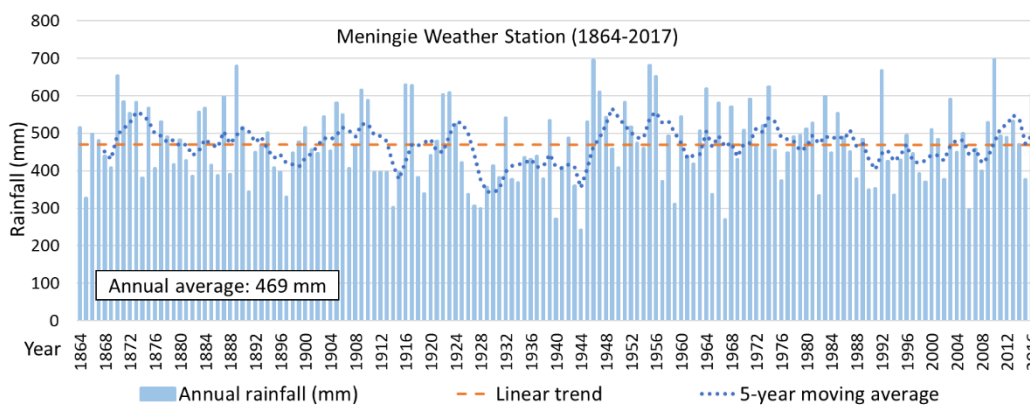


Figure 3.9 – Annual rainfall record for Meningie (SA).

The most significant decline in rainfall began in 1925, when below average rainfall occurred for 2 decades and ended in 1945. This long drought period could have contributed to the last transgressive phase of the YP dunefield, especially when combined with the increasing rabbit population (Moulton *et al.*, 2019). However, with the absence of aerial imagery or other data regarding the dunefield vegetation cover during this period there is no way of confirming this theory.

Hesp (2013) states that one of the most common ways that transgressive dunefields are initiated is by foredune erosion proceeding a major storm event. In this scenario, foredune destabilization occurs typically by dune scarping, blowout and overwash fan formation, up to a point that the foredune can be completely destroyed or segmented into many fragments, remnant knobs, or completely eroded away (Hesp, 2013). This is followed by incipient deflation

basin formation, and the sediments that once comprised the foredunes start to form a transgressive dunefield that migrates inland (Hesp, 2013, Hesp and Walker 2013, Pickart and Hesp 2019; Jackson *et al.*, 2019a).

The absence of foredunes along most of the beach and the presence of remnant knobs adjacent to the shoreline in 1949 suggests that a similar scenario to the one described by Hesp (2013) may have occurred in the northern YP. This scenario is also in accordance with Short and Hesp (1984) and Harvey (2006), who have attributed Holocene transgressive phases of the YP dunes to foreshore and foredune erosion. However, it remains an unproven hypothesis at present.

According to Hesp (2013), the eventual formation and stabilization of a new foredune reduces the beach sediment supply to the dune system, marking the end of the transgressive phase and initiating the stabilization phase (Hesp, 2013). Recent foredune formation and stabilization in the northern YP, as described previously in this work, occurred at the same time as the other landward dunes also started to become stabilized (Figure 3.5). However, reduction of sediment supply to the dunefield by the formation of new foredunes does not seem to be the most significant factor that triggered the recent stabilization phase.

Foredune formation and stabilization within the YP barrier was previously reported by Hilton *et al.* (2007) and James (2012). These studies attribute this process to the invasion of Sea-wheat grass (*Thinopyrum junceiforme*), an introduced pioneer species that commonly occurs in SE South Australia, first seen in the YP in 1978 (Hilton *et al.*, 2007). Although the spatial definition of the aerial photographs observed in this study does not enable the distinction of the pioneer species that colonized the foredune area, it is likely that *Thinopyrum* has

some contribution to the stabilization of the YP foredunes since it has been proven to outcompete native species, accelerating the foredune stabilization process and even changing its morphological evolution (Hilton *et al.*, 2006; 2007). However, the historical images show that foredune stabilization started to take place and connect the remnant knobs sometime between 1967 and 1975 (Figure 3.5), before the first report of Sea-wheat grass in the YP.

According to Hilton *et al.* (2007), the stabilization of the foredunes in the YP led to the stabilization of other dune morphologies located landward, such as blowouts and parabolic dunes. The authors argue that the rapid foredune stabilization reduced sediment availability for aeolian transport, allowing vegetation to grow at a faster rate than sand deposition (Hilton *et al.*, 2007). Despite this being a plausible theory, it is likely that this was not the main cause of stabilization and geomorphological changes seen in parabolic dunes, since the 1967 aerial images show a significant vegetation growth within the deflation basins and plains, and the absence of continuous stabilized foredunes (Figure 3.7).

Despite the significant stabilization of the dune system observed from 1949 to 2018, some sections of the transgressive dunefield remained active. This phenomenon, of active and stabilized dunes coexisting in the same geographical location, is termed dune bistability (Yizhaq *et al.*, 2007), and although the mechanisms behind it are still unclear, it is commonly attributed to interactions between wind and vegetation (Tsoar, 2005).

Gilbertson (1981) credited the reactivation of dunes in the SE portion of the YP to the increase of off-road vehicles in the early 1970's. In the northern YP, although off-road vehicles do access the beach frequently, it is unlikely that this

type of recreational activity has had much effect on the active transgressive dunefield areas.

A more likely explanation for this dune bistability in the northern YP is that dune vegetation colonized some areas faster than others due to the natural differences in the sediment volume of the dunes. Areas that were initially higher and had more sediment volume (prior to stabilization phase) took longer to be colonized by vegetation than lower areas with less sediment volume, as proved by Yizhaq *et al.* (2013) via computer modeling. Lower areas also present a faster vegetation growth rate due to the fact that they are closer to the water table (Silva *et al.*, 2019).

On high sand supply beaches such as the northern YP, where the volume of the dunefields can be very large, landward transgression does not cause major reduction of the size and volume of the dunes. In this case, quite often active dunes cannibalize the pre-existing deposits, forming overlapping dunes and even dune phases (Hesp, 2013). In the northern YP, this process occurs in some areas and not in others. Dune cannibalization can be seen in areas where active transgressive dunefields turn into a complex of smaller parabolic dunes. However, in other areas the transgressive dunes evolve into mega-parabolic dunes and migrate as a single geomorphic feature, leaving an extensive deflation plain behind (Hesp, 2001, 2013; Martinho *et al.*, 2009, 2010; Miot da Silva and Hesp, 2010).

The causes for the differences in transgressive dunefield evolution can be credited to differences in local dune volumes, landscape inheritance (Pickart and Hesp, 2019), such as the presence of older underlying dune systems and the presence and degree to which patches of vegetation act as plant colonization

spreading points, or dune-dune collision acting as a stabilizing mechanism in some areas (Barchyn and Hugenholtz, 2012).

3.7. Conclusion

In 1949 the dune system was composed mainly of active and extensive transgressive dunes and a few active parabolic dunes, all commonly connected to the beach. ~70 years later, the dunefield went through a major stabilization process.

Active transgressive dunefields suffered the most significant transformations, decreasing significantly in area due to growth of vegetation on the marginal interdune depressions and plains, forming narrow elongate vegetated ridges whose presence and expansion lead to the development of large-scale parabolic dunes. A further increase in vegetation cover lead to the formation of smaller parabolic dunes and blowouts, some still active, but many of which are now stabilized by vegetation. Highly erosional foredune segments and remnants were converted into relatively continuous foredune-blowout complexes. The result is a significantly more complex, at times chaotic dunefield landscape compared to the original 1940's morphologically simple transgressive dunefield system.

The results suggest that the stabilization of the northern YP is still on its course, and unless some drastic environmental change occurs (human or natural) (Yan and Bass, 2015), it is expected that the remaining active parabolic dunes will become stabilized by vegetation and the remaining active transgressive dunes will evolve into parabolic dunes that will eventually also become stabilized. Although the tendency is of complete dune stabilization,

formation of blowouts and parabolic dunes can produce localized reactivation of dunes in different sites at any time.

3.8. Acknowledgments

MM and GBF thank the Department of Geography, Universidade Federal Fluminense, and Flinders University for scholarships and cotutelle support for MM's research. This study was in part financed by the Coordenação de Aperfeiçoamento da Pessoa de Nível Superior - Brazil (CAPES). PH, GMdS and RK thank the Hesp Foundation, Beads Lab, and College of Science and Engineering, Flinders University for support.

3.9. References

Ardon, K., Tsoar, H., Blumberg, D.G. 2009. Dynamics of nebkhas superimposed on a parabolic dune and their effect on the dune dynamics. *Journal of Arid Environments*, 73(11), 1014-1022. <https://doi.org/10.1016/j.jaridenv.2009.04.021>

Australian Bureau of Meteorology. 2018. Climate Statistics Meningie Weather Station. Retrieved 24 July, 2018 from http://www.bom.gov.au/climate/averages/tables/cw_024518.shtml

Boak, E.H., Turner, I.L. 2005. Shoreline definition and detection: a review. *Journal of coastal research*, 688-703. <https://doi.org/10.2112/03-0071.1>

Bourman, R.P., Murray-Wallace, C.V., Belperio, A.P., Harvey N. 2000. Rapid coastal geomorphic change in the River Murray Estuary of Australia. *Marine Geology* 170(1): 141–168. [https://doi.org/10.1016/S0025-3227\(00\)00071-2](https://doi.org/10.1016/S0025-3227(00)00071-2)

Bourman, R., Harvey, N., James, K.F. 2006. Evolution of the Younghusband Peninsula, South Australia: new evidence from the northern tip. *South Australian Geographical Journal*, 105, 37-50.

Bourman, R. P., Murray-Wallace, C. V., Harvey, N. 2016. *Coastal Landscapes of South Australia*. Adedaile, SA: University of Adelaide Press. <http://dx.doi.org/10.20851/coast-sa>

Fernandez, G.B., Pereira, T.G., Rocha, T.B., Maluf, V., Moulton, M.A.B., Oliveira Filho, S.R. 2017. Classificação morfológica das dunas costeiras entre o Cabo

Frio e o Cabo Búzios, litoral do estado do Rio de Janeiro. *Revista Brasileira de Geomorfologia*, 18(3): 595-622. <http://dx.doi.org/10.20502/rbg.v18i3.862>

Flinders, M. 1814. *A voyage to Terra Australis*. Atlas, G. & W. Nicol: London. Vol. 2. 613 pp.

Gilbertson, D.D. 1981. The impact of past and present land use on a major coastal barrier system. *Applied Geography* 1(2): 97–119. [https://doi.org/10.1016/0143-6228\(81\)90028-X](https://doi.org/10.1016/0143-6228(81)90028-X)

Guan, C., Hasi, E., Zhang, P., Tao, B., Liu, D., Zhou, Y. 2017. Parabolic dune development modes according to shape at the southern fringes of the Hobq Desert, Inner Mongolia, China. *Geomorphology*, 295, 645-655. <https://doi.org/10.1016/j.geomorph.2017.08.009>

Harvey, N. 2006. Holocene coastal evolution: barriers, beach ridges, and tidal flats of South Australia. *Journal of Coastal Research* 22(1): 90–99. <https://doi.org/10.2112/05A-0008.1>

Harvey, N., Bourman, R., James, K.F. 2006. Evolution of the Youngusband Peninsula, South Australia: new evidence from the northern tip. *South Australian Geographical Journal*, 105, 37-50.

Hernández-Cordero, A.I., Hernández-Calvento, L., Hesp, P.A., Pérez-Chacón, E. 2018. Geomorphological changes in an arid transgressive coastal dune field due to natural processes and human impacts. *Earth Surf. Process. Landforms*, 43: 2167– 2180. <https://doi.org/10.1002/esp.4382>

Hesp, P.A., Thom, B.G. 1990. Geomorphology and evolution of transgressive dunefields. In: *Coastal Dunes: Processes and Morphology*, Nordstrom K, Psuty N, Carter RWG (eds). John Wiley and Sons: Chichester; 235–288.

Hesp, P.A. 2001. The Manawatu dunefield: environmental change and human impacts. *New Zealand Geographer*, 57(2), 33-40. <https://doi.org/10.1111/j.1745-7939.2001.tb01607.x>

Hesp, P. A., Martínez, M. L., 2007. Disturbance processes and dynamics in coastal dunes. In: *Plant disturbance ecology: the process and the response*, Johnson, E.A., Miyanishi, K. Burlington, MA; 215-247.

Hesp, P.A., Martínez, M., Miot da Silva, G., Rodríguez-Revelo, N., Gutierrez, E., Humanes, A., Laínez, D., Montañó, I., Palacios, V., Quesada, A., Storero, L., González Trilla, G., Trochine, C. 2011. Transgressive dunefield landforms and vegetation associations, Doña Juana, Veracruz, Mexico. *Earth Surface Processes and Landforms* 36, 285–295. <https://doi.org/10.1002/esp.2035>

Hesp, P.A. 2013. Conceptual models of the evolution of transgressive dune field systems. *Geomorphology*, 199, 138-149. <https://doi.org/10.1016/j.geomorph.2013.05.014>

Hesp, P.A., Walker, I.J. 2013. Aeolian environments: coastal dunes. In: Treatise on Geomorphology, vol. 11, Aeolian Geomorphology, Shroder J. (Editor in Chief), Lancaster N, Sherman DJ, Baas ACW (eds), Academic Press: San Diego, CA; 109–133.

Hesp, P A., Smyth, T.A. 2019. Anchored Dunes. In Aeolian Geomorphology: A new Introduction, Livingstone, I., Warren A. (Eds.), Wiley-Blackwell: Hoboken, NJ, 157-178 . <https://doi.org/10.1002/9781118945650.ch7>

Hilton, M., Harvey, N., Hart, A., James, K.F., Arbuckle, C. 2006. The impact of exotic dune grass species on foredune development in Australia and New Zealand: a case study of *Ammophila arenaria* and *Thinopyrum junceiforme*. *Australian Geographer* 37(3): 313–334. <https://doi.org/10.1080/00049180600954765>.

Hilton, M., Harvey, N., James, K.F. 2007. The impact and management of exotic dune grasses near the mouth of the Murray River, South Australia. *Australasian Journal of Environmental Management* 14(4): 220–228. <https://doi.org/10.1080/14486563.2007.9725171>.

Hugenholtz, C.H., Wolfe, S.A. 2005. Biogeomorphic model of dunefield activation and stabilization on the northern Great Plains. *Geomorphology* 70(1-2): 53–70. <https://doi.org/10.1016/j.geomorph.2005.03.011>

Jackson, D.W., Costas, S., Guisado-Pintado, E. 2019a. Large-scale transgressive coastal dune behaviour in Europe during the Little Ice Age. *Global and Planetary Change*, 175, 82-91. <https://doi.org/10.1016/j.gloplacha.2019.02.003>

James, K.F. 2012. Gaining new ground: *Thinopyrum junceiforme*, a model of success along the South Eastern Australian coastline. The University of Adelaide. Doctoral Thesis. 221 p.

Luebbers, R.A. 1981. The Coorong Report: An Archaeological Survey of the Southern Youngusband Peninsula. Report for the South Australian Department of Environment and Planning.

Luebbers, R.A. 1982. The Coorong Report. An Archaeological Survey of the Northern Coorong. Adelaide, Australia: South Australian Department of Environmental and Planning.

Miot da Silva, G., Martinho, C.T., Hesp, P.aA., Keim, B.D., & Ferligoj, Y. 2013. Changes in dunefield geomorphology and vegetation cover as a response to local and regional climate variations. *Journal of Coastal Research*, 65(sp2), 1307-1312. <https://doi.org/10.2112/SI65-221.1>

Moulton, M., Hesp, P.A., Miot da Silva, G., Bouchez, C., Lavy, M., Fernandez, G. B. 2019. Changes in vegetation cover on the Youngusband Peninsula transgressive dunefields (Australia) 1949–2017. *Earth Surface Processes and Landforms*, 44: 459– 470. <https://doi.org/10.1002/esp.4508>.

-
- Murray-Wallace, C.V. 2018. Holocene Coastal Sedimentary Environments of the Coorong Coastal Plain, Southern Australia. In: Murray-Wallace, C. V. (ed.), Quaternary History of the Coorong Coastal Plain, Southern Australia: An Archive of Environmental and Global Sea-Level Changes (pp. 81-114). Cham, Switzerland: Springer International. <https://doi.org/10.1007/978-3-319-89342-6>.
- Pickart, A.J., Hesp, P.A. 2019. Spatio-temporal geomorphological and ecological evolution of a transgressive dunefield system, Northern California, USA. *Global and planetary change*, 172, 88-103. <https://doi.org/10.1016/j.gloplacha.2018.09.012>
- Pye, K., Tsoar, H. 1990. Aeolian sand and sand dunes. Springer Science & Business Media.
- Silva, F.G., Wijnberg, K.M., de Groot, A.V., Hulscher, S.J. 2018. The influence of groundwater depth on coastal dune development at sand flats close to inlets. *Ocean Dynamics*, 68(7), 885-897. <https://doi.org/10.1007/s10236-018-1162-8>
- Short, A.D., Hesp, P. 1984. Beach and dune morphodynamics of the South East Coast of South Australia. Coastal Studies unit technical Report 84/1, Department of Geography, The University of Sydney, 142pp.
- Short, A.D. 1988. Holocene coastal dune formation in southern Australia: a case study. *Sedimentary Geology* 55(1-2): 121–142. [https://doi.org/10.1016/0037-0738\(88\)90093-0](https://doi.org/10.1016/0037-0738(88)90093-0).
- Tsoar, H. 2005. Sand dunes mobility and stability in relation to climate, *Physica A: Statistical Mechanics and its Applications*, 357(1), 50-56. <https://doi.org/10.1016/j.physa.2005.05.067>
- Tsoar, H., and Blumberg, D.G. (2002). Formation of parabolic dunes from barchan and transverse dunes along Israel's Mediterranean coast. *Earth Surface Processes and Landforms*, 27(11), 1147-1161. <https://doi.org/10.1002/esp.417>
- Yan, N., Baas, A.C. 2015. Parabolic dunes and their transformations under environmental and climatic changes: Towards a conceptual framework for understanding and prediction. *Global and Planetary Change*, 124, 123-148. <https://doi.org/10.1016/j.gloplacha.2014.11.010>
- Yan, N., Baas, A.C. 2017. Environmental controls, morphodynamic processes, and ecogeomorphic interactions of barchan to parabolic dune transformations. *Geomorphology*, 278, 209-237. <https://doi.org/10.1016/j.geomorph.2016.10.033>
- Yizhaq, H., Ashkenazy, Y., Tsoar, H. 2007. Why do active and stabilized dunes coexist under the same climatic conditions?. *Physical Review Letters*, 98(18), 188001. <https://doi.org/10.1103/PhysRevLett.98.188001>
- Yizhaq, H., Ashkenazy, Y., Levin, N., & Tsoar, H. (2013). Spatiotemporal model for the progression of transgressive dunes. *Physica A: Statistical Mechanics and its Applications*, 392(19), 4502-4515. <https://doi.org/10.1016/j.physa.2013.03.066>

Chapter 4 - Surfzone-beach-dune interactions along a variable low wave energy dissipative beach

Martim A.B. Moulton^{1,2}

Patrick A. Hesp¹

Graziela Miot da Silva¹

Robert Keane¹

Guilherme B. Fernandez²

¹BEADS Laboratory, College of Science and Engineering, Flinders University, South Australia.

²LAGEF Laboratory, Department of Geography, Universidade Federal Fluminense, Rio de Janeiro, Brazil.

4.1. Abstract

In this study, we discuss the different possible factors that influence or drive the observed volumetric and morphological variation in foredunes located along 16 km of the low wave energy, dissipative southern section of the 190 km long Youngusband Peninsula (South Australia). Grain size, wind energy, and coastline orientation are similar along this coast providing a unique site to study other drivers of coastal change. Results show that foredune height and volume progressively increases towards the north coincident with a gradual increase in wave energy. A significant correlation between foredune volume and wave energy was established, while no apparent relationship with other controlling factors was found, confirming the importance of wave energy in the dune building process on wave-dominated beaches. Results of this study indicate that (1) all other factors being equal, wave energy alone can significantly drive the morphological evolution of foredunes, and (2) minor changes in wave energy can result in differences in the long-term dune sediment budget.

Key words: Surfzone-beach-dune interactions; foredunes; wave energy; sediment transport.

4.2. Introduction

The development of dunes adjacent to the coast is determined by the combination of physical processes and environmental conditions that enable sediments to be transported from the surfzone to the beach, and onshore across the beach to accumulate behind the backshore and beyond (Trenhaile, 1997; Hesp, 2002; Davidson-Arnott, 2010; Hesp and Walker, 2013). Aeolian and hydrometeorological processes, together with the characteristics of sediments, surfzone-beach type, width and mobility, sediment supply, shoreline orientation, and presence/absence of vegetation and other roughness elements dictate the rate of landwards sediment transport that is essential for the dune building process (Short and Hesp, 1982; Sherman and Bauer, 1993; Nordstrom, 2000; Bauer *et al.*, 2009; Houser, 2009; Hesp, 2012; Hesp and Walker, 2013; McLachlan and Defeo, 2017; Brodie *et al.*, 2019; Doyle *et al.*, 2019).

Few studies have attempted to create empirical and conceptual models to explain surfzone-beach-dune interactions. Examples include Hesp (1982), Short and Hesp, (1982), Psuty (1988, 1992), and Sherman and Bauer, (1993). Several studies have subsequently attempted to either summarise these models to various degrees or analyse individual driving factors related to these models (Hesp, 1988; Sherman and Lyons, 1994; Aagaard, *et al.*, 2004; Psuty, 2008; Bauer *et al.*, 2009; Houser, 2009; Davidson-Arnott, 2010; Hesp, 2012; Aagaard *et al.*, 2013; Hesp and Smyth, 2016). Despite these efforts, the role and degree of importance of each individual factor driving the dune building process is still debatable and this is primarily due to the fact that in nature these factors cannot usually be easily separated (Bauer *et al.*, 2009).

Hesp (2012) argued that one of the many important tasks that need to be done in order to increase our understanding of the links and interactions between surfzones, beaches and dune systems, is to find and study coastal sites where one potential driving factor changes while the rest remain the same, or nearly so.

The 190 km long Younghusband Peninsula (Southeast coast of the State of South Australia) was utilized as a laboratory for the surfzone-beach-dune model developed by Hesp (1982) and Short and Hesp (1982) due to its significant variation in wave energy and minimal difference in wind energy along that barrier system. The model considers wave energy to be the principal explanatory factor for alongshore variations in foredune development and Holocene dune evolution along the barrier, assuming a minimum sediment supply is available.

In a subsequent study on the Younghusband Peninsula (YP), Hesp (1988) compared the differences between two distinct sections of the Holocene barrier-beach system that have similar grain sizes, wind energy, and dissipative modal beach state, but completely different wave energy conditions (one high, the other low). He concluded that approximately 20% of the volumetric variation in the foredunes (volumetrically greater in the high energy dissipative zone) could be credited to variations in wave-induced on-shore sediment transport to the beach and backshore alone. However, one might argue that these changes in dune development could be attributed to other factors, such as the differences in coastline orientation, wind speed variability, and aeolian sediment transport along this extensive barrier.

The southern end of the YP, however, provides an ideal laboratory to investigate the role of the different controlling factors or drivers of dune development. In this low energy dissipative surfzone-beach section of the

peninsula (Figure 4.1), there is a marked alongshore morphological variation in the active foredune and relict foredune system (landwards of the foredune). This variation occurs in an environment in which the potential driving or controlling factors are very similar. It thus provides a propitious site for studying surfzone-beach-dune interactions at a more detailed scale than previously conducted. In this study, we investigate the different potential controlling factors of the alongshore volumetric and morphological differences in foredunes situated in this 16 km long section of the YP.

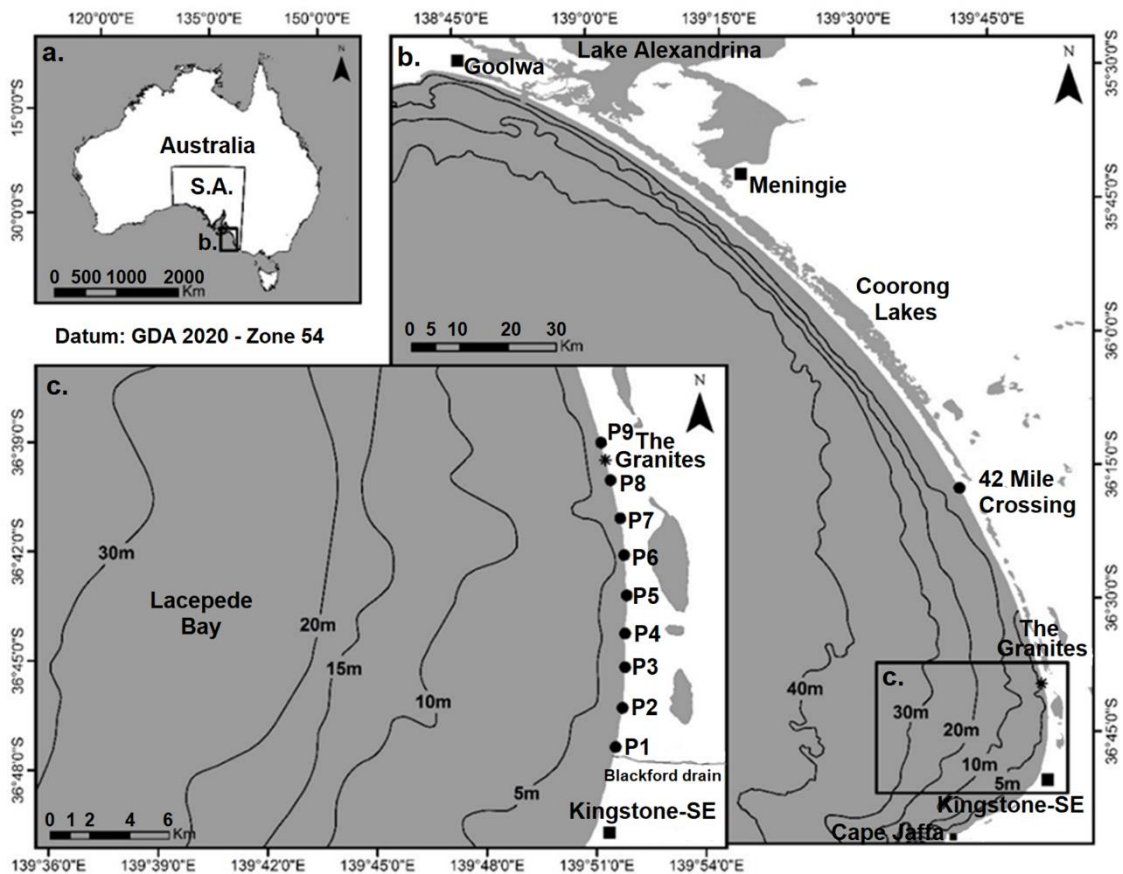


Figure 4.1 – Location of the study area in South Australia (a), at the southern end of the YP system (b), and the location of the 9 profile sites (P1 to P9) where topographic surveys were performed. (c) Bathymetric information adapted from the Australian Hydrographic Service (2001).

4.2.1. The development of Surfzone-beach-dune interaction models

In the late 1970's and 1980's several studies focused on beach morphodynamics in order to better understand the relationships between wave energy, sediment transport and beach morphology (Sonu, 1973; Chappell and Eliot, 1979; Short, 1978; 1979; 1980; 1 *et al.*, 1979; Goldsmith *et al.*, 1982; Wright and Short, 1984). Wright and Short (1984) proposed a surfzone-beach model for classifying and predicting changes in beach type or modal state (the most common morphological state of a beach) based on prior beach classification efforts from Sonu (1973), Short (1979), Wright *et al.* (1979) and others. The principle of this model is that the morphodynamic beach/surfzone spectrum is a function of the wave height at the breaking point (H_b) and beach sediment size (Wright and Short, 1984). The model has been widely accepted as it has wide applicability for micro-tidal beaches around the world (e.g. Thom and Hall, 1991; Swales, 2002; Ranasinghe *et al.*, 2004; Benedet *et al.*, 2006; Short, 2006; Pereira, *et al.*, 2010; Saravanan *et al.*, 2011), and, in fact, later in the 1990's, other researches extended this model to different tidal (Masselink, 1993; Masselink and Short, 1993; Masselink and Turner, 1999) and multi-bar surfzone types (Short and Aagaard, 1993).

By observing southeast Australian micro-tidal beaches, Wright and Short (1984) concluded that high wave energy combined with fine sediments typically generated wide, low gradient surfzones and dissipative beaches, while low wave energy associated with coarser sediments typically generated narrow, steep gradient modal reflective beaches. Between these two end members, a range of intermediate surfzone–beach types exist, typified by complex surfzone and beach morphologies and the presence of rips (Wright and Short, 1984). Variations to

this model occur due to various combinations of wave energy and sediment size. As noted by Wright and Short (1984), it is possible to have dissipative beaches in low wave energy environments due to the presence of very fine sand (with low gradients), and reflective beaches in high wave energy environments where beaches are composed of coarse sediments (e.g. cobbles to boulders).

4.2.2. Connection to the backshore and dunes

Subsequent studies extended the surfzone-beach model to the backshore and dunes (Hesp, 1982; Short and Hesp, 1982; Sherman and Bauer, 1993). Based on extensive beach profile monitoring and observations of Holocene sediment volumes on micro-tidal eastern and south-eastern beaches of Australia, Hesp (1982) and Short and Hesp (1982), were able to establish theoretical and physical links between wave energy, surfzone-beach type, intertidal/sub-aerial beach morphology and mobility, aeolian flow dynamics and sediment transport, and adjacent dune development and morphology. In this model, the authors argue that net onshore sediment transport from the surfzone to the backshore, driven by marine processes, and from backshore to dunes, driven primarily by aeolian processes, are potentially at their highest on dissipative beaches and lowest on reflective beaches.

According to Short and Hesp (1982), the differences in dune-building capability between the different beach types were related to several factors that control aeolian sediment transport and sediment supply, such as intertidal/subaerial beach morphology, beach/backshore width, and beach mobility. Despite criticism by a few authors that the model does not explain how the sediment is delivered grain by grain to the beach (e.g. Houser, 2009), this medium to long-term model rather considers net, long term transport and is widely

used or demonstrated to work within various coastal environments (e.g. Miot da Silva *et al.*, 2012; Houser and Mathew, 2011; Dillenburg *et al.*, 2016; Fernandez *et al.*, 2017; Brodie *et al.*, 2017; Short and Wright, 2018).

4.2.3. Controlling factors of foredune development

4.2.3.1. Beach morphology and wind flow

The intertidal/subaerial beach morphologies of each modal beach type produce differences in wind flow that result in variations in across-beach aeolian sediment transport (Hesp, 1982; Short and Hesp, 1982; Sherman and Lyons, 1994; Namikas and Sherman, 1997; Hesp and Smyth, 2016). On reflective beaches, the presence of steep berms, and beach faces and flat to concave terrace surfaces disturb the wind flow such that they act to reduce the wind velocity and consequently there is less aeolian sediment transport from the beach to dunes, resulting in small foredunes in the long term. In contrast, dissipative beaches display a low gradient, flat and to slightly concave sub-aerial beach morphology, no berms, and a wider backshore, providing less reduction in wind velocity across the beach and backshore that leads to a greater aeolian sand transport potential and higher/wider foredunes. Intermediate beaches display a wider range of beach/backshore morphologies, displaying at times more dissipative sub-aerial beach morphological characteristics, and at other times more reflective characteristics. Thus, aeolian transport capability can also vary considerably. Short and Hesp (1982), states that dissipative beaches have approximately 60% higher long-term net aeolian sediment transport compared to reflective beaches. These findings were confirmed by aeolian sediment transport simulations in Sherman and Lyons (1994), Namikas and Sherman (1997), and

Hesp and Smith (2016). Sherman and Lyons (1994) showed that sand transport was 20% higher on a dissipative beach compared to a reflective beach even though both model beaches had the same backshore widths (which almost never occurs in nature). When moisture was added into the model calculations, transport rates were two orders of magnitude higher on the dissipative beach (Sherman and Lyons, 1994; Hesp and Smyth, 2016).

4.2.3.2. Beach Width

The width of the beach is also regarded as an important controlling factor for cross-shore aeolian sediment transport in the model, since the extent of the beach and particularly dry backshore influences the extent of the wind fetch and therefore the amount of sediment available for aeolian transport (Short and Hesp, 1982; Davidson-Arnott and Law, 1996; Bauer and Davidson-Arnott, 2003; Davidson-Arnott *et al.*, 2005; Bauer *et al.*, 2009; Houser and Hamilton, 2009; Houser and Mathew, 2011; Silva *et al.*, 2019). Since dissipative beaches generally display wider beaches and backshores than reflective beaches, they often present a greater fetch length favouring greater dune formation (Short and Hesp, 1982). However, since moisture is a major impediment for aeolian sediment transport (Sherman and Lyons, 1994; Davidson-Arnott *et al.*, 2005; Bauer *et al.*, 2009), the tidal amplitude and extent of wave inundation by run-up must be considered (Masselink, 1993; Houser and Mathew, 2011). At short time scales, the low gradient of dissipative beaches can be a negative factor for aeolian sediment transport, since water levels, especially during storm surges, reach further landwards than on intermediate beaches for example, resulting in a reduction of dry-beach area and consequently limiting sediment availability for

wind transport (Houser and Mathew, 2011). Recent research, however, shows that the lower the gradient on dissipative beaches, the wider the dry beach becomes (Díez *et al.*, 2018).

The fetch can also be further influenced by the orientation of the beach in relation to the predominant wind direction (Short and Hesp, 1982; Bauer and Davidson-Arnott, 2003; Bauer *et al.*, 2009; Miot da Silva and Hesp, 2010; Delgado-Fernandez and Davidson-Arnott, 2011; Miot da Silva *et al.*, 2012). Onshore winds that approach the shoreline at an oblique angle tend to have greater potential for aeolian sand transport than perpendicular onshore winds, due to an increase in fetch (Arens *et al.*, 1995; Bauer and Davidson-Arnott, 2003; Miot da Silva and Hesp, 2010). The variation in aeolian sediment transport potential caused by changes in shoreline orientation, especially in narrow fetch limited beaches, can be a determinant for dune formation (Arens *et al.*, 1995; Bauer and Davidson-Arnott, 2003; Anthony *et al.*, 2006; Miot da Silva and Hesp, 2010), sometimes even more so than wind velocity (Delgado-Fernandez and Davidson-Arnott, 2011).

4.2.3.3. Beach Mobility

The degree of topographic variation of a beach over time (in essence the degree of cut and fill), termed beach mobility (Short and Hesp, 1982), also influences the long-term sediment delivery from the beach to the dunes (Short and Hesp, 1982; Short, 1988; Battiau-Queney *et al.*, 2003; Hesp and Smyth, 2016). Dissipative and reflective beaches have low mobilities and relatively lower frequency of erosional episodes. Intermediate beaches, due to the complexity of the surfzone circulation and presence of rips, have moderate to high sub-aerial beach mobility, with narrow beach widths at times and wide beach widths at

others which regularly alters the beach width, wind fetch, and airflow (due to greater topographic disturbances), therefore limiting long-term dune evolution (Short and Hesp, 1982; Hesp, 1988; Short, 1988; Battiau-Queney *et al.*, 2003). The higher mobility of intermediate beaches is one of the main arguments as to why intermediate beaches are considered to have less dune-building potential than dissipative beaches (Short and Hesp, 1982; Short, 1988; Battiau-Queney *et al.*, 2003).

4.2.3.4. Wave Energy

Wave energy is also considered to be one of the main controlling factors of dune and coastal barrier development (Short and Hesp, 1982; Short, 1988; Hesp, 1988; Aagaard *et al.*, 2004; Dillenburg *et al.*, 2009; Martinho *et al.*, 2009; Miot da Silva and Hesp, 2010; Miot da Silva *et al.*, 2012; Dillenburg *et al.*, 2016; Cohn *et al.*, 2018; 2019a), because (combined with local sediment grain size) it influences the surfzone and beach slope gradient (Wright and Short, 1984), which in turn influences the wind-driven sediment transport potential to dunes (Short and Hesp, 1982). It also drives considerable changes in onshore sediment supply to the beach and backshore (Short and Hesp, 1982; Short, 1988; Psuty, 1988; Aagaard *et al.*, 2004; Miot da Silva *et al.*, 2012; Dillenburg *et al.*, 2016; Cohn *et al.*, 2018; 2019a).

The low gradient and typically high wave energy environment of dissipative beaches provides a greater onshore wave driven sediment supply compared to intermediate and reflective beaches, according to Short and Hesp (1982). This relationship between beach type, wave energy, sediment supply, and dune growth, was also observed in both field and computer simulations (Aagaard *et al.*, 2004; Miot da Silva and Hesp, 2010; Miot da Silva *et al.*, 2012; Cohn *et al.*,

2018; 2019a), with higher wave energy resulting in higher shorewards sediment transport and an increase in foredune development. Aagaard *et al.* (2013) discussed whether high wave energy on dissipative beaches led to onshore or offshore transport and computer simulations showed dissipative beaches have relatively low rates of sediment transport compared to intermediate beaches and typically display an offshore net transport due to steady currents (cf. Van Rijn, 1999; Aagaard *et al.*, 2002).

However, more recent work supports the contention of onshore net sediment transport is, in fact, the rule on high energy dissipative beaches (Aagaard *et al.*, 2013; Cohn *et al.*, 2019a). Cohn *et al.* (2019b) have further demonstrated that wave inundation and/or erosion of the upper backshore is less common on low gradient wide beaches such as dissipative beaches than on steeper gradient high energy intermediate beaches. In addition, large-scale modelling of barrier evolution during the Holocene sea level transgression demonstrates that onshore transport is the norm (e.g. Cowell *et al.*, 1995). As Hesp and Smyth (2016) note, it is a fact that very many of the largest coastal barrier systems on Earth exist on dissipative and high energy intermediate beaches.

4.3. Study area

The Youngusband Peninsula (YP), located on the Southeast Coast of South Australia (Figure 4.1), is the longest Holocene sandy barrier in Australia, with ~190 km of continuous beach. It is considered one of the classic examples of dissipative beach systems, with fine sand and long period, high energy waves (for most of the extent of the beach) (Short, 2006). This extensive barrier displays

very distinct physiographical and morphological variations from its northern (35°33'24"S / 138°52'56"E) to its southern end (36°49'16"S / 139°51'2"E) (Short and Hesp, 1984).

Fluvial sediment input to the ocean is minimal (Bourman *et al.*, 2000), therefore the primary source of sediments to the YP is from the continental shelf, and predominantly comprises carbonate sediments which have been supplied since the post-glacial Holocene marine transgression to form the existing coastal beach-dune barrier (Thom and Roy, 1985; Short 1988; 2010; Murray-Wallace, 2018). The YP is exposed to some of the world's largest waves in the Southern Ocean (Hemer *et al.*, 2008; Hemer and Griffin 2010), with deep-water waves commonly exceeding 5 meters (Short, 1988). Wave measurements at Cape du Couedic on Kangaroo Island, (295 km from the study site), show an annual average significant wave height of 2.7 m, with a 12 s period and a predominant primary swell direction coming from the Southwest quadrant (Hemer *et al.*, 2008). Along the YP, wave energy within the surfzone progressively increases northwards mainly as a result of variations in the width and depth of the inner shelf and nearshore (Short and Hesp, 1982). According to Short and Hesp (1982), breaker wave height in the northern end of the peninsula is approximately 10 times higher than the southern end, producing surfzones that extend from 150 m to 400 m in width in the north. In contrast, the surfzone is narrow in the southern end of the peninsula (Kingston-SE), ranging from virtually non-existent surfzones near Kingston-SE (during fair weather conditions) to ~130 m wide maximum at "The Granites" (Figure 4.1).

The northern section of the YP begins at the mouth of the Murray River and is separated from the continent by the Coorong lagoon system. In this part

of the barrier, surfzones are high energy and dissipative, and transgressive dunes predominate and reach up to 40 meters above Mean Sea Level (MSL) (Short and Hesp, 1984; Hesp, 1988; Harvey, 2006; Bourman *et al.*, 2006; Moulton *et al.*, 2019). The central section is high energy intermediate and the barrier comprises mainly parabolic dunes and transgressive dunefields. In the southern end of the peninsula, the surfzone-beach type switches to a low energy dissipative system. The barrier comprises a few parabolic dunes and principally a relict foredune complex. South from “The Granites” (Figure 4.1), the barrier is dominated by a foredune plain, with negligible dune transgression. This section of the YP has a stationary to slightly prograding shoreline, with a stable foredune system (Short and Hesp 1984). The dominant seawardmost aeolian features are 2 to 6m high active foredunes (most seaward dunes) followed landwards by sequences of relict foredunes that decrease in altitude and volume from north to south (Short, 1988). The survey area in this study is located within the Southern portion of the YP, between Blackford Drain (close to Kingstone-SE) and “The Granites” (Figure 4.1), covering approximately 16 km of beach.

The meteorological station at Cape Jaffa (20 km southwest of the study site – Figure 4.1), reveals that the southern end of the YP is predominantly subjected to winds from the S to SW quadrant (Figure 4.2a), comprising 45.5% of the total winds in the region with an average wind speed of 7 ms⁻¹. Although the southerly winds are prevailing (11.95% of the occurrences), winds from SSW (9.20%), SW (8.17%), WSW (7.57%) and W (7.48%) are also common and have a high potential for sediment transport (Figure 4.2b). Northerly winds are also frequent (8.6%) but have a lower transport potential (Figure 4.2b) than winds from

the previously mentioned directions. The aeolian sediment transport resultant is to the NE (Figure 4.2b).

The tidal regime for the region is micro-tidal and semi-diurnal (0.8m). The entire barrier system is classified as a wave-dominated environment, even in the low energy southern end (Short and Hesp, 1984). Alongshore sediment transport is presumed to be minimal or absent along the YP coastline (Short and Hesp, 1982; Thom and Roy, 1985).

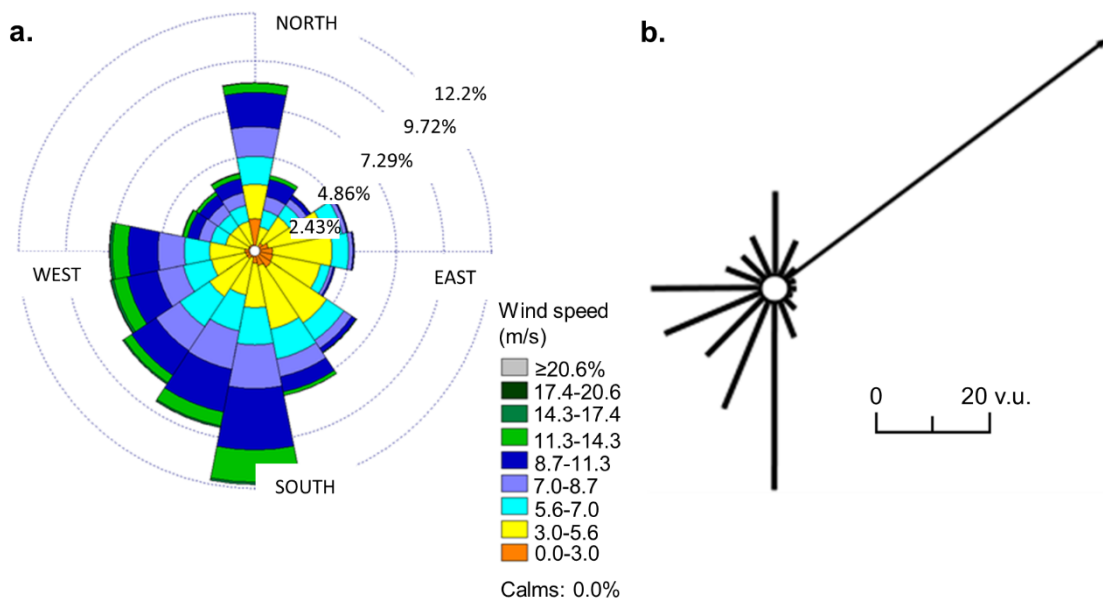


Figure 4.2 – (a) Wind rose and (b) Sand rose (based on $m\ sec^{-1}$ data) for the study area, arrow indicates the resultant sediment transport vector. (Wind data from Cape Jaffa Meteorological Station - 1991 to 2017 - Bureau of Meteorology [2017]).

4.4. Methods

Field campaigns to conduct topographic measurements, collection of sediment samples, and visual observations of breaker wave height were carried out on 16/04/2016, 15/04/2017 and 10/04/2018. In addition, numerical wave

modeling and aerial photography/satellite imagery analyses were performed to estimate alongshore wave energy and beach width.

4.4.1. Topography and bathymetry

Nine two-dimensional, cross-shore topographic profiles were spaced at 2 km starting just northwards of Kingstone-SE (Figure 4.1) in order to characterize the morphology and temporal variability of the sub-aerial beach and foredunes along the 16 km stretch of coast (Figure 4.1).

The profiles were surveyed using an Integrated GNSS System (Trimble R10), on “Continuous Topo mode”, 1 point per second, using real-time vertical correction giving a horizontal precision between 0.020 and 0.024 m, and vertical precision between 0.048 and 0.053 m. All profiles were initiated in the swale located landwards of the foredunes and extended across the beach to the swash limit. At sites 3 and 6, the topographic profiles were also extended landwards of the foredunes to the back of the Holocene barrier to verify the maximum altitude of the relict foredunes.

High resolution Light Detection and Ranging (LiDAR) data (± 50 cm horizontal and ± 15 cm vertical spatial accuracy) of the entire study area was obtained from the Department for Environment and Water of South Australia (DEW). This data is part of the Climate adaptation project led by DEW, the SA Coast Protection Board, SA Water, and local governments, to collect high precision elevation of the entire coast of the state of South Australia. The LiDAR data was used to create a Digital Elevation Model (DEM) which enabled a precise analysis of the entire Holocene barrier topography. Five equally spaced profile transects (every 4 km) extending 280 m landwards from the backshore were

generated to compare the alongshore morphological changes of the relict foredunes.

The foredune volume estimations were performed using an integration method to calculate the area of the two-dimensional topographic profiles and estimate the volume of the dune section (Birkemeier, 1984). The first swale of each profile was chosen as the most landward limit of active sedimentation and base of the foredune lee slope. The point where the backshore reaches +2 m above Australian Height Datum (AHD which = 0.0 m) was chosen as the seaward limit of the foredune as height represents the typical top of the backshore/toe of the foredune.

Digital Surface Models (DSM's) were also constructed for 3 of the profile sites using a Remotely-Piloted Aircraft (RPA), DJI Phantom 3 Professional model, in April 2017 and processed using PIX4D Mapper software. The RPA survey was consistently conducted in an area 40 m long by 40 m wide, covering the foredunes, beach and backshore. The flights were performed at a height of 10 m above ground, using a double grid mission with 70% side-overlap and 80% frontal-overlap between frames, giving an average Ground Sampling Distance (GDS) between 0.38 and 0.40 cm. The selected sites for performing the 3D morphology were P1, P5, and P9. These sites were selected due to their being representative of the southernmost, middle and northernmost portions of the study area. The objective was to obtain a more detailed 3D morphology of these different sites.

Bathymetric data were obtained from the Australian Hydrographic Service, in order to identify potential differences in nearshore topography along the study area. Data from Bathymetric Charts Aus347 and Aus127 (Australian

Hydrographic Service, 2001) were used to create a Digital Elevation Model (DEM) of the nearshore. Topographic profiles were created using ArcMap 10.4 Software, starting from each subaerial profile site to the 30 m depth contour line following a straight line at a 90° angle from the shoreline at each of the sites.

4.4.2. Beach width

Beach width and dry beach width were measured in order to evaluate potential alongshore variations that could be contributing to variations in the sediment availability for aeolian transport from the beach to the dunes. Measurements were performed both by topographic profile surveys (2016, 2017 and 2019) and remotely, using the available open source imagery with sufficient spatial resolution and visibility (7 RapidEye Satellite Imagery [from 2012 to 2018], 3 Google Earth Historical Imagery [from 2011, 2014 and 2015] and 1 orthorectified orthomosaic provided by DEW [2013]). Beach width was measured at each site from the shoreline, defined as the toe of the active foredune (Boak and Turner, 2005), to the water line. Dry beach was measured from the toe of the active foredune to the high tide swash limit (only in images where this limit was evident). An average of the beach width and dry beach width was used for each profile site, since tidal height was different in different imagery dates and between field campaigns.

4.4.3. Grain size analysis

Sediment samples were collected at all 9 profile sites during the first field campaign (16/04/2016), on the subaerial, intertidal beach (*beach* samples) and foredune crest (*dune* samples), to compare grain sizes along the survey area. Samples were processed in the laboratory after (1) 24h of drying in an oven at 80°C to facilitate sieving; (2) separation of large sediments using a 1mm sieve;

(3) granulometry analysis of sub-samples using a Malvern Mastersizer 2000; (4) data analysis using Gradistat to determine median grain size and sorting, and categorized according to the parameters of the geometric method of moments following Blott and Pye (2001).

4.4.4. Wave energy

Wave energy was measured via: (1) visual observations of breaker wave height in the field; (2) number of breaking waves; (3) surfzone width; (4) distance from the beach to the landward edge of seagrass; and (5) numerical modelling. Alongshore variations in wave height of the outermost breaking wave were obtained at each of the nine field sites by visual observation during field campaigns, following methods by Short (1985).

Additionally, breaker wave height was estimated using numerical modelling to estimate wave height and energy dissipation at each profile along the study area (Figures 4.1 and 4.3). A process-based simulation model, Delft3D Version 04.04.01 (Lesser *et al.*, 2004), coupled with SWAN (Simulating Waves Nearshore) as the wave module was utilized.

The model was set up for the Lacepede Bay large domain (spatial resolution 3 km) using Geoscience Australia bathymetric data (available from the Delft Dashboard), with a nested approach (300 meters spatial resolution) in the study area (Figure 4.3). 17 years (2000-2016) of measured wave data (height and period) from Cape du Couedic (Kangaroo Island) were analysed to extract a period representative of average and storm conditions within the data for model validation via RMSE (Root Mean Square Error) metric.

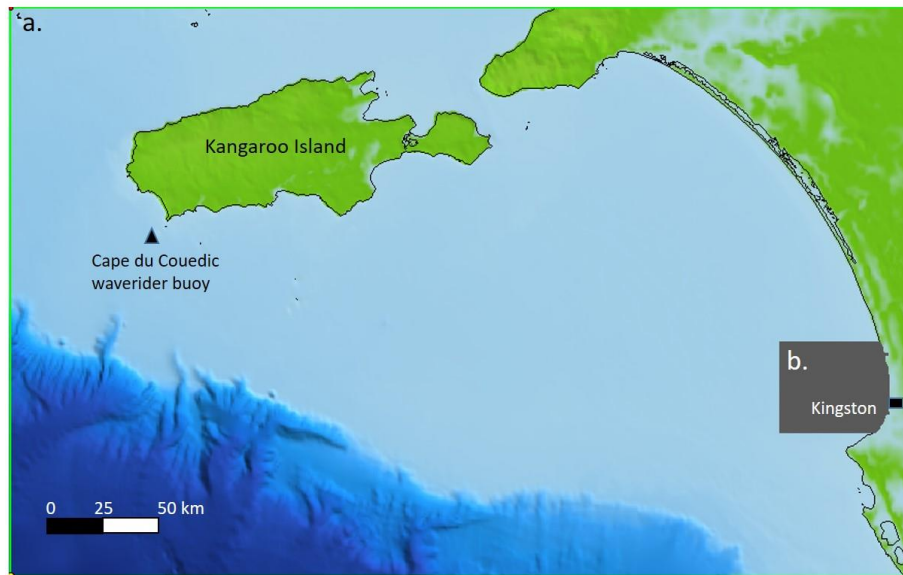


Figure 4.3 – Wave modelling domain showing the large and nested grids. Wave propagation for average and storm conditions were simulated across the large domain (a) which provided boundary conditions to the nested domain. (b) Model validation was performed using measured significant wave height (H_s) from the Cape du Couedic wave buoy (black triangle next to Kangaroo Island).

Wave energy was further measured by visual observations of the number of breaking waves at each site during field campaigns. Surfzone width (distance between the most seaward breaking wave and the swash limit), and distance from the shore to the edge of seagrass were measured using the same imagery utilised to calculate beach width. Shoreline position was considered in all measurements as being the crest of the active dune since it is the most stable and easily recognizable feature in all images (Boak and Turner, 2005). In low energy environments the inner limit of seagrass meadows is a reliable indicator of long-term nearshore wave energy (Infantes *et al.*, 2009). The lower the wave energy, the closer to the shore that seagrass may grow.

4.4.5. Shoreline orientation and aeolian drift potential

Variability in wind exposure due to changes in shoreline orientation was analyzed by measuring the angle of the shoreline relative to North (0°) at each of

the nine sites via aerial photography and comparing with aeolian Resultant Drift Potential (RDP) calculations.

RDP's were calculated for the study site via the Fryberger and Dean (1979) method, using the geographically closest available wind data (in ms^{-1}), from the Cape Jaffa Meteorological Station (data extends from 1991 to 2017). The threshold velocity (V_t) for saltation was determined based on the mean grain size of the study area following methods in Miot da Silva *et al.* (2012) and is 6.35 ms^{-1} .

RDP's were also calculated for each profile site by excluding offshore winds and alongshore winds (depending on the shoreline orientation at each site) following Arens *et al.* (1995) and Miot da Silva and Hesp (2010), in order to identify possible changes in aeolian sediment transport from the beach to the dunes due to changes in shoreline orientation relative to dominant sand transporting winds.

Alongshore winds are considered here to be winds that come directly alongshore parallel to the orientation of the foredune toe (i.e. at 0°) and to $\leq 15^\circ$ from the ocean relative to the shoreline orientation (Figure 4.4). Onshore winds are those winds approaching from the ocean and reaching the shoreline at an angle greater than $>15^\circ$. Offshore winds are all winds that arrive from the continent with an angle greater than 0° and $\leq 180^\circ$ relative to the local shoreline orientation (Figure 4.4).

To evaluate site-specific changes in terms of aeolian sediment transport rates, RDP results in vector units were converted to rates of sand drift in $\text{m}^3/\text{m}/\text{year}$ as proposed by Bullard (1997).

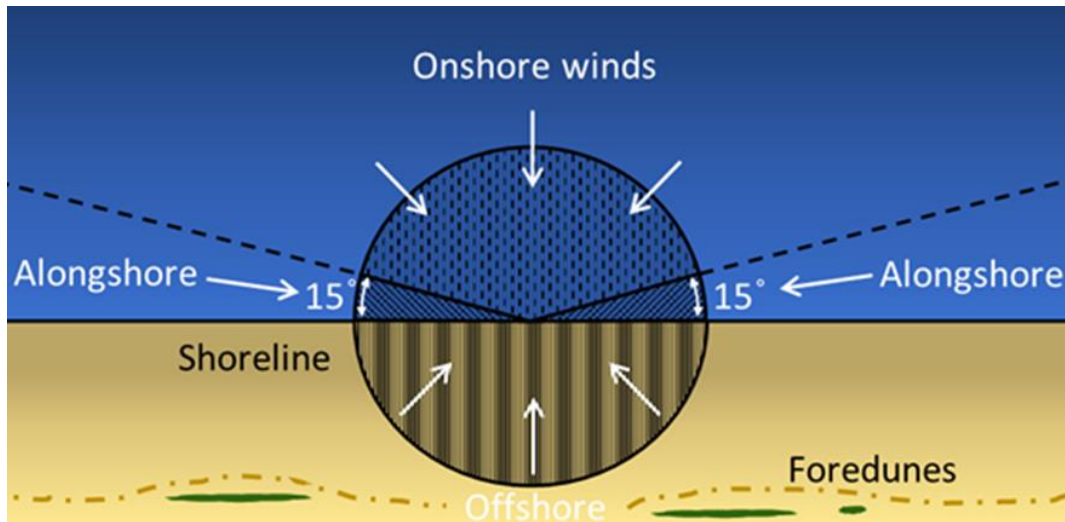


Figure 4.4 – Illustration showing the definitions used for determining onshore, alongshore and offshore winds.

4.5. Results

4.5.1. Beach and Foredune Topographic Variability

Foredune height increases from the southernmost site (P1) to the northernmost site (P9) (Figure 4.5). The topographic surveys from the 3 different years (2016, 2017 and 2018) show that at the first 4 sites, P1 to P4, foredunes have crest heights ranging from 2.5 m (P2 in 2017) to 3.5 m (P4 in 2018) above mean sea level (MSL) (Figure 4.5). These four sites also display similar morphological characteristics and occasionally also have incipient foredunes present. (Figure 4.5). A clear swale occurs in the lee of the foredunes at all these four sites, backed by relict foredunes that reach up to 5 m above MSL (Figure 4.8a). At these four profiles sites dune scarping was not present in the 2016 survey, but was present in the 2017 survey and showed signs of scarp fill and recovery in 2018 (Figure 4.5).

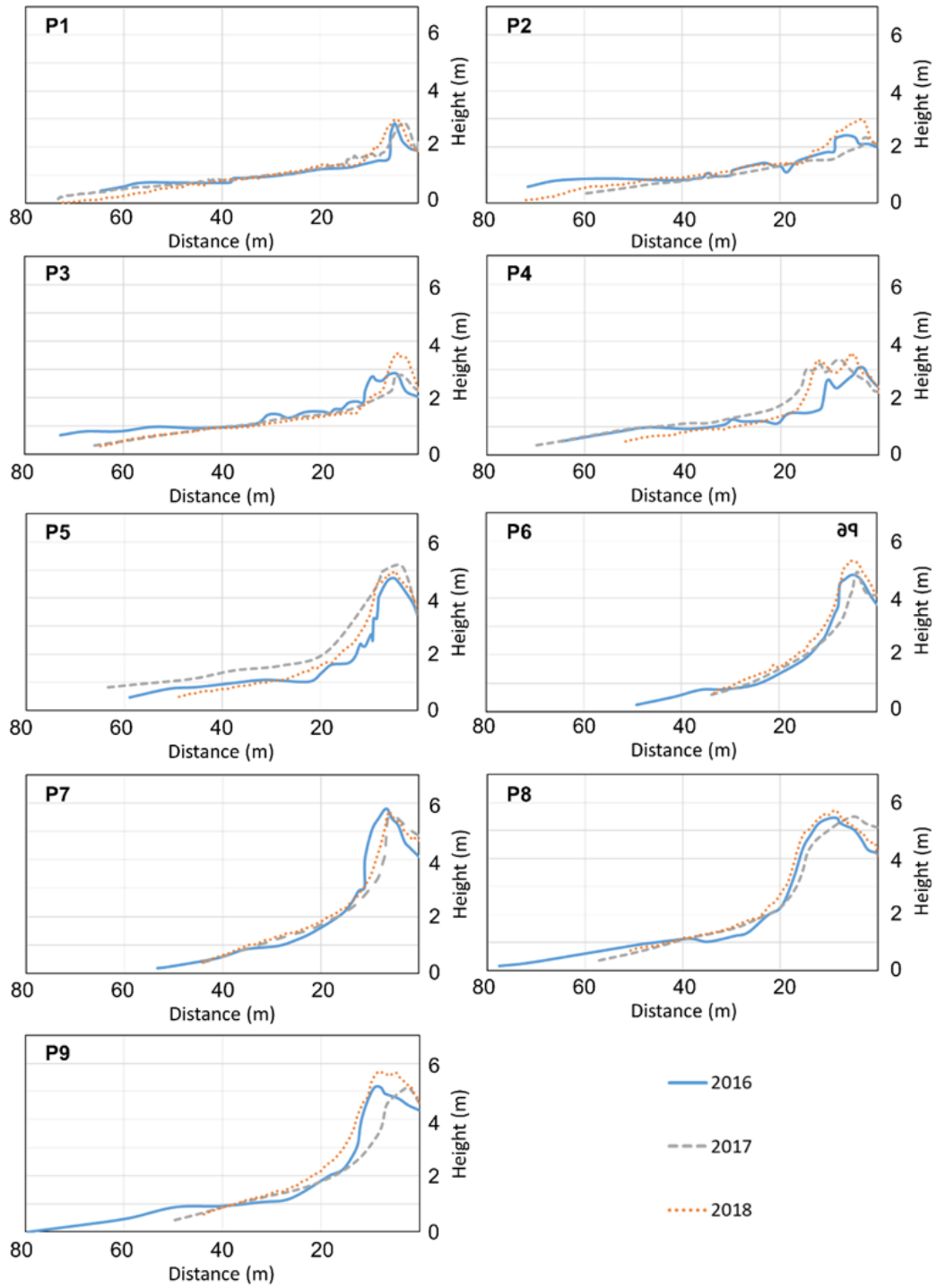


Figure 4.5 –Two-dimensional topographic profile measurements for the 9 sites between 2016 and 2018. Dune height increases from P1 to P9.

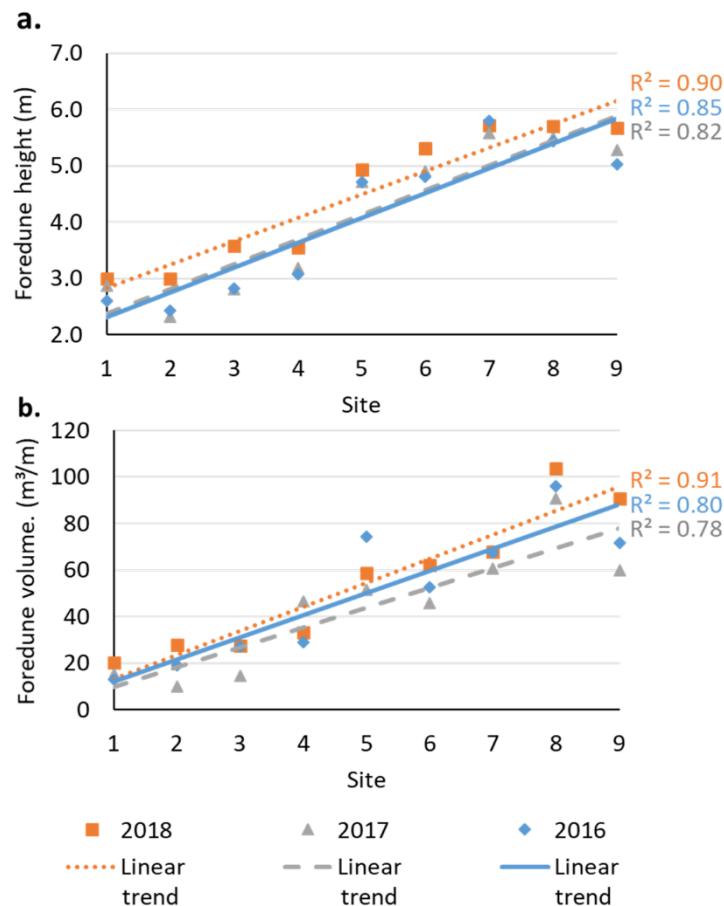


Figure 4.6 – South to North alongshore variation in (a) foredune height and (b) foredune volume at each site for each of the 3 years surveyed. In all surveys, a northwards increase in both foredune height and volume occurs from P1 to P9). Trendlines are indicated for the different years.

The foredunes at profiles P5 to P9 are considerably higher than at the first 4 profiles, with dune crests varying from 4.6 meters (P5 in 2016) to 5.8 meters (P8 in 2018) above MSL (Figure 4.5). Incipient foredune formation is absent at these sites, and the seaward slope is steeper than at the southern profiles P1 to P4 (Figure 4.5). Pronounced storm scarping with slumped sections were evident in all three surveyed years, especially 2017. In 2018 scarp/fill morphologies were observed, revealing that the foredune had gone through recovery processes.

In all of the 3 surveyed years (2016, 2017, and 2018) the foredune height (Figure 4.6a), and also the foredune volume (Figure 4.6b) showed an increasing

trend from South (P1) to North (P9). Volumetric estimates ranged from 16 m³/m (2016-2018 average of P1) to 96 m³/m (average of P8) (Figure 4.6b). A significant change in foredune volume can also be seen between the 4 first sites and the following 5 sites, with sites P1 to P4 ranging between 16 and 36 m³/m, and sites P5 to P9 ranging between 53 and 96 m³/m, with a considerable increase occurring between sites P4 and P5.

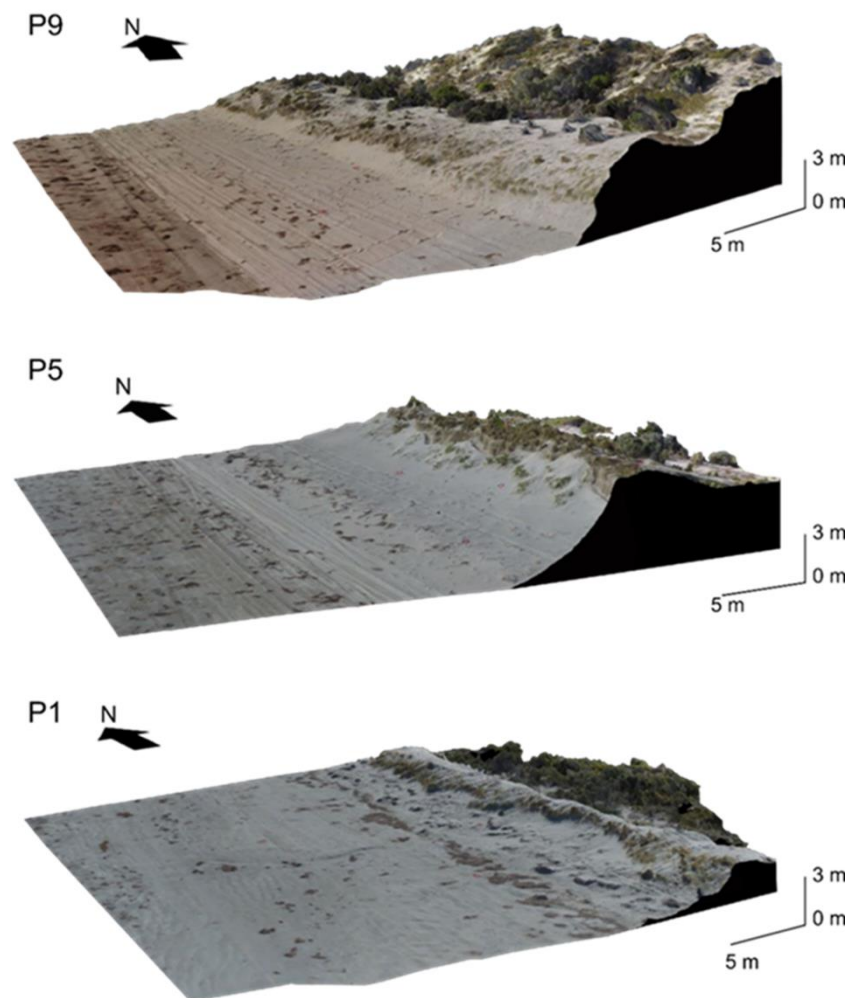


Figure 4.7 – RPA derived Digital Surface Models for P1, P5, and P9, showing the significant northwards increase in height and volume of the foredune from South (P1) to North (P9).

Although foredune height measurements do not significantly change from April 2016 to April 2017 (Figure 4.6a), foredune sediment volume does (Figure 4.6b), which could be attributed to scarping/recovery of the foredunes due to a series of storms that impacted the South Australian coast in the second half of 2016. A field excursion in July 2016 revealed that water levels reached the foredune stoss slope. However, by April 2018, the P6 to P9 foredunes had recovered and dune volumes had increased (Figures 4.5 and 4.6b).

The northwards increase in foredune height is also apparent in the Digital Surface Models (DSM's) produced from RPA surveys with the vegetation removed (Figure 4.7). The DSM's demonstrate that in the most southern site, P1, the foredune is less than 3 m high (Figure 4.7). At P5, the midpoint between the southernmost and northernmost sites, the foredune is 5m. The most northern site, P9, shows higher foredunes, with the foredune reaching 6 m in height.

Relict Foredune Plain

The Holocene barrier along this section of coast comprises a relict foredune plain as noted above. Changes in dune height and volume can also be observed in this barrier system, and the relict foredunes formed behind the modern active foredunes show a similar increase from South to North. Figure 4.8 illustrates the elevational changes in the modern foredune and landward relict foredunes.

The five profile transects (locations indicated on Figure 4.8) demonstrate a considerable increase in height and volume of the relict foredunes landwards of the modern foredune with the dunes on the most southern profile reaching a maximum height of ~6m (Figure 4.8 – P1) while the dunes at the most northern

profile reaching a maximum height of ~16m (Figure 4.8- P9). These differences indicate that the same drivers or controls on foredune morphology have been operating for the late Holocene at least, and likely the entire evolutionary period (~6,500 years) of the coastal barrier.

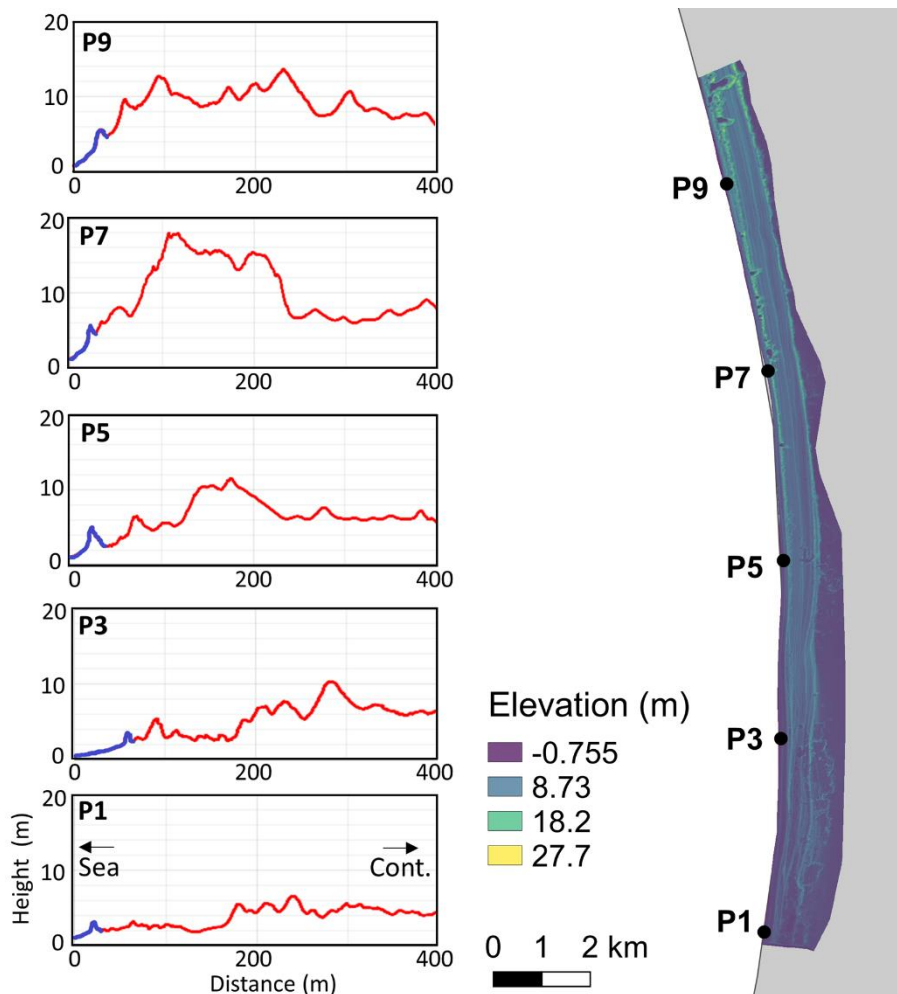


Figure 4.8 – LiDAR DEM of the study area showing elevational changes alongshore and the 5 selected profiles (P1, P3, P5, P7 and P9). A substantial difference in height and volume of the modern (blue line) and relict foredunes (red line) from south to north. LiDAR - Horizontal datum: GDA2020. Vertical datum: AHD (Australian Height Datum).

4.5.2. Beach Width

The average beach width for each profile site shows a slight decrease in beach width from P1 to P9, especially from P3 to P7 (Figure 4.9). However, when

the wet sand portion is removed from the measurements and examine only the *dry beach portion*, this decrease cannot be observed. In fact, the data shows no significant alongshore changes in average beach width for each profile site (Figure 4.9).

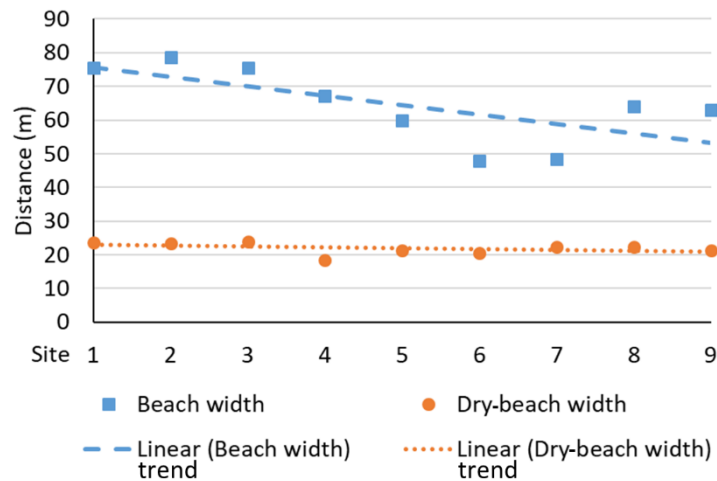


Figure 4.9 – Average beach width and dry beach width for each of the profile sites. The linear trendline shows a decrease in wet and dry beach width from North to South, but little variation in terms of dry-beach width.

4.5.3. Grain size analysis

Dune samples (collected at the foredune crest) from P1 to P9 were classified as moderately well sorted, fine to very fine sand, and display a uniform mean grain size alongshore (Figure 4.10).

Beach samples (collected in the swash zone) showed a higher heterogeneity in grain size and sorting alongshore, varying from moderately sorted to moderately well sorted, gradually increasing northwards in mean diameter from fine to medium sand (Figure 4.10). A distinction in mean grain size between P1 to P4 and P5 to P9 can be seen (Figure 4.10), with an average grain size of 0.16 mm in the four southernmost sites compared to 0.23 mm in the five northernmost sites.

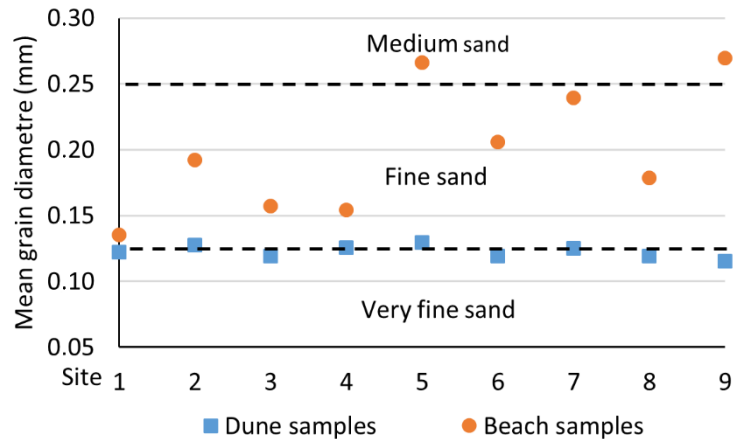


Figure 4.10 – Mean grain size diameter of beach and dune samples for each of the 9 sites. Black dashed lines represent the limits of each sediment size class.

4.5.4. Shoreline orientation and aeolian drift potentials

Resultant Drift Direction (RDD) and Resultant Drift Potential (RDP) calculated using all wind directions, indicate a NE landward sediment transport resultant for the study area (Figure 4.2b). A total Drift Potential (DP) of 155 v.u. was calculated, which is classified as a high wind-energy environment according to Bullard (1997).

Although the shoreline within the study area generally follows a N/S orientation, it nonetheless displays a gentle curvature and rotates slightly from NNE/SSW to NNW/SSE from south to north (Figure 4.11 and table 4.1). Therefore, the shoreline in the study area can be split in 3 sections according to its orientation: a NNE/SSW orientation (P1 and P2), a N/S orientation (P3 to P6) and a NNW/SSE orientation (P7 to P9) (Figure 4.11 and table 4.1).

Resultant drift potential (RDP) calculations were performed for each of these 3 sections using the average shoreline orientation angle for each (Table 4.1), in order to examine differences in onshore sand transport (if any) along the study area. These analyses first exclude offshore winds, and then offshore and

alongshore winds (Figure 1.11 and table 4.1). The results show that the slight changes in shoreline orientation could potentially affect the amount of sand transported from beach to dune by the wind (Table 4.1) due to the increased exposure to the SSW winds from P3 northwards and also S winds from P7 northwards (Figure 1.11).

Table 4.1 – Shoreline angle and estimates of aeolian drift potential and their relative rate of sand drift for sites P1 to P9 assuming equal beach sediment supply.

	Shoreline orientation (degrees)	Mean shoreline orientation (degrees)	Approximate shoreline orientation	RDP without offshore winds (v.u.)	Rate of sand drift ($\text{m}^3/\text{m}^{-1}\text{yr}^{-1}$)	RDP without offshore + alongshore winds (v.u.)	Rate of sand drift ($\text{m}^3/\text{m}^{-1}\text{yr}^{-1}$)
P1	196	192.5	NNE/SSW	96.9	8.7	85.0	7.7
P2	189						
P3	180	181.5	N/S	105.1	9.5	101.8	9.2
P4	183						
P5	180						
P6	183						
P7	165	166	NNW/SSE	125.7	11.3	107.1	9.2
P8	168						
P9	165						

However, when RDP is converted to estimated rate of sand drift, the differences in sediment transport between each section of the beach are not very significant (Table 4.1). The greatest difference in rate of sand drift was found between the 2 southern profiles and the 3 northern profiles using an RDP calculated without offshore winds, being $2.6 \text{ m}^3/\text{m}/\text{year}$. The difference between the average volume of the 2 southern profiles ($17.5 \text{ m}^3/\text{m}$ – average of the 3 surveyed years) and the 3 northern profiles ($78.7 \text{ m}^3/\text{m}$) is $61.2 \text{ m}^3/\text{m}$, far greater than the sand transport rate difference. Additionally, profiles P3 and P6 have the same shoreline orientation, therefore the same estimated rate of sand drift per year, but a significant difference in dune volume ($30 \text{ m}^3/\text{m}$).

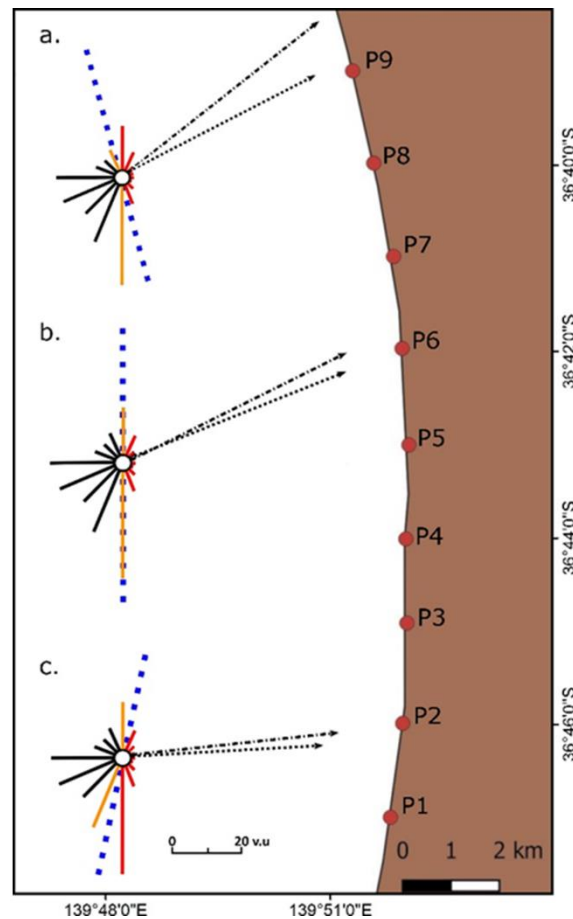


Figure 4.11 – Sand roses (a, b and c) for the 3 different sections of shoreline orientation observed in the study area. The dotted blue line in each sand rose indicates the mean orientation for that section of coast. The red solid lines are the drift potential (DP) of offshore winds and the orange solid line the DP of alongshore winds. The dashed black arrow is the RDP/RDD excluding offshore DP's. The dashed and dotted arrow is the RDP/RDD excluding offshore and alongshore DP's.

4.5.5. Wave energy alongshore variability

A consistent increase from south to north was found in all the various indicators of wave energy (Table 4.2). Breaker wave height (both visually measured and estimated by wave modeling), the number of breaking waves, surfzone width, and the distance from the shoreline to where seagrass occurs all increase from P1 to P9 (Table 4.2).

Results from breaker wave height estimations made from both visual measurements and computer modeling at each site demonstrate an increase in

wave energy from south to north (Figure 4.12). The model produced more conservative values compared to visual measurements (Figure 4.12); nonetheless, both show an increase from P1 to P9, as seen in the linear trend lines with significant R^2 regression values (0.81 and 0.96, for observed and modelled data respectively).

Table 4.2 - Indicators of wave energy measured for each site. Numbers correspond to an average calculated from both field measurements and imagery for 8 different years.

Site	Modelled breaker wave height (m)	Observed breaker wave height (m)	Mean number of breaking waves	Mean Surfzone width (m)	Mean Distance to seagrass (m)
P1	0.68	0.35	0.00	1	334
P2	0.69	0.45	1.00	28	387
P3	0.75	0.50	1.70	56	439
P4	0.81	0.50	2.00	55	456
P5	0.80	0.70	2.30	62	599
P6	0.84	0.90	3.00	79	718
P7	0.89	1.00	3.70	90	645
P8	0.82	1.00	4.00	120	744
P9	0.87	1.20	5.00	132	767

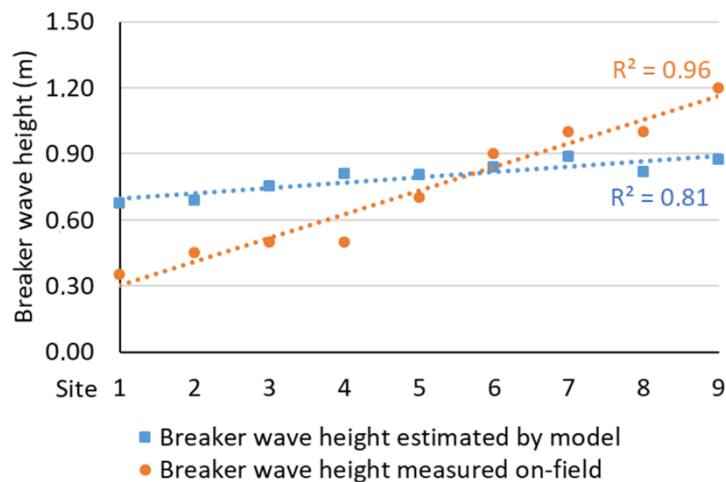


Figure 4.12 – Breaker wave height estimated by the model (square plots) and measured in-the field (round plots) at each site. Both methods show an increase in breaker wave height from South to North.

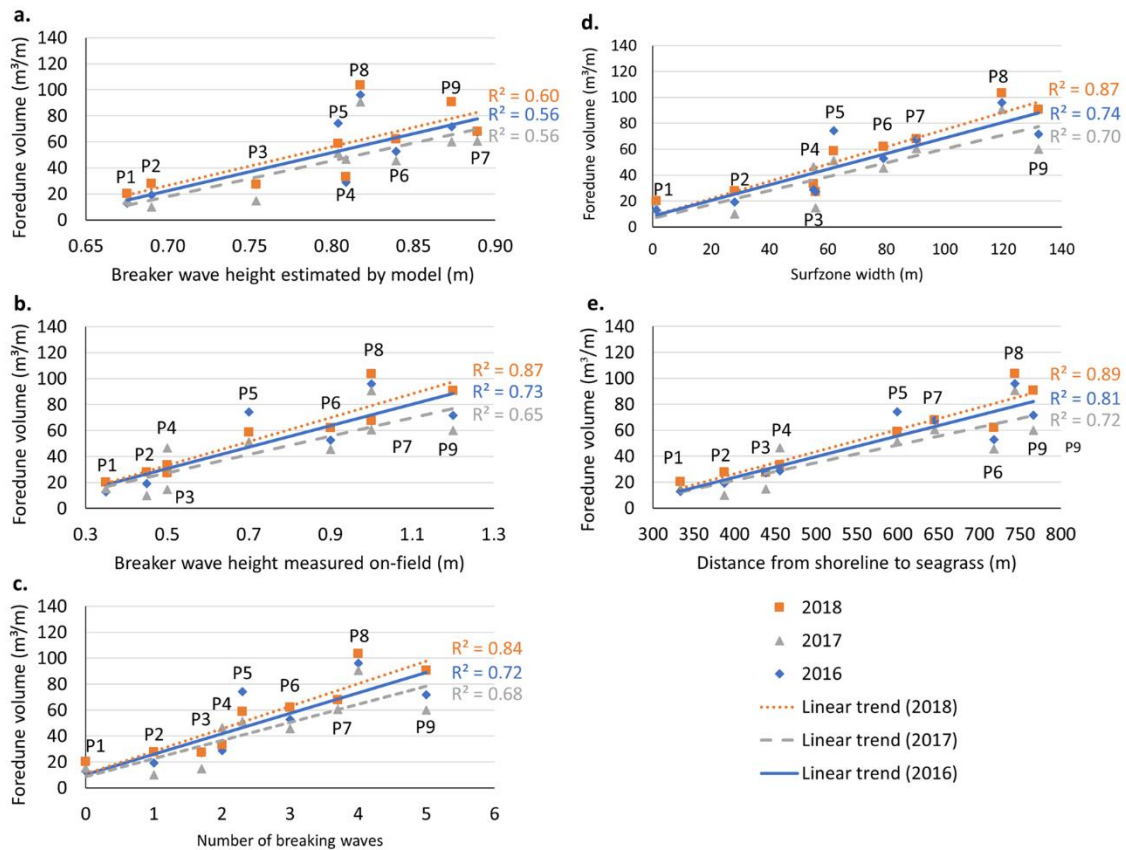


Figure 4.13 – Foredune volumes plotted against; (a) Breaker wave height estimated by the numerical model Delft3d; (b) Breaker wave height visually measured; (c) Number of breaking waves; (d) Surfzone width and (e) Distance to seagrass. All wave energy proxy indicators show a good to significant correlation with foredune volumes for the 3 different years.

Other wave energy indicators are presented here as additional methods of estimating wave energy (Table 4.2). These indicators were compared with foredune volumetric measurements, with good to excellent correlations in all of them (R^2 regressions ranging between 0.56 and 0.89) (Figure 4.13).

Volumetric measurements from 2017 had the weakest correlation with wave energy indicators of the 3 surveys (Figure 4.13), and 2018 had the most significant correlations. The weaker correlation seen in 2017 can be attributed to

a higher intensity of storm events at the end of 2016, considerably altering the foredune volume.

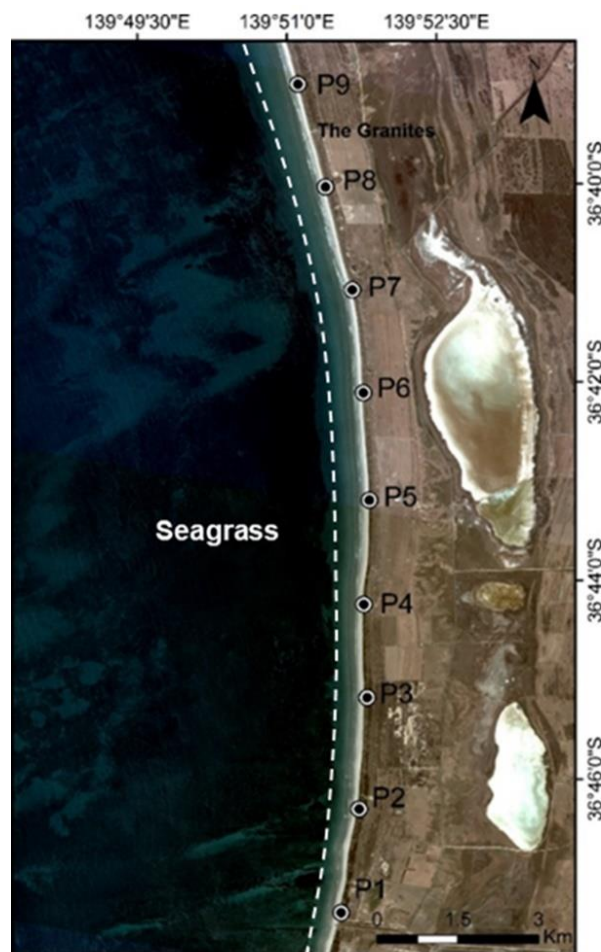


Figure 4.14 – Aerial photograph (2013) of the study area showing the seagrass meadow in the nearshore. An increase in the distance between the shoreline and the landward edge of the seagrass (white dashed line) can be observed from South to North, correlating with an increase in wave energy.

The wave energy indicator that had the least significant correlation with foredune volume was the modelled breaker wave height (Figure 4.13a) ($R^2 = 0.56$ – 2017), and the one that had the most significant correlation was distance to seagrass (Figure 4.13e) ($R^2 = 0.89$ – 2018).

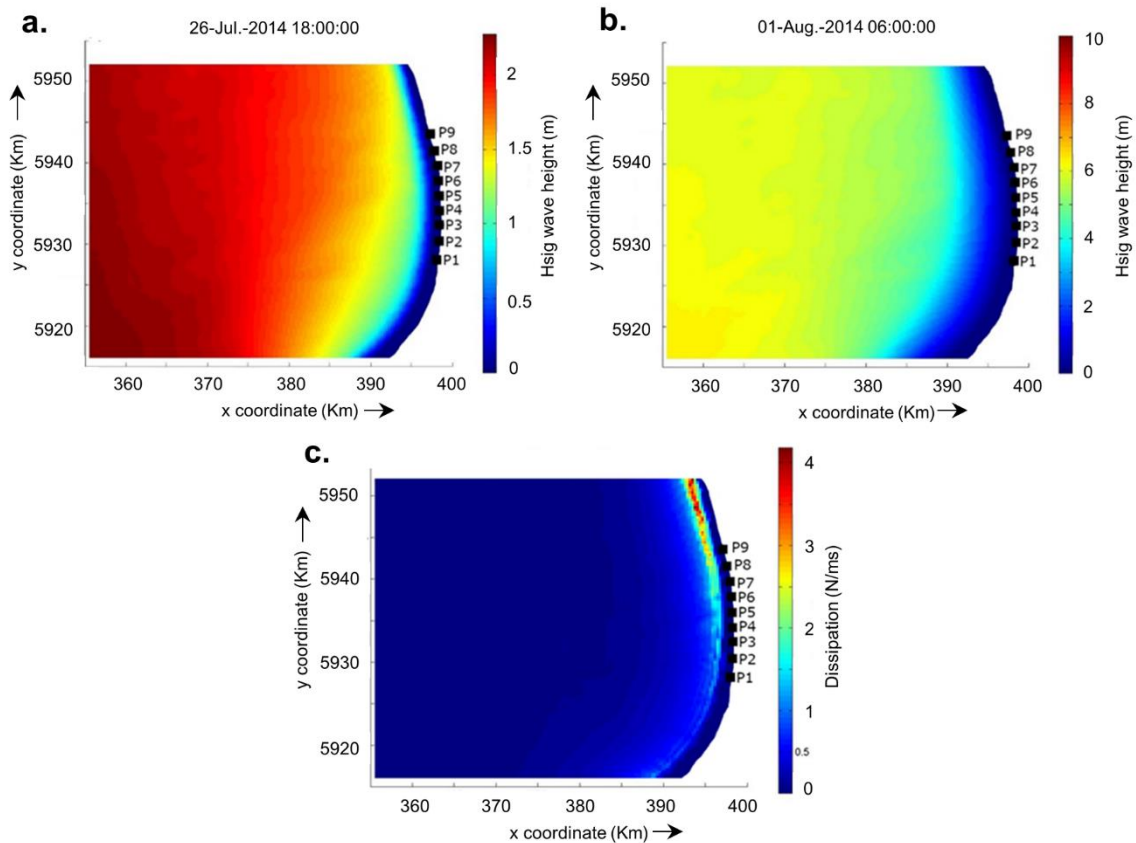


Figure 4.15 – Significant wave height (H_s) simulation for the study area using (a) storm conditions (wave direction 225° - wave period 7.7 s) and (b) average conditions (wave direction 225° - wave period 10.6 s). An increase in significant wave height (H_s) can be observed from South to North in both simulations. (c) Wave dissipation simulation results for average conditions. There is a clear increase from South to North indicating higher energy and more extensive surf zone towards the north.

The distance to seagrass showed a gradual increase from sites P1 to P9 (Figure 4.14), with the best correlation fit with foredune volume. It is noticeable however a considerable increase between P4 and P5 (Table 4.2 and Figure 4.13e). This increase in the distance of the seagrass meadow to the shoreline suggests that a more significant increase in wave energy occurs in this section of the coast, which was confirmed by visual observations (Figure 4.13b).

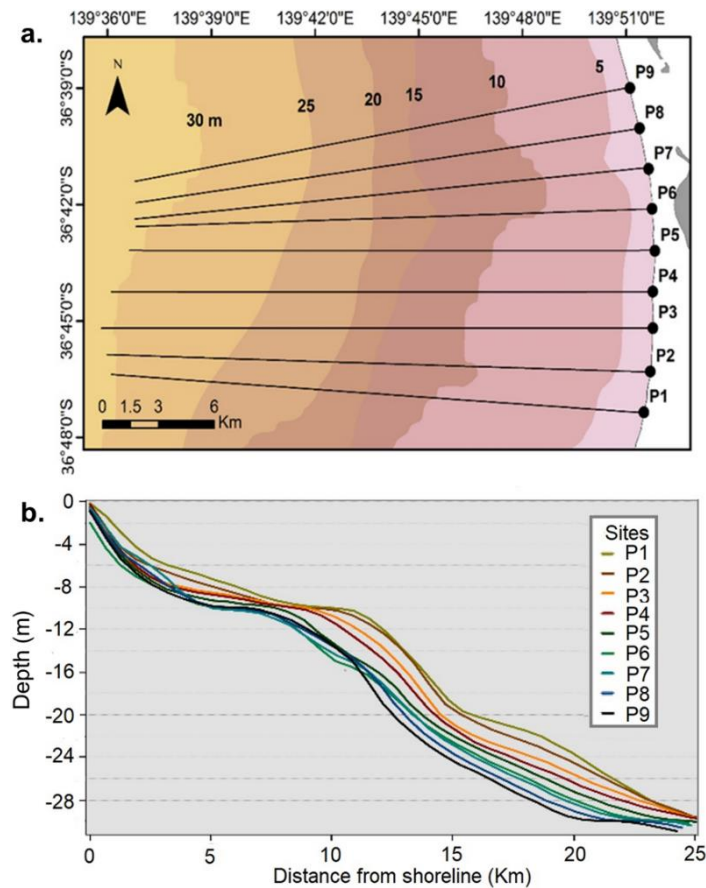


Figure 4.16 – (a) Detailed nearshore bathymetry for the study area (Adapted from the Australian Hydrographic Service, 2001) and location of the nearshore topographic profiles for each of the sites. (b) Subaqueous nearshore topographic profiles from each site revealing the slight increase in slope gradient from P1 to P9.

The wave modeling based on average wave conditions was utilised to confirm (or not) the existence of a gradual increase in breaker wave height from south to north in the study area (Figure 4.15). Despite the model validation using wave data from Cape Du Couedic buoy showing a general good agreement (RMSE = 0.598), the model tends to underestimate H_s especially during high wave energy events.

The wave modeling results also show that the alongshore variability in wave energy seen from South to North is produced by variations in nearshore slope (Figure 4.15). Slope gradient determines the degree of wave energy

dissipation, impacting directly on breaker wave height and surfzone width (Wright and Short, 1984). Detailed bathymetry of the nearshore for the study area shows an increase in steepness of the slope gradient from South to North, with significant topographic changes occurring between 0-15 m water depth (Figure 4.16a).

Bathymetric profiles of the nearshore (Figure 4.16), calculated for each of the sites, demonstrates this change with more accuracy, revealing a gradual steepening of the slope gradient from South (P1) to North (P9) (Figure 4.16b). The nearshore topographic profiles also reveal a significant increase in the slope gradient between P4 and P5 (P15b), suggesting again a more rapid increase in wave energy in this section of the coast.

4.6. Discussion

Alongshore variations in foredune volume are commonly caused by an increase in sediment availability (supply) for aeolian transport, an increase in aeolian transport due to changes in local or regional wind regimes, coastline orientation, fetch, grain size, surface roughness, beach moisture etc., surfzone-beach type changes, or a combination of these (Short and Hesp, 1982; Hesp, 1988; Psuty, 1988; Sherman and Bauer, 1993; Davidson-Arnott and Law, 1996; Houser, 2009; Houser and Mathew, 2011; Hesp and Smyth, 2016; Brodie *et al.*, 2017). The factors or drivers of the south to north increase in foredune volume measured within this 16 km section of the Younghusband Peninsula, are briefly discussed below.

One of the factors noted above that could lead to alongshore variability in cross-shore aeolian transport is sediment grain size variability. However, beach sand samples taken along the 16 km shoreline show a slight increase in mean

grain size from South to North (Figure 4.10), which in theory would lead to a decrease in aeolian sediment transport and lower foredune volumes towards the north. This minor increase from South to North, possibly related to the observed increase in wave energy (Prodger *et al.*, 2017), suggests that grain size does not have a significant impact on aeolian sediment transport within the study area

Changes in aeolian sediment transport due to variations in shoreline orientation may also be discarded as having any major effect on dune volumetric changes alongshore. While there is, in fact, subtle changes in shoreline orientation that lead to a minor increase in potential aeolian sand transport between sections of the study area (Table 4.2 and Figure 4.11), this corresponds to minimal changes in terms of m^3 of sand transport per year, and does not explain the alongshore differences in foredune volume (Table 4.2), as it does on many beaches (Davidson-Arnott *et al.*, 2005; Davidson-Arnott and Bauer, 2009; Delgado-Fernandez, 2010; Miot da Silva and Hesp, 2010; Delgado-Fernandez and Davidson-Arnott, 2011).

Amongst the many factors that could explain an increase in sediment availability, beach width does not provide any explanatory relationship. Not only do the dry beach width measurements show very little alongshore variability (Figure 4.9), but the beach width (including the wet to saturated zone) decreases from P1 to P9, which in theory means less sediment available for aeolian transport in the more northerly sites. In comparison to the findings of, for example, Davidson-Arnott and Law (1996), Díez *et al.* (2018), and Silva *et al.* (2019), where beach width, and especially dry beach width, was strongly correlated with sediment availability and foredune development, sediment availability does not seem to be influenced by this factor within the study area.

Wave energy, including all proxies of wave energy, was found to be the only variable that shows significant changes alongshore in parallel with foredune height and volume (Figure 4.11). There is also an abrupt rise in foredune height and volume between sites P4 and P5, exactly where the nearshore bathymetry (Figure 15b) and distance from seagrass measurements (Figure 11a) show a more acute increase in wave energy.

This suggests that higher wave energy results in higher sediment supply to the intertidal beach and backshore. This increase in sediment availability northwards then results in a higher net aeolian sediment transport from beach/backshore to the dunes creating low dunes in the south and higher, larger dunes in the north. This wave energy driver has also been operating throughout the past 6-7,000 years driving volumetric and elevational changes throughout the evolution of the entire barrier system.

4.7. Conclusion

A variety of factors such as grain size, beach width, wave energy, coastal orientation, and aeolian sediment transport, that might drive or produce an alongshore increase in foredune height and volume (including along and across the Holocene barrier) have been examined along 16 km of the low energy dissipative Younghusband Peninsula. A south to north increase in wave energy alongshore is considered the single most important factor influencing an alongshore increase in foredune height and volume.

These findings indicate that alongshore sand supply variability is more important than aeolian transport limitations for dictating foredune evolution in the

YP, and wave driven sediment supply to the beach and backshore is the principal control or driver of foredune (and relict foredune) evolution within the study area.

Results of this study indicate that all other factors being equal, wave energy alone can significantly drive the morphological evolution of foredunes, and, minor changes in wave energy can result in small to significant differences in long-term dune sediment budgets and dunefield evolution.

4.8. Acknowledgments

MM, PH and GMdS thank Flinders University for scholarships and cotutelle support for MM's research. MM and GBF thank the Department of Geography, Universidade Federal Fluminense for support. This study was financed by the Coordenação de Aperfeiçoamento da Pessoa de Nível Superior - Brazil (CAPES), the Hesp Foundation and BEADS Laboratory. PH and GMdS thank the College of Science and Engineering, Flinders University for support.

4.9. References

- Aagaard, T., Black, K.P., Greenwood, B. 2002. Cross-shore suspended sediment transport in the surf zone: A field-based parameterization. *Marine Geology*, 185(3–4): 283–302. [https://doi.org/10.1016/S0025-3227\(02\)00193-7](https://doi.org/10.1016/S0025-3227(02)00193-7).
- Aagaard, T., Davidson-Arnott, R., Greenwood, B., Nielsen, J. 2004. Sediment supply from shoreface to dunes: linking sediment transport measurements and long-term morphological evolution. *Geomorphology*, 60(1-2): 205-224. <https://doi.org/10.1016/j.geomorph.2003.08.002>.
- Aagaard, T., Greenwood, B., Hughes, M. 2013. Sediment transport on dissipative, intermediate and reflective beaches. *Earth-science reviews*, 124: 32-50. <https://doi.org/10.1016/j.earscirev.2013.05.002>.
- Anthony, E.J., Vanhee, S., Ruz, M.H. 2006. Short-term beach–dune sand budgets on the north sea coast of France: Sand supply from shoreface to dunes, and the role of wind and fetch. *Geomorphology*, 81(3-4): 316-329. <https://doi.org/10.1016/j.geomorph.2006.04.022>.

Arens, S.M., Van Kaam-Peters, H.M.E., Van Boxel, J.H., 1995. Air flow over foredunes and implications for sand transport. *Earth Surface Process Landforms*, 20: 315–332. <https://doi.org/10.1002/esp.3290200403>.

Australian Hydrographic Service. 2001. AUS 347 - Backstairs Passage to Cape Martin Nautical Chart (1:300000).

Battiau-Queney, Y., Billet, J.F., Chaverot, S., Lanoy-Ratel, P. 2003. Recent shoreline mobility and geomorphologic evolution of macrotidal sandy beaches in the north of France. *Marine Geology*, 194(1-2): 31-45. [https://doi.org/10.1016/S0025-3227\(02\)00697-7](https://doi.org/10.1016/S0025-3227(02)00697-7).

Bauer, B.O., Davidson-Arnott, R.G. 2003. A general framework for modeling sediment supply to coastal dunes including wind angle, beach geometry, and fetch effects. *Geomorphology*, 49(1-2): 89-108. [https://doi.org/10.1016/S0169-555X\(02\)00165-4](https://doi.org/10.1016/S0169-555X(02)00165-4).

Bauer, B.O., Davidson-Arnott, R.G.D., Hesp, P.A., Namikas, S.L., Ollerhead, J., Walker, I.J. 2009. Aeolian sediment transport on a beach: Surface moisture, wind fetch, and mean transport. *Geomorphology*, 105(1-2): 106-116. <https://doi.org/10.1016/j.geomorph.2008.02.016>.

Benedet, L., Finkl, C.W., Klein, A.H.F. (2006). Morphodynamic classification of beaches on the Atlantic coast of Florida: geographical variability of beach types, beach safety and coastal hazards. *Journal of Coastal Research*, sp39: 360-365. <http://www.jstor.org/stable/25741596>.

Birkemeier, W.A. 1984. Time scales of nearshore profile changes. In: *Proceedings of the 19th International Conference on Coastal Engineering* (pp. 1507-1521), Houston, Texas: Amer Society of Civil Engineers (ASCE). <https://doi.org/10.1061/9780872624382.103>.

Blott, S.J., Pye, K. 2001. GRADISTAT: a grain size distribution and statistics package for the analysis of unconsolidated sediments. *Earth surface processes and Landforms*, 26(11): 1237-1248. <https://doi.org/10.1002/esp.261>.

Bourman, R.P., Murray-Wallace, C V., Belperio, A.P., Harvey, N. 2000. Rapid coastal geomorphic change in the River Murray Estuary of Australia. *Marine Geology*, 170(1-2): 141-168. [https://doi.org/10.1016/S0025-3227\(00\)00071-2](https://doi.org/10.1016/S0025-3227(00)00071-2).

Bourman, R., Harvey, N., James, K.F. 2006. Evolution of the Younghusband Peninsula, South Australia: new evidence from the northern tip. *South Australian Geographical Journal*, 105: 37-50.

Brodie, K.L., Palmsten, M.L., Spore, N.J. 2017. Coastal Fore-dune Evolution, Part 1: Environmental Factors and Forcing Processes Affecting Morphological Evolution. US Army Corps of Engineers Coastal and Hydraulics Engineering Technical Note: 1-10. <https://apps.dtic.mil/dtic/tr/fulltext/u2/1028704.pdf>.

Brodie, K.L., Conery, I., Cohn, N., Spore, N., Palmsten, M. 2019. Spatial Variability of Coastal Fore-dune Evolution, Part A: Timescales of Months to Years.

Journal of Marine Science and Engineering, 7(5), 124.
<https://doi.org/10.3390/jmse7050124>

Bullard, J.E. 1997. A note on the use of the " Fryberger method" for evaluating potential sand transport by wind. *Journal of Sedimentary Research*, 67(3); 499-501. <http://dx.doi.org/10.1306/D42685A9-2B26-11D7-8648000102C1865D>.

Bureau of Meteorology - Climate statistics for Australian locations: Cape Jaffa. 2017. Retrieved September 18, 2017, from http://www.bom.gov.au/climate/averages/tables/cw_026095.shtml.

Chappell, J., Eliot, I.G. 1979. Surf-beach dynamics in time and space—an Australian case study, and elements of a predictive model. *Marine Geology*, 32(3-4): 231-250. [https://doi.org/10.1016/0025-3227\(79\)90066-5](https://doi.org/10.1016/0025-3227(79)90066-5).

Cohn, N., Ruggiero, P., de Vries, S., Kaminsky, G. 2018. New insights on the relative contributions of marine and aeolian processes to coastal foredune growth. *Geophysics Research Letters*, 45: 4965-4973. <https://doi.org/10.1029/2018GL077836>.

Cohn, N., Hoonhout, B.M., Goldstein, E.B., De Vries, S., Moore, L.J., Durán Vinent, O., Ruggiero, P. 2019a. Exploring Marine and Aeolian Controls on Coastal Foredune Growth Using a Coupled Numerical Model. *Journal of Marine Science and Engineering*, 7(1): 13. <https://doi.org/10.3390/jmse7010013>.

Cohn, N., Ruggiero, P., García-Medina, G., Anderson, D., Serafin, K.A., Biel, R. 2019b. Environmental and morphologic controls on wave-induced dune response. *Geomorphology*, 329: 108-128. <https://doi.org/10.1016/j.geomorph.2018.12.023>.

Cowell, P.J., Roy, P.S., Jones, R.A. 1995. Simulation of large-scale coastal change using a morphological behaviour model. *Marine Geology*, 126(1-4), 45-61. [https://doi.org/10.1016/0025-3227\(95\)00065-7](https://doi.org/10.1016/0025-3227(95)00065-7)

Davidson-Arnott, R.G., Law, M.N. 1996. Measurement and prediction of long-term sediment supply to coastal foredunes. *Journal of Coastal Research*, 12(3): 654-663. <https://www.jstor.org/stable/4298513>.

Davidson-Arnott, R.G.D., MacQuarrie, K., Aagaard, T., 2005. The effect of wind gusts, moisture content and fetch length on sand transport on a beach. *Geomorphology*, 63: 115–129. <https://doi.org/10.1016/j.geomorph.2004.04.008>.

Davidson-Arnott, R.G.D., Bauer, B.O. 2009. Aeolian sediment transport on a beach: thresholds, intermittency, and high frequency variability. *Geomorphology*, 105: 117–126.

Davidson-Arnott, R. 2010. *Introduction to Coastal Processes and Geomorphology*. Cambridge, UK: Cambridge University Press.

Delgado-Fernandez, I. 2010. A review of the application of the fetch effect to modelling sand supply to coastal foredunes. *Aeolian Research*, 2(2-3): 61-70.

Delgado-Fernandez, I., Davidson-Arnott, R. 2011. Meso-scale aeolian sediment input to coastal dunes: The nature of aeolian transport events. *Geomorphology*, 126(1-2): 217-232. <https://doi.org/10.1016/j.geomorph.2010.11.005>.

Díez, J., Cohn, N., Kaminsky, G. M., Medina, R., Ruggiero, P. 2018. Spatial and temporal variability of dissipative dry beach profiles in the Pacific Northwest, USA. *Journal of Coastal Research*, 34(3): 510-523. <https://doi.org/10.2112/JCOASTRES-D-17-00149.1>.

Dillenburg, S.R., Barboza, E.G., Tomazelli, L.J., Hesp, P.A., Clerot, L.C.P., Ayup-Zouain, R.N. 2009. The Holocene Coastal Barriers of Rio Grande do Sul. In: *Lecture Notes in Earth Sciences: Geology and Geomorphology of Holocene Coastal Barriers of Brazil* (Vol.107, pp.53-91), Dillenburg, S.R. and Hesp, P.A. (eds.). Berlin, Heidelberg: Springer.

Dillenburg, S.R., Hesp, P.A., Cecilio, R., Miot da Silva, G. 2016. Wave Energy as a Control on Dune Development on two Regressive Barriers in Southern Brazil. *Journal of Coastal Research*, 75(sp1): 273-277. <https://doi.org/10.2112/SI75-55.1>.

Doyle, T.B., Short, A.D., Ruggiero, P., Woodroffe, C.D. 2019. Interdecadal Foredune Changes along the Southeast Australian Coastline: 1942–2014. *Journal of Marine Science and Engineering*, 7(6), 177. <https://doi.org/10.3390/jmse7060177>

Fernandez, G.B., Pereira, T.G., Rocha, T.B., Maluf, V., Moulton, M.A.B., Oliveira Filho, S.R. 2017. Classificação morfológica das dunas costeiras entre o Cabo Frio e o Cabo Búzios, litoral do estado do Rio de Janeiro. *Revista Brasileira de Geomorfologia*, 18(3): 595-622. <http://dx.doi.org/10.20502/rbg.v18i3.862>.

Fryberger, S.G., Dean, G. 1979. Dune forms and wind regime. In: *A study of Global Sand Seas*, McKee E.D. (ed.), U.S. Geological Survey Professional Paper 1052 (pp. 137-169). Washington, D.C.: U.S. Government Printing Office <https://doi.org/10.3133/001052>.

Silva, G.F., Wijnberg, K.M., de Groot, A.V., Hulscher, S.J. 2019. The effects of beach width variability on coastal dune development at decadal scales. *Geomorphology*, 329: 58-69. <https://doi.org/10.1016/j.geomorph.2018.12.012>

Goldsmith, V., Bowman, D., Kiley, K. 1982. Sequential stage development of crescentic bars; HaHoterim Beach, southeastern Mediterranean. *Journal of Sedimentary Research*, 52(1): 233-249. <https://doi.org/10.1306/212F7F22-2B24-11D7-8648000102C1865D>.

Infantes, E., Terrados, J., Orfila, A., 2009. Wave energy and the upper depth limit distribution of *Posidonia oceanica*. *Botanica Marina*, 52(5), 419-427. <https://doi.org/10.1515/BOT.2009.050>.

Harvey, N. 2006. Holocene coastal evolution: Barriers, beach ridges, and tidal flats of South Australia. *Journal of Coastal Research*, 22(1): 90-99. <https://doi.org/10.2112/05A-0008.1>.

-
- Hemer, M.A., Simmonds, I., Keay, K. 2008. A classification of wave generation characteristics during large wave events on the Southern Australian margin. *Continental Shelf Research*, 28(4): 634-652. <https://doi.org/10.1016/j.csr.2007.12.004>.
- Hemer, M.A., Griffin, D.A. 2010. The wave energy resource along Australia's southern margin. *Journal of renewable and sustainable energy*, 2(4): 043108. <https://doi.org/10.1063/1.3464753>.
- Hesp, P. A. 1982. Morphology and Dynamics of Foredunes in Eastern Australia. Unpubl. Ph.D Thesis, Dept. Geography, University of Sydney.
- Hesp, P. A. 1988. Surfzone, beach, and foredune interactions on the Australian South East Coast [Special issue]. *Journal of Coastal Research*, 3: 15-25. <https://www.jstor.org/stable/40928722>.
- Hesp, P. A. 2002. Foredunes and blowouts: initiation, geomorphology and dynamics. *Geomorphology*, 48(1-3), 245-268. [https://doi.org/10.1016/S0169-555X\(02\)00184-8](https://doi.org/10.1016/S0169-555X(02)00184-8).
- Hesp, P. A. 2012. Surfzone-beach-dune interactions. In: NCK-days 2012: Crossing Borders in Coastal Research. Jubilee Conference Proceedings 20th NCK-days, Netherlands Centre for Coastal Research (pp. 35-40). <http://dx.doi.org/10.3990/2.168>.
- Hesp, P.A., Walker, I.J. 2013. Aeolian environments: coastal dunes. In: *Treatise on Geomorphology*, vol. 11, Aeolian Geomorphology, Shroder, J. (Editor in Chief), Lancaster, N., Sherman, D.J., Baas, A.C.W. (eds.), Academic Press: San Diego, CA; 109–133.
- Hesp, P.A., Smyth, T.A. (2016). Surfzone-Beach-Dune interactions: Flow and Sediment Transport across the Intertidal Beach and Backshore. *Journal of Coastal Research*, 75(sp1), 8-12. <https://doi.org/10.2112/SI75-002.1>.
- Houser, C. 2009. Synchronization of transport and supply in beach-dune interaction. *Progress in Physical Geography*, 33(6), 733-746. <https://doi.org/10.1177/0309133309350120>.
- Houser, C., Hamilton, S. 2009. Sensitivity of post-hurricane beach and dune recovery to event frequency. *Earth Surface Processes and Landforms*, 34, 613–628. <https://doi.org/10.1002/esp.1730>.
- Houser, C., Mathew, S. 2011. Alongshore variation in foredune height in response to transport potential and sediment supply: South Padre Island, Texas. *Geomorphology*, 125(1): 62-72. <https://doi.org/10.1016/j.geomorph.2010.07.028>.
- Lesser, G. R., Roelvink, J. V., Van Kester, J. A. T. M., Stelling, G. S. 2004. Development and validation of a three-dimensional morphological model. *Coastal engineering*, 51(8-9): 883-915. <https://doi.org/10.1016/j.coastaleng.2004.07.014>.
- McLachlan, A., Defeo, O. 2017. *The Ecology of Sandy Shores*. London, UK: Academic Press.

-
- Martinho, C. T., Dillenburg, S. R., Hesp, P. A. 2009. Wave energy and longshore sediment transport gradients controlling barrier evolution in Rio Grande do Sul, Brazil. *Journal of Coastal Research*, 25(2): 285-293. <https://doi.org/10.2112/06-0645.1>.
- Masselink, G. 1993. Simulating the effects of tides on beach morphodynamics. *Journal of Coastal Research*, sp15: 180-197. <https://www.jstor.org/stable/25735729>.
- Masselink, G., Short, A.D. 1993. The effect of tide range on beach morphodynamics and morphology: a conceptual beach model. *Journal of Coastal Research*, 9(3): 785-800. <https://www.jstor.org/stable/4298129>.
- Masselink, G. Turner, I.L. 1999. The effect of tides on beach morphodynamics. In: *Handbook of beach and shoreface morphodynamics* (pp. 204-229), Short, A. D. (ed.). Chichester, West Sussex: John Wiley & Sons.
- Moulton, M., Hesp, P.A., Miot da Silva, G., Bouchez, C., Lavy, M., Fernandez, G. B. 2019. Changes in vegetation cover on the Youngusband Peninsula transgressive dunefields (Australia) 1949–2017. *Earth Surface Processes and Landforms*, 44: 459– 470. <https://doi.org/10.1002/esp.4508>.
- Miot da Silva, G., Hesp, P.A. 2010. Coastline orientation, aeolian sediment transport and foredune and dunefield dynamics of Moçambique Beach, Southern Brazil. *Geomorphology*, 120(3-4), 258-278. <https://doi.org/10.1016/j.geomorph.2010.03.039>.
- Miot da Silva, G.M., Mousavi, S.M.S., Jose, F. 2012. Wave-driven sediment transport and beach-dune dynamics in a headland bay beach. *Marine Geology*, 323: 29-46. <https://doi.org/10.1016/j.margeo.2012.07.015>.
- Murray-Wallace, C.V. 2018. Holocene Coastal Sedimentary Environments of the Coorong Coastal Plain, Southern Australia. In: Murray-Wallace, C. V. (ed.), *Quaternary History of the Coorong Coastal Plain, Southern Australia: An Archive of Environmental and Global Sea-Level Changes* (pp. 81-114). Cham, Switzerland: Springer International. <https://doi.org/10.1007/978-3-319-89342-6>.
- Namikas, S., Sherman, D.J. 1997. Predicting aeolian sand transport: revisiting the White model. *Earth Surface Processes and Landforms*, 22: 601-604. [https://doi.org/10.1002/\(SICI\)1096-9837\(199706\)22:6<601::AID-ESP783>3.0.CO;2-5](https://doi.org/10.1002/(SICI)1096-9837(199706)22:6<601::AID-ESP783>3.0.CO;2-5).
- Nordstrom, K.F. 2000. *Beaches and Dunes of Developed Coasts*. Cambridge, UK: Cambridge University Press. <https://doi.org/10.1017/CBO9780511549519>
- Pereira, P.S., Calliari, L. J., do Carmo Barletta, R. 2010. Heterogeneity and homogeneity of Southern Brazilian beaches: A morphodynamic and statistical approach. *Continental Shelf Research*, 30(3-4): 270-280. <https://doi.org/10.1016/j.csr.2009.11.007>.

Prodger, S., Russell, P., Davidson, M. 2017. Grain-size distributions on high-energy sandy beaches and their relation to wave dissipation. *Sedimentology*, 64(5): 1289-1302. <https://doi.org/10.1111/sed.12353>.

Psuty, N.P. 1988. Sediment budget and dune/beach interaction [Special issue]. *Journal of Coastal Research*, 3: 1–4.

Psuty, N.P. 1992. Spatial variation in coastal foredune development. In: Carter, R.W., Curtis, T.G.F., Sheehy-Skeffington, M.J. (eds.), *Coastal dunes: geomorphology, ecology and management for conservation: Proceedings of the 3rd European Dune Congress Galway, Ireland, 17-21 June 1992* (pp. 3-13). A.A. Balkema. Rotterdam.

Psuty N.P. 2008. The Coastal Foredune: A Morphological Basis for Regional Coastal Dune Development. In: Martínez M. L., Psuty N.P. (eds.), *Coastal Dunes. Ecological Studies*, vol 171. (pp. 11-27). Berlin, Heidelberg: Springer https://doi.org/10.1007/978-3-540-74002-5_2.

Ranasinghe, R., Symonds, G., Black, K., Holman, R. 2004. Morphodynamics of intermediate beaches: a video imaging and numerical modelling study. *Coastal Engineering*, 51(7): 629-655. <https://doi.org/10.1016/j.coastaleng.2004.07.018>.

Saravanan, S., Chandrasekar, N., Mujabar, P.S., Hentry, C. 2011. An overview of beach morphodynamic classification along the beaches between Ovari and Kanyakumari, Southern Tamilnadu Coast, India. *Physical Oceanography*, 21(2): 129-141. <https://doi.org/10.1007/s11110-011-9110-x>.

Sherman, D.J., Bauer, B.O. 1993. Dynamics of beach-dune systems. *Progress in Physical Geography*, 17(4): 413-447. <https://doi.org/10.1177/030913339301700402>.

Sherman, D.J., Lyons, W. 1994. Beach-state controls on aeolian sand delivery to coastal dunes. *Physical Geography*, 15(4): 381-395. <https://doi.org/10.1080/02723646.1994.10642524>.

Short, A.D. 1978. Wave power and beach-stages: a global model. In: *Proceedings of 16th Conference on Coastal Engineering* (pp. 1145-1162). Hamburg, Germany: Amer Society of Civil Engineers (ASCE). <https://doi.org/10.1061/9780872621909.068>.

Short, A.D. 1979. Three dimensional beach-stage model. *The Journal of Geology*, 87(5): 553-571. <https://doi.org/10.1086/628445>.

Short, A.D. 1980. Beach response to variations in breaker height. In: *17th International Conference on Coastal Engineering, Sydney, 23-28 March 1980: abstracts-in-depth*. (pp. 1016-1035). Camberra, Barton, A.C.T: Institution of Engineers, Australia. <https://doi.org/10.1061/9780872622647.063>.

Short, A D., Hesp, P. A. 1982. Wave, beach and dune interactions in southeastern Australia. *Marine geology*, 48(3-4), 259-284. [https://doi.org/10.1016/0025-3227\(82\)90100-1](https://doi.org/10.1016/0025-3227(82)90100-1).

Short, A.D., Hesp, P.A. 1984. Beach and dune morphodynamics of the South East coast of South Australia. Coastal Studies Unit Technical Report 84/1. Coastal Studies Unit, Department of Geography, University of Sydney.

Short, A.D. 1985. Rip-current type, spacing and persistence, Narrabeen Beach, Australia. *Marine geology*, 65(1-2): 47-71. [https://doi.org/10.1016/0025-3227\(85\)90046-5](https://doi.org/10.1016/0025-3227(85)90046-5).

Short, A.D. 1988. Holocene coastal dune formation in southern Australia: a case study. *Sedimentary geology*, 55(1-2), 121-142. [https://doi.org/10.1016/0037-0738\(88\)90093-0](https://doi.org/10.1016/0037-0738(88)90093-0).

Short, A., Aagaard, T. 1993. Single and Multi-Bar Beach Change Models. *Journal of Coastal Research*, 141-157. <http://www.jstor.org/stable/25735727>.

Short, A.D. 2006. Australian beach systems—nature and distribution. *Journal of Coastal Research*, 11-27. <https://doi.org/10.2112/05A-0002.1>.

Short, A.D. 2010. Sediment transport around Australia—sources, mechanisms, rates, and barrier forms. *Journal of Coastal Research*, 26(3) 395-402. <https://doi.org/10.2112/05A-0002.1>.

Short, A.D., Wright, L.D. 2018. Morphodynamics of beaches and surf zones in Australia. In: Komar, P. (eds.), *Handbook of Coastal Processes and Erosion* (pp. 35-64). Boca Raton, Florida: CRC Press. <https://doi.org/10.1201/9781351072908>.

Sonu, C.J. 1973. Three-dimensional beach changes. *The Journal of Geology*, 81(1): 42-64. <https://doi.org/10.1086/627806>.

Swales, A. 2002. Geostatistical estimation of short-term changes in beach morphology and sand budget. *Journal of Coastal Research*, 18(2): 338-351. <https://www.jstor.org/stable/4299079>.

Thom, B.G., Roy, P.S. 1985. Relative sea levels and coastal sedimentation in southeast Australia in the Holocene. *Journal of Sedimentary Research*, 55(2): 257-264. <https://doi.org/10.1306/212F8693-2B24-11D7-8648000102C1865D>.

Thom, B.G., Hall, W. 1991. Behaviour of beach profiles during accretion and erosion dominated periods. *Earth Surface Processes and Landforms*, 16(2): 113-127. <https://doi.org/10.1002/esp.3290160203>.

Trenhaile A.S. 1997. *Coastal Dynamics and Landforms*. Gloucestershire, UK: Clarendon Press.

Van Rijn, L.C., Ruessink, B.G., Grasmeijer, B.T., 1999. Generation and migration of nearshore bars under non-to macrotidal conditions. In: *Coastal Sediments '99: Proceedings of the 4th International Symposium on Coastal Engineering and Science of Coastal Sediment* (pp. 463-478). Houston, Texas: Amer Society of Civil Engineers (ASCE).

Wright, L.D.; Chappell, J.; Thorn, B.G.; Bradshaw, M. P., Cowell, P. 1979. Morphodynamics of reflective and dissipative beach and inshore systems:

Southeastern Australia. *Marine Geology*, 32(1-2): 105-140.
[https://doi.org/10.1016/0025-3227\(79\)90149-X](https://doi.org/10.1016/0025-3227(79)90149-X).

Wright, L.D., Short, A.D. 1984. Morphodynamic variability of surf zones and beaches: a synthesis. *Marine Geology*, 56(1-4): 93-118.
[https://doi.org/10.1016/0025-3227\(84\)90008-2](https://doi.org/10.1016/0025-3227(84)90008-2)

Chapter 5 - Thesis final conclusions

5.1. Summary of findings

The three studies contained in this thesis investigated the different biotic and abiotic controlling factors, drivers and different processes that lead to coastal dune changes, along various portions of the Youngusband Peninsula (South Australia). These changes were also quantified using different field and remote sensing techniques. In the northern part of the Youngusband Peninsula, dune vegetation cover was quantified for the past ~70 years and the possible driving factors causing this change were investigated (chapter 2). In a separate study, geomorphological transformations associated with this vegetation cover change for the same time period were mapped (chapter 3), and the evolutionary processes that transformed different dune types during these past decades were investigated. In the southern end of the Peninsula, alongshore differences in foredune height and volume were documented using topographic surveying from 3 different years, and the possible controlling factors and processes that contribute to the foredune topographic variance were examined (chapter 4).

By investigating these environmental controls of coastal dune formation and transformation, this thesis is an original contribution to knowledge, since it provides new findings regarding the roles of biotic and abiotic factors and their impact on the morphology of large-scale dune systems.

The key findings from each of the three studies are as follows:

- i. In the past ~70 years, the vegetation cover of the northern Youngusband peninsula increased significantly. Results show a net increase in the vegetation cover from ~7% to ~39% in the period 1949 to 2017. The changes

in vegetation cover were compared to the different biotic and abiotic driving factors that could have led this increase in vegetation cover. The results show that the decline in exotic rabbit abundance, especially in the 1950's after the introduction of the Myxomatosis virus as part of a nation-wide rabbit control program, presented significant correlation to periods of greater vegetation growth. Other factors such as wind and rainfall variability, did not present any explanatory correlations, suggesting a secondary role in this process.

ii. The geomorphological changes that occurred in the Youngusband peninsula in the past 7 decades are of great magnitude and the observed vegetation increase marked a new stabilization phase of the dunefield. Geomorphological mapping of the northern Youngusband Peninsula shows that active transgressive dunefields displayed the most significant transformations, representing 60% of the landscape in 1949 and only 11% in 2018. The growth of vegetation on the marginal interdune depressions and plains played an important role in this process, forming narrow elongate vegetated ridges expanding over time, that led to the development of large-scale parabolic dunes. The result of this stabilization process is a significantly more complex, at times chaotic dunefield landscape compared to the 1940's morphologically simple transgressive dunefield system. It is possible to suggest that the stabilization of the northern YP is still on its course, and unless some drastic environmental change occurs (human or natural), the remaining active dunes are expected to become fully stabilized by vegetation.

iii. Topographic beach profile surveys showed an alongshore increase in foredune height and volume from South to North, within the 16 km stretch of the Southern YP coastline. Within the several possible controlling factors of the

volumetric/morphological difference in the foredunes, wave energy was found to have the strongest positive correlation. While wind is the primary agent of sediment transport from the beach to the dunes, wave energy was found to be the only controlling factor that presented significant alongshore variability. The study concludes that a relationship between wave energy and foredune volume is established. This positive relationship suggests that due to a possible variation alongshore in wave-driven sediment supply to the beach, onshore sediment supply is lower in the southern end (lower wave energy), and greater in the northern end (higher wave energy), resulting in the differences in foredune evolution alongshore.

The research concludes that the Youngusband Peninsula Holocene dune system is undergoing a stabilization phase due to an increase in vegetation cover, which has significantly changed the dunefield geomorphology in the past ~70 years. This stabilization process might not have been possible without the decline of the exotic rabbit population in the dunefields.

Results presented in this work suggest that local factors play a more significant role in the stabilization process of dunefields than regional or global factors, and this has also been identified in other recent studies (Delgado-Fernandez *et al.*, 2019; Rodgers *et al.*, 2019). Although it is possible that climate change is contributing to the stabilization of dunes around the world, mainly due to an increase in temperature and rainfall (Jackson *et al.*, 2019b), local factors, such as the one presented in this work, can significantly alter this process. Therefore, future coastal researches, as well as decision-makers, should also look into local biotic factors when investigating possible driving factors of vegetation cover changes in dunes.

Since dune landward transgression is a serious problem around the world, and vegetation plays a critical role in this phenomenon by reducing the rate of migration by naturally fixating these systems, the observed impacts of exotic herbivores in the vegetation cover and dune transgression need to be considered when implementing coastal management strategies.

Results also show the importance of oceanographic forces in the foredune building processes. Foredunes, are a vital element within the larger coastal dune system, retaining and providing sediments to the landward system, and also represent an important coastal defense mechanism to humans. Better understanding of the mechanisms driving foredune development is critical.

Although other studies have reported the role of waves as a dune building agent (Short and Hesp, 1982; Short, 1988; Hesp, 1988; Aagaard *et al.*, 2004; Dillenburg *et al.*, 2009; Martinho *et al.*, 2009; Miot da Silva and Hesp, 2010; Miot da Silva *et al.*, 2012; Dillenburg *et al.*, 2016; Cohn *et al.*, 2018; 2019a), this research provides unique insights into marine controls on dune characteristics, taking a semi-conceptual and semi-quantitative approach to linking the surfzone-beach-dune interactions. For the first time, an investigative study of the role of the driving factors of foredunes takes place in an uncontrolled environment where only one driving factor (wave energy) significantly changes, while others remain the same (or nearly so).

The results obtained in each of the main chapters of this thesis represent a significant contribution to the field and may be regarded as an important baseline for future coastal research within the Youngusband Peninsula and other analogue coastal areas.

5.2. Future work

To better understand the mesoscale drivers of dune dynamics further research is obviously required. The role of exotic herbivores on coastal dune vegetation and its implications to the geomorphological evolution of dune systems needs to be further investigated in other sites, especially in Australia. To further understand the role of exotic rabbits in dune vegetation changes in SA an investigation on the vegetation changes and their drivers in large-scale dune systems that have similar climatic and environmental conditions to the YP, but no exotic herbivores, would be ideal.

With the technological advances in the next decades, higher spatial and temporal resolution open source satellite data will allow more precise analyses of the changes and dynamics of dune systems. This will enable a finer meso-scale analysis of vegetation changes and geomorphological evolution of large-scale dune systems. Higher resolution spatial data could be used to differentiate plant species and investigate the growth rate of different plants as well as show if and how exotic species are colonizing/stabilizing dunes. With a higher temporal resolution data, seasonal variation of vegetation cover and different plant species could be analyzed.

The investigation of possible effects of climate change in dunefield stabilization on a global scale can also benefit from the technological evolution of satellite imagery. Combined with the advances in computer modeling of global environmental changes, our understanding of how climate change is influencing dune stabilization will improve significantly. However, these studies have to be carried out along-side with other studies that look into local biotic and abiotic factors in order to better understand this complex process.

Spatial resolution of meso-scale geomorphological analysis on large-scale dune systems will also be significantly increased if LiDAR surveys become more frequent (Doyle and Woodroffe, 2018). The funding of such surveys by government agencies, like the one performed in 2018 by DEW covering the entire SA coastline, quite possibly will become more recurrent as they realize the benefits of these data for coastal research and reduction of coastal hazards. Despite having a smaller spatial reach, technological advances in Remotely-Piloted Aircraft (RPA) surveying will also greatly enrich vegetation and geomorphological studies related to coastal dunes. RPAs represent a cheaper and more independent way of monitoring coastal changes in high-resolution.

The need to further investigate the drivers or controlling factors of meso-scale foredune changes is also crucial. Further surfzone-beach-dune morphodynamics investigations in other coastal areas where a single driving/controlling factor of foredune evolution can be decoupled from the rest as much as possible is certainly needed.

Thesis references

- Aagaard, T., Black, K.P., Greenwood, B. 2002. Cross-shore suspended sediment transport in the surf zone: A field-based parameterization. *Marine Geology*, 185(3–4), 283–302. [https://doi.org/10.1016/S0025-3227\(02\)00193-7](https://doi.org/10.1016/S0025-3227(02)00193-7)
- Aagaard, T., Davidson-Arnott, R., Greenwood, B., Nielsen, J. 2004. Sediment supply from shoreface to dunes: linking sediment transport measurements and long-term morphological evolution. *Geomorphology*, 60(1-2), 205-224. <https://doi.org/10.1016/j.geomorph.2003.08.002>
- Aagaard, T., Greenwood, B., Hughes, M. 2013. Sediment transport on dissipative, intermediate and reflective beaches. *Earth-science reviews*, 124, 32-50. <https://doi.org/10.1016/j.earscirev.2013.05.002>
- Anthony, E.J., Vanhee, S., Ruz, M.H. 2006. Short-term beach–dune sand budgets on the north sea coast of France: Sand supply from shoreface to dunes, and the role of wind and fetch. *Geomorphology*, 81(3-4), 316-329. <https://doi.org/10.1016/j.geomorph.2006.04.022>
- Ardon, K., Tsoar, H., Blumberg, D.G. 2009. Dynamics of nebkhas superimposed on a parabolic dune and their effect on the dune dynamics. *Journal of Arid Environments*, 73(11), 1014-1022. <https://doi.org/10.1016/j.jaridenv.2009.04.021>
- Arens, S.M., Van Kaam-Peters, H.M.E., Van Boxel, J.H. 1995. Air flow over foredunes and implications for sand transport. *Earth Surface Process Landforms*, 20, 315–332. <https://doi.org/10.1002/esp.3290200403>
- Arens, S.M., Slings, Q.L., Geelen, L.H., Van der Hagen, H.G. 2013. Restoration of dune mobility in the Netherlands. In: *Restoration of coastal dunes*, Martínez, L.M., Gallego-Fernández, J.B., Hesp, P.A. (Eds.). Berlin: Springer. 107-124. https://doi.org/10.1007/978-3-642-33445-0_7
- Atkinson, P.M., Lewis, P. 2000. Geostatistical classification for remote sensing: an introduction. *Computers & Geosciences*, 26(4), 361-371. [https://doi.org/10.1016/S0098-3004\(99\)00117-X](https://doi.org/10.1016/S0098-3004(99)00117-X)
- Australian Bureau of Meteorology. 2017. La Niña – Detailed Australian Analysis. Retrieved 23 January, 2017 from <http://www.bom.gov.au/climate/enso/lnlist/>
- Australian Bureau of Meteorology. 2018. Climate Statistics Meningie Weather Station. Retrieved 24 July, 2018 from http://www.bom.gov.au/climate/averages/tables/cw_024518.shtml
- Australian Hydrographic Service. 2001. AUS 347 - Backstairs Passage to Cape Martin Nautical Chart (1:300000).
- Barchyn, T.E., Hugenholtz, C.H. 2012. Aeolian dune field geomorphology modulates the stabilization rate imposed by climate. *Journal of Geophysical Research: Earth Surface*, 117(F2). <https://doi.org/10.1029/2011JF002274>

-
- Battiau-Queney, Y., Billet, J.F., Chaverot, S., Lanoy-Ratel, P. 2003. Recent shoreline mobility and geomorphologic evolution of macrotidal sandy beaches in the north of France. *Marine Geology*, 194(1-2), 31-45. [https://doi.org/10.1016/S0025-3227\(02\)00697-7](https://doi.org/10.1016/S0025-3227(02)00697-7)
- Bauer, B.O., Davidson-Arnott, R.G. 2003. A general framework for modeling sediment supply to coastal dunes including wind angle, beach geometry, and fetch effects. *Geomorphology*, 49(1-2), 89-108. [https://doi.org/10.1016/S0169-555X\(02\)00165-4](https://doi.org/10.1016/S0169-555X(02)00165-4)
- Bauer, B.O., Davidson-Arnott, R.G.D., Hesp, P.A., Namikas, S.L., Ollerhead, J., Walker, I.J. 2009. Aeolian sediment transport on a beach: Surface moisture, wind fetch, and mean transport. *Geomorphology*, 105(1-2), 106-116. <https://doi.org/10.1016/j.geomorph.2008.02.016>
- Belperio, A.P., Harvey, N., Bourman, R.P. 2002. Spatial and temporal variability in the Holocene sea-level record of the South Australian coastline. *Sedimentary Geology*, 150(1), 153-169. [https://doi.org/10.1016/S0037-0738\(01\)00273-1](https://doi.org/10.1016/S0037-0738(01)00273-1)
- Benedet, L., Finkl, C.W., Klein, A.H.F. 2006. Morphodynamic classification of beaches on the Atlantic coast of Florida: geographical variability of beach types, beach safety and coastal hazards. *Journal of Coastal Research*, 360-365. <http://www.jstor.org/stable/25741596>
- Bird, P., Mutze, G., Peacock, D., Jennings, S. 2012. Damage caused by low-density exotic herbivore populations: the impact of introduced European rabbits on marsupial herbivores and *Allocasuarina* and *Bursaria* seedling survival in Australian coastal shrubland. *Biological Invasions*, 14(3), 743-755. <https://doi.org/10.1007/s10530-011-0114-8>
- Birkemeier, W.A. 1984. Time scales of nearshore profile changes. In: *Proceedings of the 19th International Conference on Coastal Engineering* (pp. 1507-1521). Houston, Texas: Amer Society of Civil Engineers (ASCE). <https://doi.org/10.1061/9780872624382.103>
- Blott, S.J., Pye, K. 2001. GRADISTAT: a grain size distribution and statistics package for the analysis of unconsolidated sediments. *Earth surface processes and Landforms*, 26(11), 1237-1248. <https://doi.org/10.1002/esp.261>
- Boak, E.H., Turner, I.L. 2005. Shoreline definition and detection: a review. *Journal of coastal research*, 688-703. <https://doi.org/10.2112/03-0071.1>
- Bourman, R.P., Murray-Wallace, C.V., Belperio, A.P., Harvey, N. 2000. Rapid coastal geomorphic change in the River Murray Estuary of Australia. *Marine Geology* 170(1): 141–168. [https://doi.org/10.1016/S0025-3227\(00\)00071-2](https://doi.org/10.1016/S0025-3227(00)00071-2)
- Bourman, R., Harvey, N., James, K.F. 2006. Evolution of the Youngusband Peninsula, South Australia: new evidence from the northern tip. *South Australian Geographical Journal*, 105, 37-50.

Bourman, R. P., Murray-Wallace, C. V., Harvey, N. 2016. Coastal Landscapes of South Australia. Adedaile, SA: University of Adelaide Press. <http://dx.doi.org/10.20851/coast-sa>

Brodie, K.L., Palmsten, M.L., Spore, N.J. 2017. Coastal Fore-dune Evolution, Part 1: Environmental Factors and Forcing Processes Affecting Morphological Evolution. US Army Corps of Engineers Coastal and Hydraulics Engineering Technical Note, 1-10. <https://apps.dtic.mil/dtic/tr/fulltext/u2/1028704.pdf>

Brodie, K.L., Conery, I., Cohn, N., Spore, N., Palmsten, M. 2019. Spatial Variability of Coastal Fore-dune Evolution, Part A: Timescales of Months to Years. Journal of Marine Science and Engineering, 7(5), 124. <https://doi.org/10.3390/jmse7050124>

Bullard, J.E. 1997. A note on the use of the "Fryberger method" for evaluating potential sand transport by wind. Journal of Sedimentary Research, 67(3), 499-501. <http://dx.doi.org/10.1306/D42685A9-2B26-11D7-8648000102C1865D>

Bureau of Meteorology - Climate statistics for Australian locations: Cape Jaffa. 2017. Retrieved September 18, 2017, from http://www.bom.gov.au/climate/averages/tables/cw_026095.shtml

Cape Grim Greenhouse Gas Data – CSIRO. 2018. CSIRO Marine and Atmospheric Research and the Australian Bureau of Meteorology (Cape Grim Baseline Air Pollution Station). Retrieved from <http://capegrim.csiro.au/>

Chappell, J., Eliot, I.G. 1979. Surf-beach dynamics in time and space—an Australian case study, and elements of a predictive model. Marine Geology, 32(3-4), 231-250. [https://doi.org/10.1016/0025-3227\(79\)90066-5](https://doi.org/10.1016/0025-3227(79)90066-5)

Clarke, M.L., Rendell, H.M. 2009. The impact of North Atlantic storminess on western European coasts: a review. Quaternary International, 195(1), 31-41. <https://doi.org/10.1016/j.quaint.2008.02.007>

Clemmensen, L.B., Andreasen, F., Nielsen, S. T., Sten, E. 1996. The late Holocene coastal dunefield at Vejers, Denmark: characteristics, sand budget and depositional dynamics. Geomorphology, 17(1-3), 79-98. [https://doi.org/10.1016/0169-555X\(95\)00096-N](https://doi.org/10.1016/0169-555X(95)00096-N)

Clemmensen, L.B., Pye, K., Murray, A., Heinemeier, J. 2001. Sedimentology, stratigraphy and landscape evolution of a Holocene coastal dune system, Lodbjerg, NW Jutland, Denmark. Sedimentology, 48(1), 3-27. <https://doi.org/10.1111/j.1365-3091.2001.00345.x>

Clemmensen, L.B., Murray, A. 2006. The termination of the last major phase of aeolian sand movement, coastal dunefields, Denmark. Earth Surface Processes and Landforms, 31(7), 795-808. <https://doi.org/10.1002/esp.1283>

Cohn, N., Ruggiero, P., de Vries, S., Kaminsky, G. 2018. New insights on the relative contributions of marine and aeolian processes to coastal fore-dune growth. Geophys. Res. Lett, 45, 4965-4973. <https://doi.org/10.1029/2018GL077836>

-
- Cohn, N., Hoonhout, B.M., Goldstein, E.B., De Vries, S., Moore, L.J., Durán Vinent, O., Ruggiero, P. 2019a. Exploring Marine and Aeolian Controls on Coastal Fore-dune Growth Using a Coupled Numerical Model. *Journal of Marine Science and Engineering*, 7(1), 13. <https://doi.org/10.3390/jmse7010013>
- Cohn, N., Ruggiero, P., García-Medina, G., Anderson, D., Serafin, K.A., Biel, R. 2019b. Environmental and morphologic controls on wave-induced dune response. *Geomorphology*, 329, 108-128. <https://doi.org/10.1016/j.geomorph.2018.12.023>
- Cooke, B.D. 1988. The effects of rabbit grazing on regeneration of sheoaks, *Allocasuarina verticillata* and saltwater ti-trees, *Melaleuca halmaturorum*, in the Coorong National Park, South Australia. *Australian Journal of Ecology*, 13(1), 11-20. <https://doi.org/10.1111/j.1442-9993.1988.tb01414.x>
- Cooke, B.D. 2014. Australia's war against rabbits: the story of rabbit haemorrhagic disease. Collingwood, Victoria: CSIRO Publishing.
- Cooper, W.S., 1958. Coastal Sand Dunes of Oregon and Washington. *Geological Society of America Memoirs*, Boulder, CO; No.72, 169 pp. <https://ir.library.oregonstate.edu/concern/defaults/hq37vs212>
- Cooper, W.S., 1967. Coastal Sand Dunes of California. *Geological Society of America Memoirs*, Boulder, CO; No. 104, 131 pp. <https://doi.org/10.1130/MEM104-p1>
- Cowell, P.J., Roy, P.S., Jones, R.A. 1995. Simulation of large-scale coastal change using a morphological behaviour model. *Marine Geology*, 126(1-4), 45-61. [https://doi.org/10.1016/0025-3227\(95\)00065-7](https://doi.org/10.1016/0025-3227(95)00065-7)
- Davidson-Arnott, R.G.D., Law, M.N. 1996. Measurement and prediction of long-term sediment supply to coastal foredunes. *Journal of Coastal Research*, 12(3), 654-663. <https://www.jstor.org/stable/4298513>
- Davidson-Arnott, R.G.D., MacQuarrie, K., Aagaard, T., 2005. The effect of wind gusts, moisture content and fetch length on sand transport on a beach. *Geomorphology*, 63, 115–129. <https://doi.org/10.1016/j.geomorph.2004.04.008>
- Davidson-Arnott, R.G.D., Bauer, B.O. 2009. Aeolian sediment transport on a beach: thresholds, intermittency, and high frequency variability. *Geomorphology*, 105, 117–126. <https://doi.org/10.1016/j.geomorph.2008.02.018>
- Davidson-Arnott, R.G.D. 2010. *Introduction to Coastal Processes and Geomorphology*. Cambridge, UK: Cambridge University Press.
- Davies, J.L. 1980. *Geographical variation in coastal development*. London: Longman. 212 pp.
- Delgado-Fernandez, I. 2010. A review of the application of the fetch effect to modelling sand supply to coastal foredunes. *Aeolian Research*, 2(2-3), 61-70. <https://doi.org/10.1016/j.aeolia.2010.04.001>

-
- Delgado-Fernandez, I., Davidson-Arnott, R. 2011. Meso-scale aeolian sediment input to coastal dunes: The nature of aeolian transport events. *Geomorphology*, 126(1-2), 217-232. <https://doi.org/10.1016/j.geomorph.2010.11.005>
- Delgado-Fernandez, I., O'Keeffe, N., Davidson-Arnott, R.G. 2019. Natural and human controls on dune vegetation cover and disturbance. *Science of The Total Environment*, 672, 643-656. <https://doi.org/10.1016/j.scitotenv.2019.03.494>
- Díez, J., Cohn, N., Kaminsky, G.M., Medina, R., Ruggiero, P. 2018. Spatial and temporal variability of dissipative dry beach profiles in the Pacific Northwest, USA. *Journal of Coastal Research*, 34(3), 510-523. <https://doi.org/10.2112/JCOASTRES-D-17-00149.1>
- Dillenburg, S.R., Barboza, E.G., Tomazelli, L.J., Hesp, P.A., Clerot, L.C.P., Ayup-Zouain, R.N. 2009. The Holocene Coastal Barriers of Rio Grande do Sul. In: *Lecture Notes in Earth Sciences: Geology and Geomorphology of Holocene Coastal Barriers of Brazil* (Vol.107, pp.53-91), Dillenburg S.R., Hesp, P.A. (Eds). Berlin, Heidelberg: Springer.
- Dillenburg, S.R., Hesp, P.A., Cecilio, R., Miot da Silva, G. 2016. Wave Energy as a Control on Dune Development on two Regressive Barriers in Southern Brazil. *Journal of Coastal Research*, Special Issue 75(1), 273-277. <https://doi.org/10.2112/SI75-55.1>
- Doyle, T.B., Woodroffe, C.D. 2018. The application of LiDAR to investigate foredune morphology and vegetation. *Geomorphology*, 303, 106-121. <https://doi.org/10.1016/j.geomorph.2017.11.005>
- Doyle, T.B., Short, A.D., Ruggiero, P., Woodroffe, C.D. 2019. Interdecadal Foredune Changes along the Southeast Australian Coastline: 1942–2014. *Journal of Marine Science and Engineering*, 7(6), 177. <https://doi.org/10.3390/jmse7060177>
- Durán, O., Herrmann, H.J. 2006. Vegetation against dune mobility. *Physical Review Letters*, 97(18), 188001. <https://doi.org/10.1103/PhysRevLett.97.188001>
- Everard, M., Jones, L., Watts, B. 2010. Have we neglected the societal importance of sand dunes? An ecosystem services perspective. *Aquatic Conservation: Marine and Freshwater Ecosystems*, 20(4), 476-487. <https://doi.org/10.1002/aqc.1114>
- Fensham, R.J., Fairfax, R.J. 2002. Aerial photography for assessing vegetation change: a review of applications and the relevance of findings for Australian vegetation history. *Australian Journal of Botany*, 50(4), 415-429. <https://doi.org/10.1071/BT01032>
- Fernandez, G.B., Pereira, T.G., Rocha, T.B., Maluf, V., Moulton, M., Oliveira Filho, S.R. 2017. Classificação morfológica das dunas costeiras entre o Cabo Frio e o Cabo Búzios, litoral do estado do Rio de Janeiro. *Revista Brasileira de Geomorfologia*, 18(3), 595-622. <http://dx.doi.org/10.20502/rbg.v18i3.862>

Flinders, M. 1814. A voyage to Terra Australis. Atlas, G. & W. Nicol: London. Vol. 2. 613 pp.

Fryberger, S.G., Dean, G. 1979. Dune forms and wind regime. In: McKee E.D. (Ed.), A study of Global Sand Seas, U.S. Geological Survey Professional Paper 1052 (pp. 137-169). Washington, D.C.: U.S. Government Printing Office
<https://doi.org/10.3133/001052>

Gilbertson, D.D. 1977. The off-road use of vehicles and aspects of the bio-physical systems of the lower Coorong region. In: Gilbertson, D.D., Foale, M.R. (eds.), The southern Coorong and lower Younghusband Peninsula of South Australia (pp.71–91). Adelaide, South Australia: The Nature Conservation Society of South Australia.

Gilbertson, D.D. 1981. The impact of past and present land use on a major coastal barrier system. *Applied Geography*, 1(2), 97-119.
[https://doi.org/10.1016/0143-6228\(81\)90028-X](https://doi.org/10.1016/0143-6228(81)90028-X)

Gilbertson, D.D., Schwenninger, J.L., Kemp, R.A., Rhodes, E.J. 1999. Sand-drift and soil formation along an exposed North Atlantic coastline: 14,000 years of diverse geomorphological, climatic and human impacts. *Journal of Archaeological Science*, 26(4), 439-469. <https://doi.org/10.1006/jasc.1998.0360>

Goldsmith, V. 1978. Coastal dunes. In: Davis, R.A., (Ed.), *Coastal Sedimentary Environments*. Springer, New York, NY, pp. 171–230.

Goldsmith, V., Bowman, D., Kiley, K. 1982. Sequential stage development of crescentic bars; HaHoterim Beach, southeastern Mediterranean. *Journal of Sedimentary Research*, 52(1), 233-249. <https://doi.org/10.1306/212F7F22-2B24-11D7-8648000102C1865D>

Goldsmith, V. 1989. Coastal sand dunes as geomorphological systems. *Proceedings of the Royal Society of Edinburgh. Section B. Biological Sciences*, 96, 3–15. <https://doi.org/10.1017/S0269727000010824>

Guan, C., Hasi, E., Zhang, P., Tao, B., Liu, D., Zhou, Y. 2017. Parabolic dune development modes according to shape at the southern fringes of the Hobq Desert, Inner Mongolia, China. *Geomorphology*, 295, 645-655.
<https://doi.org/10.1016/j.geomorph.2017.08.009>

Harris, D., Davy, A.J. 1986. Strandline colonization by *Elymus farctus* in relation to sand mobility and rabbit grazing. *The Journal of Ecology*, 1045-1056.
<https://doi.org/10.2307/2260232>

Harvey, N. 2006. Holocene coastal evolution: barriers, beach ridges, and tidal flats of South Australia. *Journal of Coastal Research* 22(1): 90–99.
<https://doi.org/10.2112/05A-0008.1>.

Harvey, N., Bourman, R., James, K.F. 2006. Evolution of the Younghusband Peninsula, South Australia: new evidence from the northern tip. *South Australian Geographical Journal*, 105, 37-50.

-
- Hemer, M.A., Simmonds, I., Keay, K. 2008. A classification of wave generation characteristics during large wave events on the Southern Australian margin. *Continental Shelf Research*, 28(4), 634-652. <https://doi.org/10.1016/j.csr.2007.12.004>
- Hemer, M.A., Griffin, D.A. 2010. The wave energy resource along Australia's southern margin. *Journal of renewable and sustainable energy*, 2(4), 043108. <https://doi.org/10.1063/1.3464753>
- Hernández-Cordero, A.I., Hernández-Calvento, L., Hesp, P.A., Pérez-Chacón, E. 2018. Geomorphological changes in an arid transgressive coastal dune field due to natural processes and human impacts. *Earth Surf. Process. Landforms*, 43: 2167– 2180. <https://doi.org/10.1002/esp.4382>.
- Hesp, P.A., Thom, B.G. 1990. Geomorphology and evolution of transgressive dunefields. In: *Coastal Dunes: Processes and Morphology*, Nordstrom, K., Psuty, N., Carter, R.W.G. (eds). Chichester: John Wiley and Sons; 235–288.
- Hesp, P.A. 1982. Morphology and Dynamics of Foredunes in Eastern Australia. Unpubl. Ph.D Thesis, Dept. Geography, University of Sydney.
- Hesp, P.A. 1988. Surfzone, beach, and foredune interactions on the Australian South East Coast. *Journal of Coastal Research*, Special Issue 3, 15-25. <https://www.jstor.org/stable/40928722>
- Hesp, P.A., Thom, B.G. 1990. Geomorphology and evolution of transgressive dunefields. In: Nordstrom, K.; Psuty, N. and Carter, R.W.G. (Eds.). *Coastal Dunes: Processes and Morphology* (pp. 235-288). Chichester: John Wiley & Sons.
- Hesp, P.A. 2001. The Manawatu dunefield: environmental change and human impacts. *New Zealand Geographer*, 57(2), 33-40. <https://doi.org/10.1111/j.1745-7939.2001.tb01607.x>
- Hesp, P.A. 2002. Foredunes and blowouts: initiation, geomorphology and dynamics. *Geomorphology*, 48(1-3), 245-268. [https://doi.org/10.1016/S0169-555X\(02\)00184-8](https://doi.org/10.1016/S0169-555X(02)00184-8)
- Hesp, P.A., Martínez, M.L., 2007. Disturbance processes and dynamics in coastal dunes. In: *Plant disturbance ecology: the process and the response*, Johnson, E.A., Miyanishi, K. Burlington, MA; 215-247.
- Hesp, P.A. 2011. Dune Coasts. In: *Treatise on Estuarine and Coastal Science*, vol. 3, Wolanski, E., McLusky, D.S. (eds.), Waltham: Academic Press; 193–221.
- Hesp, P.A., Martinez, M., Miot da Silva, G., Rodríguez-Revelo, N., Gutierrez, E., Humanes, A., Lainez, D., Montano, I., Palacios, V., Quesada, A., Storero, L., Trilla, G.G., Trochine, C. 2011. Transgressive dunefield landforms and vegetation associations, Doña Juana, Veracruz, Mexico. *Earth Surface Processes and Landforms*, 36(3), 285-295. <https://doi.org/10.1002/esp.2035>

-
- Hesp, P.A. 2012. Surfzone-beach-dune interactions. In: NCK-days 2012: Crossing Borders in Coastal Research. Jubilee Conference Proceedings 20th NCK-days, Netherlands Centre for Coastal Research (pp. 35-40). <http://dx.doi.org/10.3990/2.168>
- Hesp, P.A. 2013. Conceptual models of the evolution of transgressive dune field systems. *Geomorphology*, 199, 138-149. <https://doi.org/10.1016/j.geomorph.2013.05.014>
- Hesp, P.A., Walker, I.J. 2013. Aeolian environments: coastal dunes. In: Treatise on Geomorphology, vol. 11, Shroder J. (Editor in Chief), Lancaster, N., Sherman, D.J., Baas, A.C.W. (eds.), San Diego, CA: Academic Press; 109–133.
- Hesp, P.A., Hilton, M.J. 2013. Restoration of foredunes and transgressive dunefields: case studies from New Zealand. In: Restoration of coastal dunes, Martínez, L.M., Gallego-Fernández, J.B., & Hesp, P.A. (Eds.). Berlin, Heidelberg: Springer, 67-92. https://doi.org/10.1007/978-3-642-33445-0_5
- Hesp, P.A., Smyth, T.A. 2016. Surfzone-Beach-Dune interactions: Flow and Sediment Transport across the Intertidal Beach and Backshore. *Journal of Coastal Research*, Special Issue 75(1), 8-12. <https://doi.org/10.2112/SI75-002.1>
- Hesp, P.A., Smyth, T.A. 2019. Anchored Dunes. In *Aeolian Geomorphology: A new Introduction*, Livingstone, I., Warren A. (Eds.), Wiley-Blackwell: Hoboken, NJ, 157-178 . <https://doi.org/10.1002/9781118945650.ch7>
- Hilton, M., Harvey, N., Hart, A., James, K.F., Arbuckle, C. 2006. The impact of exotic dune grass species on foredune development in Australia and New Zealand: a case study of *Ammophila arenaria* and *Thinopyrum junceiforme*. *Australian Geographer*, 37(3), 313-334. <https://doi.org/10.1080/00049180600954765>
- Hilton, M., Harvey, N., James, K. 2007. The impact and management of exotic dune grasses near the mouth of the Murray River, South Australia. *Australasian Journal of Environmental Management*, 14(4), 220-228. <https://doi.org/10.1080/14486563.2007.9725171>
- Houser, C. 2009. Synchronization of transport and supply in beach-dune interaction. *Progress in Physical Geography*, 33(6), 733-746. <https://doi.org/10.1177/0309133309350120>
- Houser, C., Hamilton, S. 2009. Sensitivity of post-hurricane beach and dune recovery to event frequency. *Earth Surface Processes and Landforms*, 34, 613–628. <https://doi.org/10.1002/esp.1730>
- Houser, C., Mathew, S. 2011. Alongshore variation in foredune height in response to transport potential and sediment supply: South Padre Island, Texas. *Geomorphology*, 125(1), 62-72. <https://doi.org/10.1016/j.geomorph.2010.07.028>

-
- Hugenholtz, C.H., Wolfe, S.A. 2005. Biogeomorphic model of dunefield activation and stabilization on the northern Great Plains. *Geomorphology* 70(1-2): 53–70. <https://doi.org/10.1016/j.geomorph.2005.03.011>.
- Infantes, E., Terrados, J., Orfila, A., 2009. Wave energy and the upper depth limit distribution of *Posidonia oceanica*. *Botanica Marina*, 52(5), 419-427. <https://doi.org/10.1515/BOT.2009.050>
- Jackson, N.L., Nordstrom, K.F. 2019. Trends in research on beaches and dunes on sandy shores, 1969–2019. *Geomorphology*. <https://doi.org/10.1016/j.geomorph.2019.04.009>
- Jackson, D.W., Costas, S., Guisado-Pintado, E. 2019a. Large-scale transgressive coastal dune behaviour in Europe during the Little Ice Age. *Global and Planetary Change*, 175, 82-91. <https://doi.org/10.1016/j.gloplacha.2019.02.003>
- Jackson, D.W., Costas, S., González-Villanueva, R., Cooper, A. 2019b. A global 'greening' of coastal dunes: An integrated consequence of climate change? *Global and Planetary Change*, 182, 103026. <https://doi.org/10.1016/j.gloplacha.2019.103026>
- James, K.F. 2012. Gaining new ground: *Thinopyrum junceiforme*, a model of success along the South Eastern Australian coastline. The University of Adelaide. Doctoral Thesis. 221 p.
- Jones, M.L.M., Sowerby, A., Rhind, P.M. 2010. Factors affecting vegetation establishment and development in a sand dune chronosequence at Newborough Warren, North Wales. *Journal of Coastal Conservation*, 14(2), 127-137. <https://doi.org/10.1007/s11852-009-0071-x>
- Knutson, T.R., McBride, J.L., Chan, J., Emanuel, K., Holland, G., Landsea, C., Held, I., Kossin, J.P., Srivastava, A.K., Sugi, M. 2010. Tropical cyclones and climate change. *Nature geoscience*, 3(3), 157-163.
- Kutiel, P., Cohen, O., Shoshany, M., Shub, M. 2004. Vegetation establishment on the southern Israeli coastal sand dunes between the years 1965 and 1999. *Landscape and urban planning*, 67(1), 141-156. [https://doi.org/10.1016/S0169-2046\(03\)00035-5](https://doi.org/10.1016/S0169-2046(03)00035-5)
- Lesser, G.R., Roelvink, J.V., Van Kester, J.A.T.M., Stelling, G.S. 2004. Development and validation of a three-dimensional morphological model. *Coastal engineering*, 51(8-9), 883-915. <https://doi.org/10.1016/j.coastaleng.2004.07.014>
- Levin, N. 2011. Climate-driven changes in tropical cyclone intensity shape dune activity on Earth's largest sand island. *Geomorphology*, 125(1), 239-252. <https://doi.org/10.1016/j.geomorph.2010.09.021>
- Levin, N., Jablon, P.E., Phinn, S., Collins, K. 2017. Coastal dune activity and foredune formation on Moreton Island, Australia, 1944–2015. *Aeolian Research*, 25, 107-121.

Luebbers, R.A. 1981. The Coorong Report: An Archaeological Survey of the Southern Youngusband Peninsula. Report for the South Australian Department of Environment and Planning.

Luebbers, R.A. 1982. The Coorong Report. An Archaeological Survey of the Northern Coorong. Adelaide, Australia: South Australian Department of Environmental and Planning.

Marcomini, S.C., Maidana, N. 2006. Response of eolian ecosystems to minor climatic changes [Special issue]. *Journal of Coastal Research*, 39, 204-208. <https://www.jstor.org/stable/25741562>

Martínez, M.L., Psuty, N.P. 2004. *Coastal Dunes: Ecology and Conservation*. Berlin: Springer. Ecological Studies, vol 171. Berlin, Heidelberg: Springer.

Hesp, P.A., Martínez, M.L., 2007. Disturbance processes and dynamics in coastal dunes. In: *Plant disturbance ecology: the process and the response*, Johnson, E.A., Miyanishi, K. Burlington, MA; 215-247.

Martinho, C.T., Dillenburg, S.R., Hesp, P.A. 2009. Wave energy and longshore sediment transport gradients controlling barrier evolution in Rio Grande do Sul, Brazil. *Journal of Coastal Research*, 25(2), 285-293. <https://doi.org/10.2112/06-0645.1>

Martinho, C.T., Hesp, P.A., Dillenburg, S.R. 2010. Morphological and temporal variations of transgressive dunefields of the northern and mid-littoral Rio Grande do Sul coast, Southern Brazil. *Geomorphology*, 117(1), 14-32. <https://doi.org/10.1016/j.geomorph.2009.11.002>

Masselink, G. 1993. Simulating the effects of tides on beach morphodynamics. *Journal of Coastal Research*, 180-197. <https://www.jstor.org/stable/25735729>

Masselink, G., Short, A.D. 1993. The effect of tide range on beach morphodynamics and morphology: a conceptual beach model. *Journal of Coastal Research*, 9(3), 785-800. <https://www.jstor.org/stable/4298129>

Masselink, G., Turner, I.L. 1999. The effect of tides on beach morphodynamics. In: Short, A. D. (Ed.). *Handbook of beach and shoreface morphodynamics* (pp. 204-229). Chinchester, West Sussex: John Wiley & Sons.

McGranahan, G., Balk, D., Anderson, B. 2007. The rising tide: assessing the risks of climate change and human settlements in low elevation coastal zones. *Environment and urbanization*, 19(1), 17-37.

McLachlan, A., Defeo, O. 2017. *The Ecology of Sandy Shores*. London, UK: Academic Press.

Miot da Silva, G., Hesp, P.A. 2010. Coastline orientation, aeolian sediment transport and foredune and dunefield dynamics of Moçambique Beach, Southern Brazil. *Geomorphology*, 120(3-4), 258-278. <https://doi.org/10.1016/j.geomorph.2010.03.039>

Miot da Silva, G., Mousavi, S.M.S., Jose, F. 2012. Wave-driven sediment transport and beach-dune dynamics in a headland bay beach. *Marine Geology*, 323, 29-46. <https://doi.org/10.1016/j.margeo.2012.07.015>

Miot da Silva, G., Hesp, P.A. 2013. Increasing rainfall, decreasing winds, and historical changes in Santa Catarina dunefields, southern Brazil. *Earth Surface Processes and Landforms*, 38(9), 1036-1045. <https://doi.org/10.1002/esp.3390>

Miot da Silva, G., Martinho, C.T., Hesp, P.aA., Keim, B.D., & Ferligoj, Y. 2013. Changes in dunefield geomorphology and vegetation cover as a response to local and regional climate variations. *Journal of Coastal Research*, 65(sp2), 1307-1312. <https://doi.org/10.2112/SI65-221.1>

Moulton, M.A.B., Hesp, P.A., Miot da Silva, G., Bouchez, C., Lavy, M., Fernandez, G.B. 2019. Changes in vegetation cover on the Youngusband Peninsula transgressive dunefields (Australia) 1949–2017. *Earth Surface Processes and Landforms*, 44, 459–470. <https://doi.org/10.1002/esp.4508>

Murray-Wallace, C.V. 2018. Holocene Coastal Sedimentary Environments of the Coorong Coastal Plain, Southern Australia. In: Murray-Wallace, C. V. (Ed.), *Quaternary History of the Coorong Coastal Plain, Southern Australia: An Archive of Environmental and Global Sea-Level Changes* (pp. 81-114). Cham, Switzerland: Springer International. <https://doi.org/10.1007/978-3-319-89342-6>

Mutze, G., Kovaliski, J., Butler, K., Capucci, L., McPhee, S. 2010. The effect of rabbit population control programmes on the impact of rabbit haemorrhagic disease in south-eastern Australia. *Journal of Applied Ecology*, 47(5), 1137-1146. <https://doi.org/10.1111/j.1365-2664.2010.01844.x>

Mutze, G., Bird, P., Jennings, S., Peacock, D., de Preu, N., Kovaliski, J., Cooke, B., & Capucci, L. 2014a. Recovery of South Australian rabbit populations from the impact of rabbit haemorrhagic disease. *Wildlife Research*, 41(7), 552-559. <https://doi.org/10.1071/WR14107>

Mutze, G., Cooke, B., Lethbridge, M., Jennings, S. 2014b. A rapid survey method for estimating population density of European rabbits living in native vegetation. *The Rangeland Journal*, 36(3), 239-247. <https://doi.org/10.1071/RJ13117>

Mutze, G., Cooke, B., Jennings, S. 2016. Estimating density-dependent impacts of European rabbits on Australian tree and shrub populations. *Australian Journal of Botany*, 64(2), 142-152. <https://doi.org/10.1071/BT15208>

Namikas, S., Sherman, D.J. 1997. Predicting aeolian sand transport: revisiting the White model. *Earth Surface Processes and Landforms*, 22, 601-604. [https://doi.org/10.1002/\(SICI\)1096-9837\(199706\)22:6<601::AID-ESP783>3.0.CO;2-5](https://doi.org/10.1002/(SICI)1096-9837(199706)22:6<601::AID-ESP783>3.0.CO;2-5)

Nicholls, N. 2010. Local and remote causes of the southern Australian autumn-winter rainfall decline, 1958–2007. *Climate dynamics*, 34(6), 835-845. <https://doi.org/10.1007/s00382-009-0527-6>

-
- Nordstrom, K.F. 2000. *Beaches and Dunes of Developed Coasts*. Cambridge, UK: Cambridge University Press. <https://doi.org/10.1017/CBO9780511549519>
- Nordstrom, K.F. 2008. *Beach and Dune Restoration*. Cambridge: Cambridge University Press. <https://doi.org/10.1017/CBO9780511535925>
- Olson, J.S. 1958. Lake Michigan dune development. 1-2-3. *Journal of Geology* 56, 254–263, 345–351, 413–483. <https://doi.org/10.1086/626503>
- Orme, A.R., Tchakerian, V.P. 1986. Quaternary dunes of the Pacific coast of the Californias. In: Nickling, W.G. (Ed.), *Aeolian Geomorphology*. Allen and Unwin, London, 149–175.
- Paton, D.C. 2010. *At the end of the river: the Coorong and lower lakes/David*. ATF Press: Adelaide. <https://doi.org/10.1071/PC110290>
- Pereira, P.S., Calliari, L.J., do Carmo Barletta, R. 2010. Heterogeneity and homogeneity of Southern Brazilian beaches: A morphodynamic and statistical approach. *Continental Shelf Research*, 30(3-4), 270-280. <https://doi.org/10.1016/j.csr.2009.11.007>
- Pickart, A.J., Hesp, P.A. 2019. Spatio-temporal geomorphological and ecological evolution of a transgressive dunefield system, Northern California, USA. *Global and planetary change*, 172, 88-103. <https://doi.org/10.1016/j.gloplacha.2018.09.012>
- Planet Team. 2017. *Planet Application Program Interface: In Space for Life on Earth*. San Francisco, California. <https://api.planet.com>
- Prodger, S., Russell, P., Davidson, M. 2017. Grain-size distributions on high-energy sandy beaches and their relation to wave dissipation. *Sedimentology*, 64(5), 1289-1302. <https://doi.org/10.1111/sed.12353>
- Provoost, S., Jones, M.L.M., Edmondson, S.E. 2011. Changes in landscape and vegetation of coastal dunes in northwest Europe: a review. *Journal of Coastal Conservation*, 15(1), 207-226. <https://doi.org/10.1007/s11852-009-0068-5>
- Psuty, N.P. 1988. Sediment budget and dune/beach interaction. *Journal of Coastal Research*, Special Issue 3, 1–4.
- Psuty, N.P. 1992. Spatial variation in coastal foredune development. In: Carter, R.W., Curtis, T.G.F., Sheehy-Skeffington, M.J. (Eds.), *Coastal dunes: geomorphology, ecology and management for conservation: Proceedings of the 3rd European Dune Congress Galway, Ireland, 17-21 June 1992* (pp. 3-13). A.A. Balkema. Rotterdam.
- Psuty N.P. 2004. *The Coastal Foredune: A Morphological Basis for Regional Coastal Dune Development*. In: Martínez M.L., Psuty N.P. (eds) *Coastal Dunes: Ecology and Conservation*. Ecological Studies, vol 171. Berlin, Heidelberg: Springer.
- Psuty, N.P. 2008. *The Coastal Foredune: A Morphological Basis for Regional Coastal Dune Development*. In: Martínez M. L., Psuty N. P. (Eds.). *Coastal*

Dunes. *Ecological Studies*, vol 171. (pp. 11-27). Berlin, Heidelberg: Springer
https://doi.org/10.1007/978-3-540-74002-5_2

Pye, K., Tsoar, H. 1990. *Aeolian Sands and Sand Dunes*. Unwin Hyman, London.

Ranasinghe, R., Symonds, G., Black, K., Holman, R. 2004. Morphodynamics of intermediate beaches: a video imaging and numerical modelling study. *Coastal Engineering*, 51(7), 629-655. <https://doi.org/10.1016/j.coastaleng.2004.07.018>

Ranwell, D.S. 1960. Newborough Warren, Anglesey: III. Changes in the vegetation on parts of the dune system after the loss of rabbits by myxomatosis. *The Journal of Ecology*, 48(2) 385-395. <https://doi.org/10.2307/2257524>

Rodgers, S., Keeffe, N. O., Delgado-Fernandez, I. 2019. Factors affecting dune mobility in Newborough, Wales. In Durán R, Guillén J, Simarro G (eds) *Proceedings of the X Jornadas de Geomorfología Litoral*, Castelldefels 4–6 September 2019, 129–132.

Saravanan, S., Chandrasekar, N., Mujabar, P.S., Hentry, C. 2011. An overview of beach morphodynamic classification along the beaches between Ovari and Kanyakumari, Southern Tamilnadu Coast, India. *Physical Oceanography*, 21(2), 129-141. <https://doi.org/10.1007/s11110-011-9110-x>

Saunders, G., Cooke, B., McColl, K., Shine, R., Peacock, T. 2010. Modern approaches for the biological control of vertebrate pests: an Australian perspective. *Biological Control*, 52(3), 288-295. doi: <https://doi.org/10.1016/j.biocontrol.2009.06.014>

Sherman, D.J., Bauer, B.O. 1993. Dynamics of beach-dune systems. *Progress in Physical Geography*, 17(4), 413-447. <https://doi.org/10.1177/030913339301700402>

Sherman, D.J., Lyons, W. 1994. Beach-state controls on aeolian sand delivery to coastal dunes. *Physical Geography*, 15(4), 381-395. <https://doi.org/10.1080/02723646.1994.10642524>

Short, A.D. 1978. Wave power and beach-stages: a global model. In: *Proceedings of 16th Conference on Coastal Engineering* (pp. 1145-1162). Hamburg, Germany: Amer Society of Civil Engineers (ASCE). <https://doi.org/10.1061/9780872621909.068>

Short, A.D. 1979. Three dimensional beach-stage model. *The Journal of Geology*, 87(5), 553-571. <https://doi.org/10.1086/628445>

Short, A.D. 1980. Beach response to variations in breaker height. In: *17th International Conference on Coastal Engineering*, Sydney, 23-28 March 1980: abstracts-in-depth. (pp. 1016-1035). Canberra, Barton, A.C.T: Institution of Engineers, Australia. <https://doi.org/10.1061/9780872622647.063>

Short, A.D., Hesp, P.A. 1982. Wave, beach and dune interactions in southeastern Australia. *Marine geology*, 48(3-4), 259-284. [https://doi.org/10.1016/0025-3227\(82\)90100-1](https://doi.org/10.1016/0025-3227(82)90100-1)

Short, A.D., Hesp, P. 1984. Beach and dune morphodynamics of the South East Coast of South Australia. Coastal Studies unit technical Report 84/1, Department of Geography, The University of Sydney, 142pp.

Short, A.D. 1985. Rip-current type, spacing and persistence, Narrabeen Beach, Australia. *Marine geology*, 65(1-2), 47-71. [https://doi.org/10.1016/0025-3227\(85\)90046-5](https://doi.org/10.1016/0025-3227(85)90046-5)

Short, A.D. 1988. Holocene coastal dune formation in southern Australia: a case study. *Sedimentary Geology* 55(1-2): 121–142. [https://doi.org/10.1016/0037-0738\(88\)90093-0](https://doi.org/10.1016/0037-0738(88)90093-0).

Short, A.D., Aagaard, T. 1993. Single and Multi-Bar Beach Change Models. *Journal of Coastal Research*, 141-157. <http://www.jstor.org/stable/25735727>

Short, A.D. 2006. Australian beach systems—nature and distribution. *Journal of Coastal Research*, 11-27. <https://doi.org/10.2112/05A-0002.1>

Short, A.D. 2010. Sediment transport around Australia—sources, mechanisms, rates, and barrier forms. *Journal of Coastal Research*, 26(3) 395-402. <https://doi.org/10.2112/05A-0002.1>

Short, A.D., Wright, L.D. 2018. Morphodynamics of beaches and surf zones in Australia. In: Komar, P. (Eds.), *Handbook of Coastal Processes and Erosion* (pp. 35-64). Boca Raton, Florida: CRC Press. <https://doi.org/10.1201/9781351072908>

Silva, F.G., Wijnberg, K.M., de Groot, A.V., Hulscher, S.J. 2019. The effects of beach width variability on coastal dune development at decadal scales. *Geomorphology*, 329, 58-69. <https://doi.org/10.1016/j.geomorph.2018.12.012>

Sonu, C.J. 1973. Three-dimensional beach changes. *The Journal of Geology*, 81(1), 42-64. <https://doi.org/10.1086/627806>

Steffen, W., Hughes., L. 2011. The critical decade: South Australian impacts (Report). Canberra: A.C.T. Climate Commission Secretariat. Retrieved from <https://climatecommission.angrygoats.net/report/the-critical-decade-south-australian-impacts/>

Sutton, J. 1925. A trip to the Coorong. *South Australian Ornithologist*, 8(3), 75-95.

Swales, A. 2002. Geostatistical estimation of short-term changes in beach morphology and sand budget. *Journal of Coastal Research*, 18(2), 338-351. <https://www.jstor.org/stable/4299079>

Sweet, W. V., Kopp, R. E., Weaver, C. P., Obeysekera, J., Horton, R. M., Thieler, E. R., Zervas, C. 2017. Global and regional sea level rise scenarios for the United States.

Tastet, J.P., Pontee, N.I. 1998. Morpho-chronology of coastal dunes in Médoc. A new interpretation of Holocene dunes in Southwestern France. *Geomorphology*, 25(1-2), 93-109. [https://doi.org/10.1016/S0169-555X\(98\)00035-X](https://doi.org/10.1016/S0169-555X(98)00035-X)

-
- Thom, B.G., Roy, P.S. 1985. Relative sea levels and coastal sedimentation in southeast Australia in the Holocene. *Journal of Sedimentary Research*, 55(2), 257-264. <https://doi.org/10.1306/212F8693-2B24-11D7-8648000102C1865D>
- Thom, B.G., Hall, W. 1991. Behaviour of beach profiles during accretion and erosion dominated periods. *Earth Surface Processes and Landforms*, 16(2), 113-127. <https://doi.org/10.1002/esp.3290160203>
- Trenhaile, A.S. 1997. *Coastal Dynamics and Landforms*. Gloucestershire, UK: Clarendon Press.
- Tsoar, H., Blumberg, D.A.N. 2002. Formation of parabolic dunes from barchan and transverse dunes along Israel's Mediterranean coast. *Earth Surface Processes and Landforms*, 27(11), 1147-1161. <https://doi.org/10.1002/esp.417>
- Tsoar, H. 2005. Sand dunes mobility and stability in relation to climate, *Physica A: Statistical Mechanics and its Applications*, 357(1), 50-56. <https://doi.org/10.1016/j.physa.2005.05.067>
- Tsoar, H., Levin, N., Porat, N., Maia, L.P., Herrmann, H.J., Tatumi, S.H., Claudino-Sales, V. 2009. The effect of climate change on the mobility and stability of coastal sand dunes in Ceará State (NE Brazil). *Quaternary Research*, 71(2), 217-226. <https://doi.org/10.1016/j.yqres.2008.12.001>
- Van Rijn, L.C., Ruessink, B.G., Grasmeijer, B.T., 1999. Generation and migration of nearshore bars under non-to macrotidal conditions. In: *Coastal Sediments '99: Proceedings of the 4th International Symposium on Coastal Engineering and Science of Coastal Sediment* (pp. 463-478). Houston, Texas: Amer Society of Civil Engineers (ASCE).
- Verdon-Kidd, D.C., Kiem, A.S. 2009. Nature and causes of protracted droughts in southeast Australia: Comparison between the Federation, WWII, and Big Dry droughts. *Geophysical Research Letters*, 36(22), L22707, <https://doi.org/10.1029/2009GL041067>
- Walker, I.J., Davidson-Arnott, R.G., Bauer, B.O., Hesp, P.A., Delgado-Fernandez, I., Ollerhead, J., Smyth, T.A. 2017. Scale-dependent perspectives on the geomorphology and evolution of beach-dune systems. *Earth-Science Reviews*, 171, 220-253. <https://doi.org/10.1016/j.earscirev.2017.04.011>
- White, D.J.B. 1961. Some observations on the vegetation of Blakeney Point, Norfolk, following the disappearance of the rabbits in 1954. *Journal of Ecology*, 49(1), 113-118. <https://www.jstor.org/stable/2257428>
- Wolfe, S.A, Hugenholtz, C.H. 2009. Barchan dunes stabilized under recent climate warming on the northern Great Plains. *Geology* 37(11), 1039-1042. <https://doi.org/10.1130/G30334A.1>
- Wright, L.D., Chappell, J., Thorn, B.G., Bradshaw, M.P., Cowell, P. 1979. Morphodynamics of reflective and dissipative beach and inshore systems: Southeastern Australia. *Marine Geology*, 32(1-2), 105-140. [https://doi.org/10.1016/0025-3227\(79\)90149-X](https://doi.org/10.1016/0025-3227(79)90149-X)

Wright, L.D., Short, A.D. 1984. Morphodynamic variability of surf zones and beaches: a synthesis. *Marine Geology*, 56(1-4), 93-118. [https://doi.org/10.1016/0025-3227\(84\)90008-2](https://doi.org/10.1016/0025-3227(84)90008-2)

Yan, N., Baas, A.C. 2015. Parabolic dunes and their transformations under environmental and climatic changes: Towards a conceptual framework for understanding and prediction. *Global and Planetary Change*, 124, 123-148. <https://doi.org/10.1016/j.gloplacha.2014.11.010>

Yan, N., Baas, A.C. 2017. Environmental controls, morphodynamic processes, and ecogeomorphic interactions of barchan to parabolic dune transformations. *Geomorphology*, 278, 209-237. <https://doi.org/10.1016/j.geomorph.2016.10.033>

Yizhaq, H., Ashkenazy, Y., Tsoar, H. 2007. Why do active and stabilized dunes coexist under the same climatic conditions? *Physical Review Letters*, 98 (18), 188001. <https://doi.org/10.1103/PhysRevLett.98.188001>

Yizhaq, H., Ashkenazy, Y., Tsoar, H. 2009. Sand dune dynamics and climate change: A modeling approach, *Journal of Geophysical Research.*, 114, F01023. <https://doi.org/10.1029/2008JF001138>

Yizhaq, H., Ashkenazy, Y., Levin, N., Tsoar, H. 2013. Spatiotemporal model for the progression of transgressive dunes. *Physica A: Statistical Mechanics and its Applications*, 392(19), 4502-4515. <https://doi.org/10.1016/j.physa.2013.03.066>